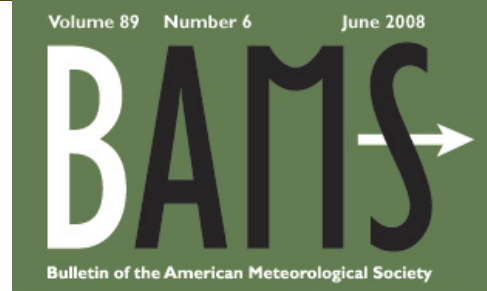# Constituent and Aerosol Assimilation

R. Bradley Pierce

National Ocean and Atmospheric Administration
National Environmental Satellite, Data, and Information Service
Center for Satellite Applications and Research (STAR)

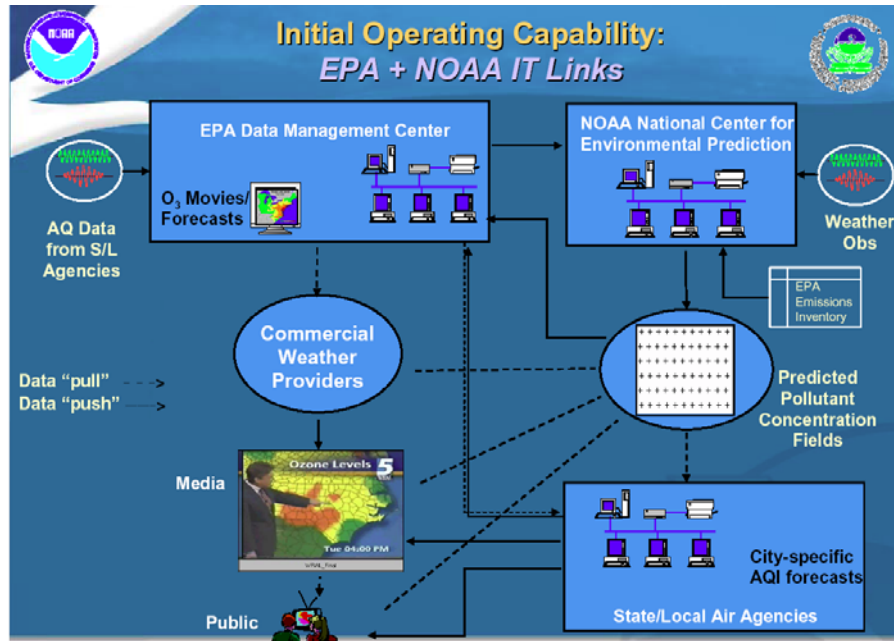**JCSDA Summer Colloquium on Data Assimilation Stevenson, Washington**

Motivation

Changes in atmospheric composition since the industrial revolution

• Decreases in stratospheric ozone and increases in surface ultraviolet radiation

• Occurrence of urban smog and increased ozone background in the northern troposphere

• Increases in greenhouse gases and aerosols and associated climate change

• Acid rain and eutrophication of surface waters

• Enhanced aerosol and photo-oxidant levels due to biomass burning

• Increases in fine particles, reduction in visibility and human health effects

• Long-range transport of air pollution

"Many of these changes in atmospheric composition have socio-economic consequences through adverse effects on human and ecosystem health, on water supply and quality, and on crop growth."

IGACO
THE INTEGRATED GLOBAL ATMOSPHERIC CHEMISTRY OBSERVATIONS THEME

IGOS
Integrated Global Observing Strategy

For the Monitoring of our Environment from Space and from Earth

September 2004
An international partnership for cooperation in Earth observations

From IGOS Atmospheric Chemistry Theme Report 2004
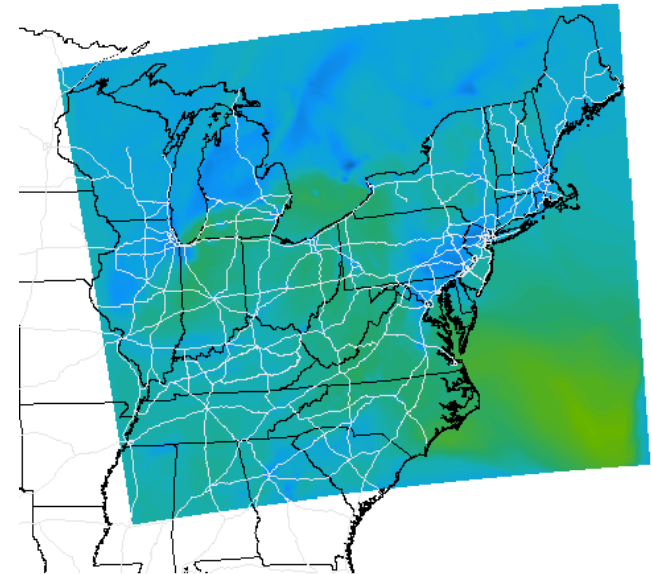
National Air Quality Forecasting

Initial Operating Capability: EPA + NOAA IT Links

The Congressional Energy Policy Act of 2002 [H.R. 4, 2002] Directed the Department of Commerce, through NOAA, to "establish a program to provide operational air quality forecasts And warnings for specific regions of the United States".

In September 2004, the first phase of NOAA Air Quality forecasting became operational, providing twice daily predictions of ground-level ozone over the NE US.

1Hr Avg Ozone Concentration(PPB) Ending Thu Nov 04 2004 12PM EST
(Thu Nov 04 2004 17Z)
National Digital Guidance Database
Experimental graphic created 11/04/2004 10:22AM EST

Current (February, 2008) Status

National Air Quality Forecast Capability
End-to-End Operational Capability

Model Components: Linked numerical prediction system

Operationally integrated on NCEP's supercomputer

- NCEP mesoscale NWP: WRF-NMM
- NOAA/EPA community model for AQ: CMAQ

Observational Input:

- NWS weather observations; NESDIS fire locations
- EPA emissions inventory

Gridded forecast guidance products

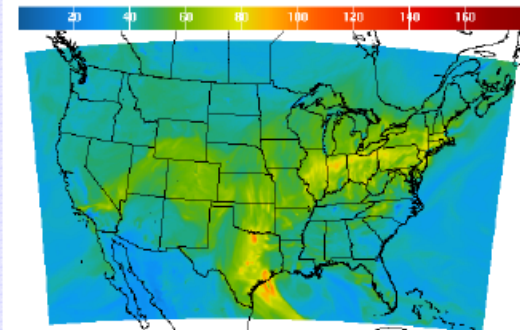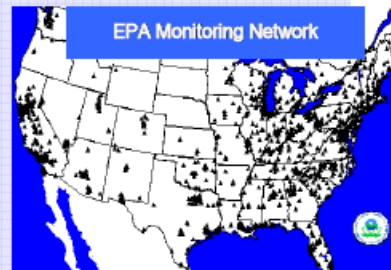- On NWS Telecommunications Gateway and EPA servers
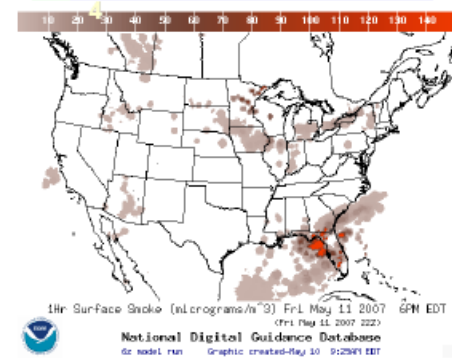- Updated 2x daily

Verification basis

EPA compilation:

- Ground-level ozone observations

Customer outreach/feedback

- State & Local AQ forecasters coordinated with EPA
- Public and Private Sector AQ constituents

1Hr Avg Ozone Concentration(PPB) Ending Thu Oct 04 2007 4PM EDT
(Thu Oct 04 2007 20Z)
National Digital Guidance Database
06z model run   Graphic created-Oct 04 7:23AM EDT

AQI: Peak Oct

EPA Monitoring Network

1Hr Surface Smoke (micrograms/m^3) Fri May 11 2007 6PM EDT
(Fri May 11 2007 22Z)
National Digital Guidance Database
6z model run   Graphic created-May 10 9:25PM EDT

http://www.weather.gov/ost/air_quality/

Current (February, 2008) Status

National Air Quality Forecast Capability
End-to-End Operational Capability

Model Components: Linked numerical prediction system

Operationally integrated on NCEP's supercomputer

- *NCEP mesoscale NWP: WRF-NMM*
- *NOAA/EPA community model for AQ: CMAQ*

Observational Input:

- *NWS weather observations; NESDIS fire locations*
- *EPA emissions inventory*

Gridded forecast guidance products

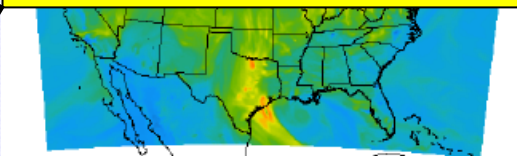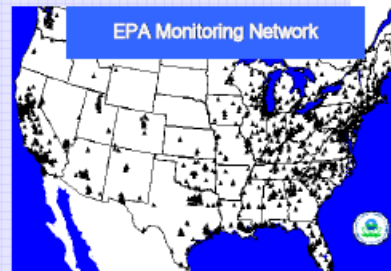- On NWS Telecommunications Gateway and EPA servers
- Updated 2x daily

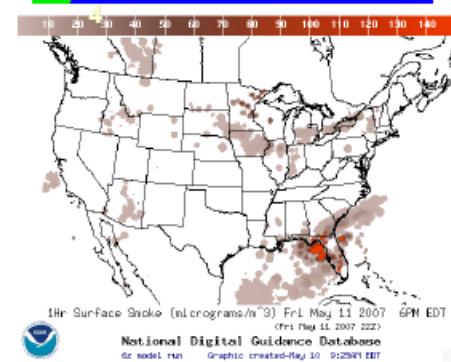## Verification basis

EPA compilation:

- Ground-level ozone observations

Customer outreach/feedback

- State & Local AQ forecasters coordinated with EPA
- Public and Private Sector AQ constituents

No composition or aerosol data to constrain initial conditions

EPA Monitoring Network

1Hr Avg Ozone Concentration(PPB) Ending Thu Oct 04 2007 4PM EDT
(Thu Oct 04 2007 20Z)
National Digital Guidance Database
06z model run   Graphic created-Oct 04 7:23AM EDT

AQI: Peak Oct

1Hr Surface Smoke (micrograms/m^3) Fri May 11 2007 6PM EDT
(Fri May 11 2007 22Z)
National Digital Guidance Database
6z model run   Graphic created-May 10 9:25AM EDT

http://www.weather.gov/ost/air_quality/

Background

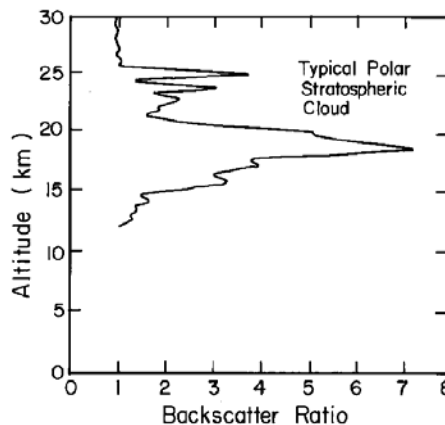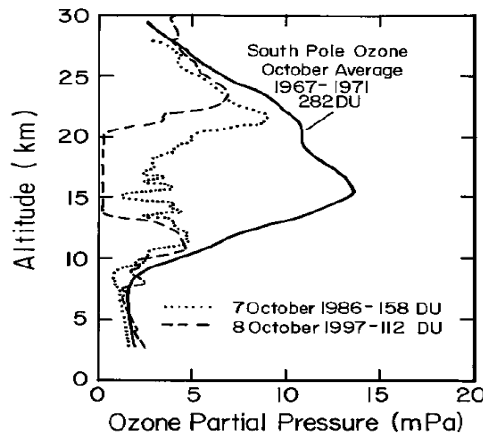## 1. Stratospheric Chemistry/Aerosols

- **Antarctic/Arctic ozone loss**

- **Volcanic injection of sulfate aerosols**

2. Tropospheric Air quality

- **Health effects (PM2.5, O3)**

- **Tropospheric aerosol formation**

- **NOx/VOC chemistry**

Stratospheric Chemistry
Antarctic Ozone Depletion

$$ClO + ClO \xrightarrow{M} Cl_2O_2$$

$$Cl_2O_2 + h\nu \rightarrow Cl + ClOO$$

$$ClOO \xrightarrow{M} Cl + O_2$$

$$2(Cl + O_3 \rightarrow ClO + O_2)$$

$$\text{net:} \quad 2O_3 \rightarrow 3O_2$$

Molina and Molina [1987] showed that very rapid ozone depletion can occur through a catalytic cycle involving formation and photolysis of a *ClO dimer*, Cl_2O_2. This cycle is responsible for about 75% of the ozone removal in the ozone hole.

From Solomon [Reviews of Geophysics,1999]
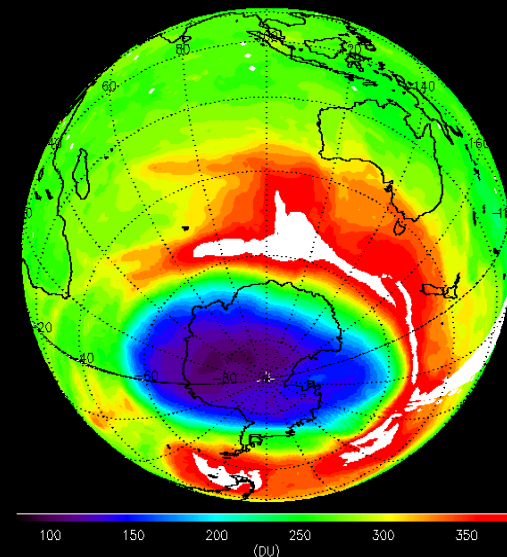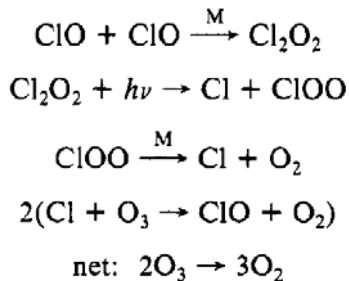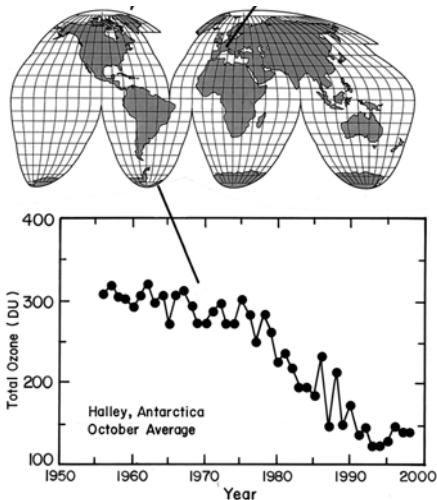
OMI October 15, 2006

**RAQMS Analysis
October 15, 2006**
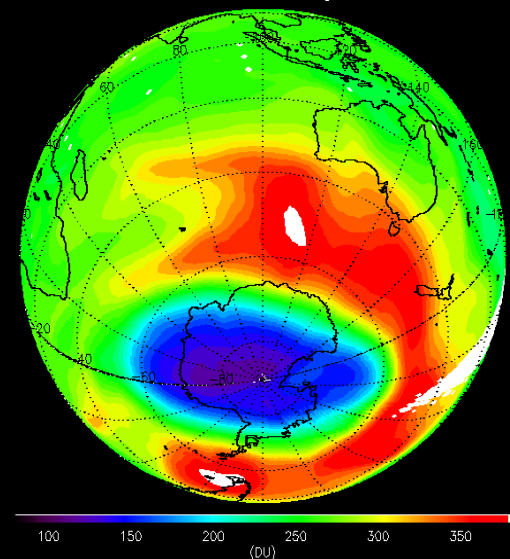
**Record breaking ozone loss
during October, 2006**

Stratospheric Aerosols: Volcanic Injection
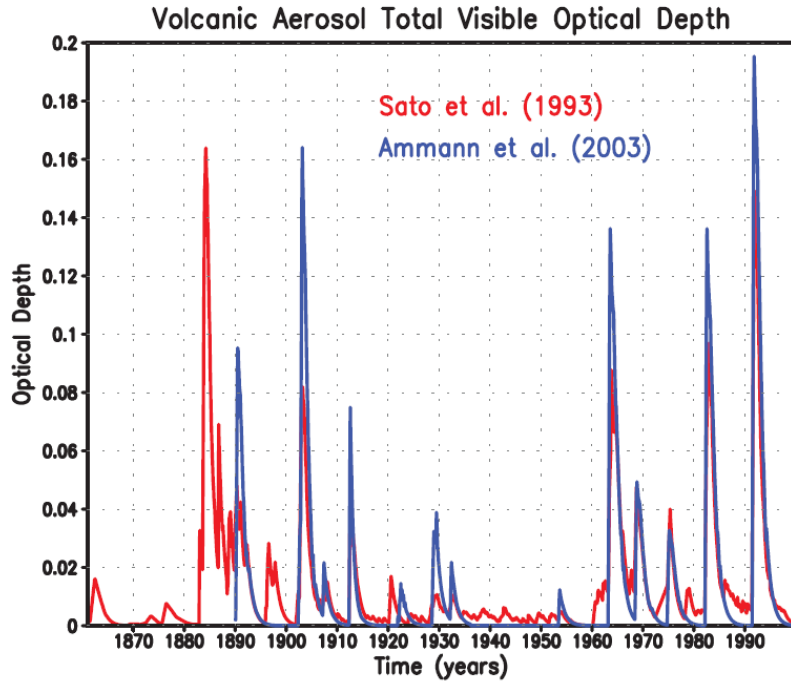
Figure 2.18. *Visible (wavelength 0.55 μm) optical depth estimates of stratospheric sulphate aerosols formed in the aftermath of explosive volcanic eruptions that occurred between 1860 and 2000. Results are shown from two different data sets that have been used in recent climate model integrations. Note that the Ammann et al. (2003) data begins in 1890.*

Simulations of the 1991 Mt. Pinatubo eruption show a large negative perturbation in radiative forcing (-3 W m^{-2}) (Ramachandran et al., 2000; Hansen et al., 2002)

From Forster, P., V. et. al., [IPCC, 2007]
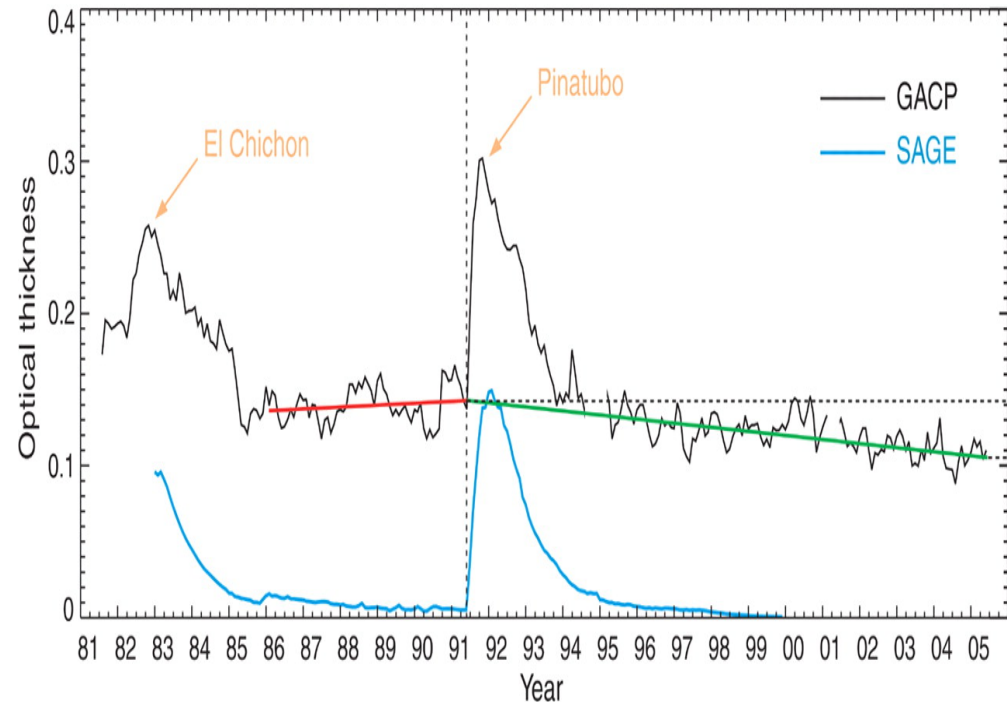
Global Aerosol Climatology Project (GACP) data shows a decrease of the global optical thickness of tropospheric aerosols during the period from 1991 to 2005, mirroring the increase in solar radiation fluxes at Earth's surface.

From Mishchenko, M. I., et al. [Science 2007]

Table 3. Summary of selected chemical model data assimilation experiments.

References	Method	Assimilated constituent dataset	Chemistry
Austin, 1992	Nudging	Ozone, H_2O, HNO_3 and NO_2 profiles (LIMS)	CTM: extended family approach
Fisher and Lary, 1995	4D-Var	Ozone (UARS MLS) and NO_2 (UARS CLAES) profiles; synthetic data	Trajectory box model: reduced stratospheric chemistry
Levelt et al., 1998	Sequential statistical interpolation	Ozone profiles (UARS MLS)	CTM: extensive photochemical scheme; heterogeneous chemistry
Khattatov et al., 1999	4D-Var and Kalman filter	Ozone, HNO_3, NO_2, $ClONO_2$, N_2O and CH_4 (UARS CLAES); ClO and H_2O (UARS MLS)	Photochemical box model: gas-phase chemistry
Khattatov et al., 2000	Kalman filter	Ozone profiles (UARS MLS)	CTM: extensive set of photochemical reactions; heterogeneous processes
Ménard et al., 2000; Ménard and Chang, 2000	Kalman filter	CH_4 profiles (UARS CLAES and HALOE)	CTM: no chemistry
Errera and Fonteyn, 2001; BIRA-IASB system was operational 2002–2004	4D-Var	Ozone, CH_4, N_2O, CFC-11, HNO_3, $ClONO_2$ and N_2O_5 profiles (CRISTA)	CTM: detailed chemical scheme
Fonteyn et al., 2001	4D-Var	Aerosol (SAGE-II)	Simple aerosol model
Chipperfield et al. (2002)	Kalman filter	O_3, CH_4, H_2O, and HCl profiles (UARS HALOE)	CTM: detailed gas-phase stratospheric chemistry; CH_4 oxidation scheme; long-lived tracers
Küll et al., 2002	Nudging	Ozone, CH_4, N_2O, HNO_3, $ClONO_2$, NO_2 and N_2O_5 profiles (CRISTA)	CTM: detailed chemical scheme and aerosol parametrization

From **Lahoz, W. A. et al.,** Atmos. Chem. Phys., 7, 5745–5773, 2007

Lagrangian four-dimensional variational data assimilation of chemical species

By M. FISHER[*1] and D. J. LARY[2]

[1]*Meteorological Office, UK*
[2]*Cambridge University, UK*

SUMMARY

For the first time, the method of four-dimensional variational data assimilation is applied to the analysis of chemically active trace species. By combining observations with a numerical model to analyse simultaneously several species over a period of a few days, the analysis method is able to exploit information which is not available to conventional analysis techniques. Moreover, effective use can be made of asynoptic observations even for species which have strong diurnal cycles. Synoptic analyses are produced. A Lagrangian approach is adopted, allowing a separation of dynamics and chemistry which considerably reduces the computational expense of the method.

KEYWORDS: Atmospheric chemistry   Data analysis   Lagrangian model   Stratosphere   Variational data assimilation
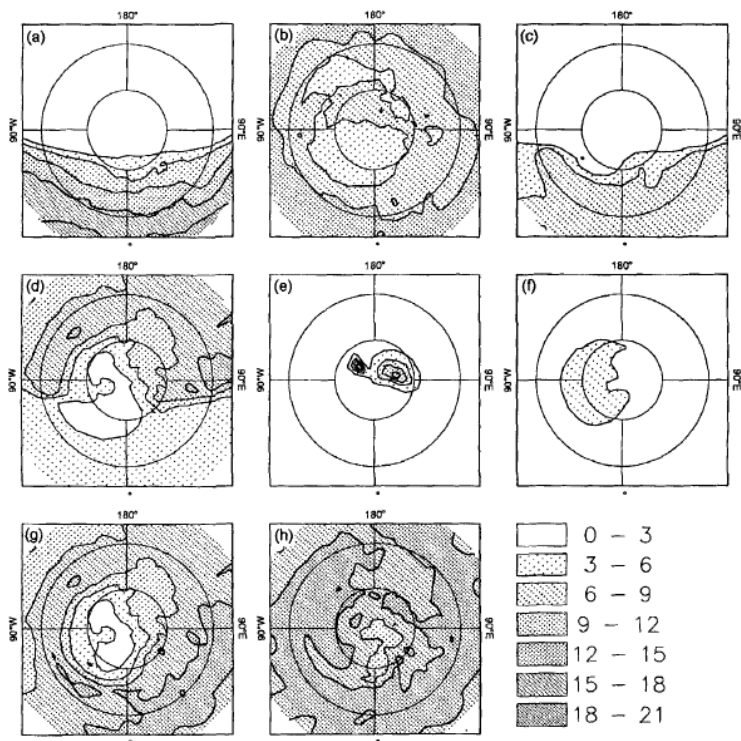
Simplified O3/NOy chemistry photochemical 'box' model which simulates the evolution of chemical trace species for a number of independent air parcels.

The constraints of the model chemical equations were incorporated into the analysis by regarding the cost function (in the minimization), as a function of the initial concentrations only.

The analysis uses O3 retrievals (version 3) from the Microwave Limb Sounder (MLS) and NO+NO2 from the Cryogenic Limb Array Etalon Spectrometer (CLAES) instruments on the Upper Atmosphere Research Satellite (UARS)

Figure 8. Analysed mixing ratios for the 1100 K isentrope for 12 UTC on 10 January 1992. (a) $O(^3P)$ (pptv), (b) O_3 (ppmv), (c) NO (ppbv), (d) NO_2 (ppbv), (e) NO_3 (pptv), (f) N_2O_5 (ppbv), (g) $NO+NO_2$ (ppbv), (h) $NO+NO_2+NO_3+2N_2O_5$ (ppbv). The circles plotted on each map represent 30°N and 60°N.

TABLE 1.   THE REACTION SCHEME USED IN THIS STUDY. THE RATES OF ALL THESE REACTIONS ARE TAKEN FROM DeMORE *et al.* (1992)

$O(^3P)$	+	O_3	$\longrightarrow$	O_2	+	O_2	k_{b1}
$O(^3P)$	+	NO_2	$\longrightarrow$	NO	+	O_2	k_{b2}
$O(^3P)$	+	NO_3	$\longrightarrow$	O_2	+	NO_2	k_{b3}
O_3	+	NO	$\longrightarrow$	NO_2	+	O_2	k_{b4}
NO	+	NO_3	$\longrightarrow$	NO_2	+	NO_2	k_{b5}
O_3	+	NO_2	$\longrightarrow$	NO_3	+	O_2	k_{b6}
NO_2	+	NO_3	$\longrightarrow$	NO	+	NO_2 + O_2	k_{b7}
$O(^3P)$	+	O_2	$\overset{M}{\longrightarrow}$	O_3			k_{t1}
$O(^3P)$	+	NO	$\overset{M}{\longrightarrow}$	NO_2			k_{t2}
$O(^3P)$	+	NO_2	$\overset{M}{\longrightarrow}$	NO_3			k_{t3}
NO_2	+	NO_3	$\overset{M}{\longrightarrow}$	N_2O_5			k_{t4}
N_2O_5			$\overset{M}{\longrightarrow}$	NO_2	+	NO_3	k_{t5}
O_2	+	$h\nu$	$\longrightarrow$	$O(^3P)$	+	$O(^3P)$	j_1
O_3	+	$h\nu$	$\longrightarrow$	O_2	+	$O(^3P)$	j_2
NO_2	+	$h\nu$	$\longrightarrow$	NO	+	$O(^3P)$	j_3
NO_3	+	$h\nu$	$\longrightarrow$	NO	+	O_2	j_4
NO_3	+	$h\nu$	$\longrightarrow$	NO_2	+	$O(^3P)$	j_5
N_2O_5	+	$h\nu$	$\longrightarrow$	NO_3	+	NO_2	j_6
N_2O_5	+	$h\nu$	$\longrightarrow$	NO_3	+	NO + $O(^3P)$	j_7

Assimilation of satellite observations of long-lived chemical species in global chemistry transport models

Boris V. Khattatov,[1] Jean-Francois Lamarque,[1] Lawrence V. Lyjak,[1] Richard Menard,[2] Pieternel Levelt,[3] Xuexi Tie,[1] Guy P. Brasseur,[4] and John C. Gille[1]

Abstract. Use of data assimilation techniques such as optimal interpolation or the Kalman filter in global chemistry transport models (CTM) is becoming more common. However, owing to high computational requirements, it is often difficult to apply these techniques to multidimensional models containing extensive photochemical schemes. We present a sequential assimilation approach developed for use with general global chemistry transport models. It allows fast assimilation and mapping of satellite observations and provides estimates of analysis errors. The suggested data assimilation scheme evolved from the one described by *Levelt et al.* [1998]. It is a variant of the suboptimal Kalman filter and is based on ideas described by *Menard et al.* [2000] and *Menard and Chang* [2000]. One of the most important features of the developed scheme is its ability to routinely estimate variance of the analysis and to predict variance evolution in the model. The developed technique (or its variants) has been successfully interfaced with a number of different global models and used for assimilation of several types of measurements, including aerosol extinction ratios. Some of these experiments are described by *Lamarque et al.* [1999] and W. D. Collins et al. (Forecasting aerosols using a chemical transport model with assimilation of satellite aerosol retrievals: Methodology for INDOEX, submitted to *Journal of Geophysical Research*, 2000, hereinafter referred to as Collins et al., submitted manuscript, 2000). We illustrate the method using assimilation of ozone observations made by the Upper Atmosphere Research Satellite/Microwave Limb Sounder in the three-dimensional chemistry transport model ROSE [Research for Ozone in the Stratosphere and its Evolution; *Rose and Brasseur*, 1989].

Research for Ozone in the Stratosphere and its Evolution (ROSE) [Rose and Brasseur, 1989] 3D CTM. Family approach for oxygen, nitrogen, carbon, chlorine, hydrogen, and bromine) heterogeneous (aerosol) processes.

3D sequential data assimilation method based on Menard et al. [2000] with parameterized calculations of off-diagonal elements of forecast error covariance (constant functional relationship based on diagonal elements)

Allows fast and accurate mapping of sparse satellite data and facilitates comparisons with correlative data
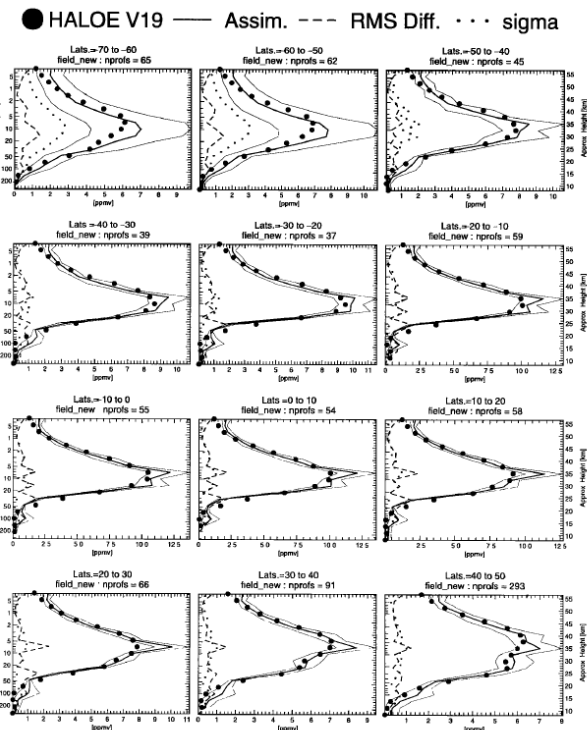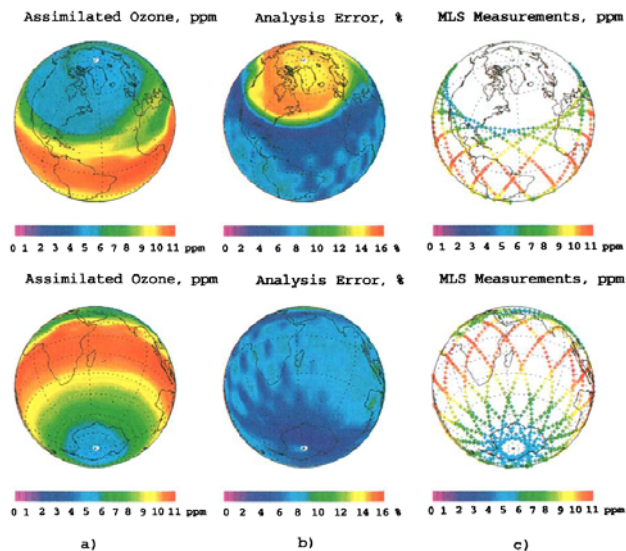

Plate 1. Results of the assimilation for January 13, 1993, at 10 mbar. (a) Analyzed ozone at 1300 UT, ppmv; (b) analysis error in percent at 1300 UT; (c) MLS ozone observations.

Figure 3. Monthly (January) and zonally averaged ozone profiles from HALOE (solid circles) and the assimilation (thick lines) for different latitude bins. Also shown are the average RMS differences between HALOE and assimilation (dotted lines) and average assimilation analysis error (dashed lines). Thin solid lines represent error bars of the assimilation analysis.

Assimilation of ozone profiles from the Improved Limb Atmospheric Spectrometer-II: Study of Antarctic ozone

Ivanka Stajner,[1,2] Krzysztof Wargan,[1,2] Lang-Ping Chang,[1,2] Hiroo Hayashi,[1,3] Steven Pawson,[1] and Hideaki Nakajima[4]

[1] Ozone data from the Improved Limb Atmospheric Spectrometer-II (ILAS-II) were included in addition to other satellite observations in the ozone assimilation system at the Global Modeling and Assimilation Office (GMAO) of NASA/Goddard. The control run assimilated data from NOAA 16 Solar Backscatter Ultraviolet/2 (SBUV/2) and Polar Ozone and Aerosol Measurement III (POAM III) instruments. Persistent impacts over Antarctica and transient impacts over northern middle and high latitudes are seen from April to October 2003, when ILAS-II provided good coverage. The largest improvements with respect to independent ozone sonde data are seen over the South Pole station. Ozone analyses and forecasts from the assimilation of SBUV/2, POAM III and ILAS-II data are used to investigate the transport of ozone to southern middle latitudes following the breakup of the Antarctic vortex. The quality of analyses and forecasts is evaluated by comparison with independent Stratospheric Aerosol and Gas Experiment III (SAGE III) ozone data near 46°S. Anomaly correlations between SAGE III data and forecasts are improved at 70 hPa when occultation data are included.
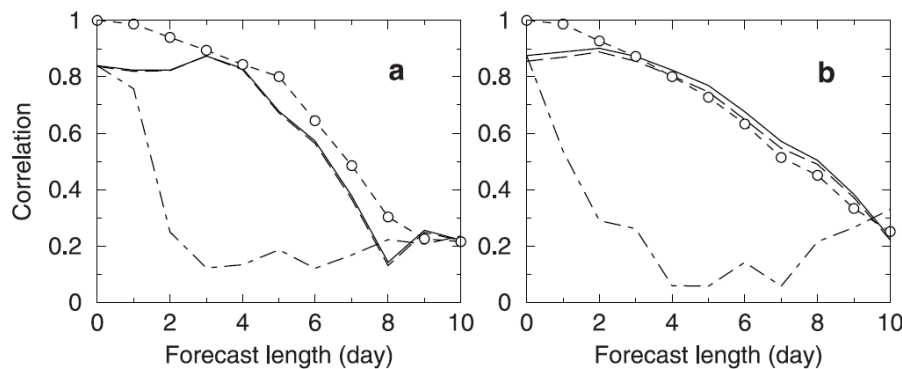
NASA Global Modeling and Assimilation Office (GMAO) Physical-space Statistical Analysis System (PSAS) [Cohn et al.,1998] univariate assimilation system at NASA/Goddard [Stajner et al., 2001]

Evaluation of the impacts of assimilating Improved Limb Atmospheric Spectrometer-II (ILAS-II) ozone

Anomaly correlations exceed 0.6 for up to 5–7 days in the middle and lower stratosphere (30, 50 and 70 hPa). The loss in the forecast skill with advanced forecast length related to transport errors.
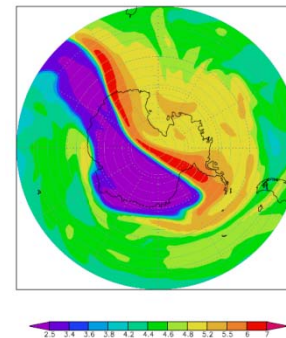

Figure 6. Ozone field (ppmv) at 30 hPa at 1200 UT on 5 November shown in the south polar stereographic projection poleward of 45°S.

Figure 9. Anomaly correlations between SAGE III and collocated ozone forecasts as a function of forecast length started from the analyses of POAM III, ILAS-II and SBUV/2 data (solid curve). Same is shown for forecasts started from SBUV/2-only assimilation (dashed) and for persistence (dot-dashed). In each case, forecast time zero corresponds to the analysis. Anomaly correlations of forecasts from analyses of POAM III, ILAS-II and SBUV/2 data against those analyses at 46°S are shown (dashed with circles). (a) At 30 hPa and (b) at 70 hPa.
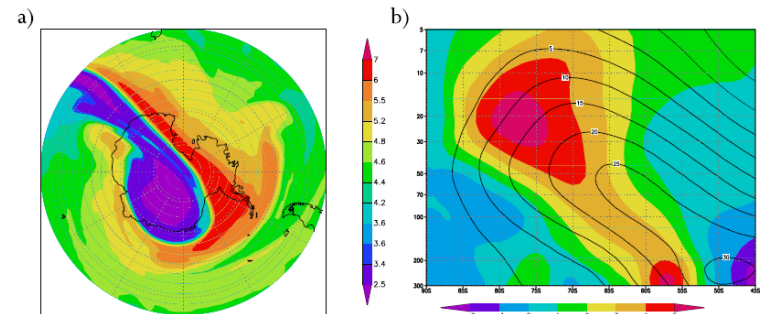

Figure 11. (a) Five-day ozone forecast (ppmv) at 30 hPa for 5 November at 1200 UT shown (compare analysis in Figure 6). (b) Average analysis zonal wind (m/s) for 1–10 November (contour) and the average difference between 5-day wind forecast and analysis (color) shown for 90−45°S and 300−5 hPa.

Tropospheric Air Quality is largely determined by the abundance of *Aerosols* and *Ozone*

What are *tropospheric aerosols*?

Aerosols are a mixture of microscopic solids and liquid droplets suspended in air. This pollution, also known as particulate matter, is made up of a number of components, including acids (such as nitrates and sulfates), organic chemicals, metals, soil or dust particles, and allergens (such as fragments of pollen or mold spores).
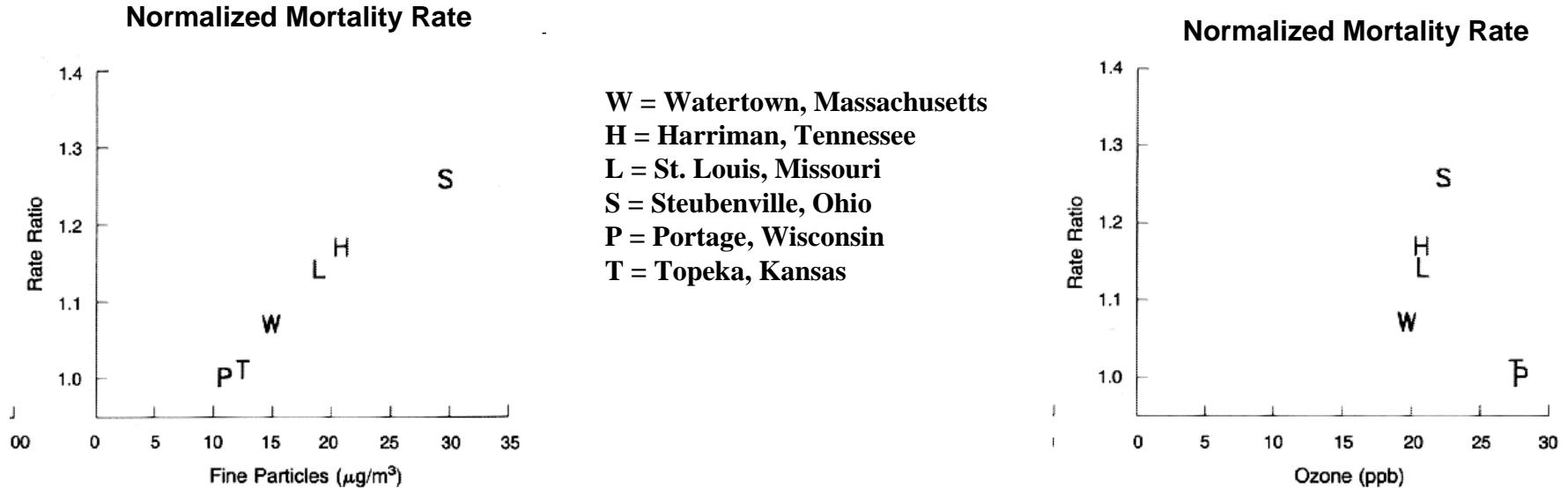

Particles contribute to haze, such as this brown haze over Boston.

Ground-level *ozone*, a primary ingredient in smog, is formed when volatile organic compounds (VOCs) and NOx react chemically in the presence of sunlight. Car, trucks, power plants and industrial facilities are primary sources of these emissions. Ozone pollution is a concern during the summer months when the weather conditions needed to form ground-level ozone – lots of sun and hot temperatures – normally occur.

Impacts of poor Air Quality

In a 6 city study of the association between air pollution and mortality (lung cancer and cardiopulmonary disease) the adjusted mortality-rate ratio for the most polluted of the cities as compared with the least polluted was 1.26 (95 percent confidence interval, 1.08 to 1.47). Increased mortality (excluding smoking) was most strongly associated with air pollution with fine particulates, including sulfates. [*Dockery, et al. NEJM, 329, 1753-1759,1993*]
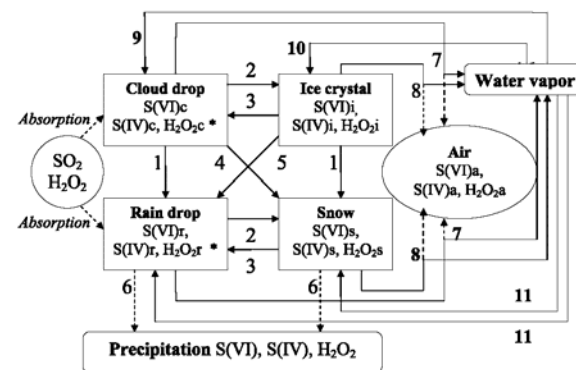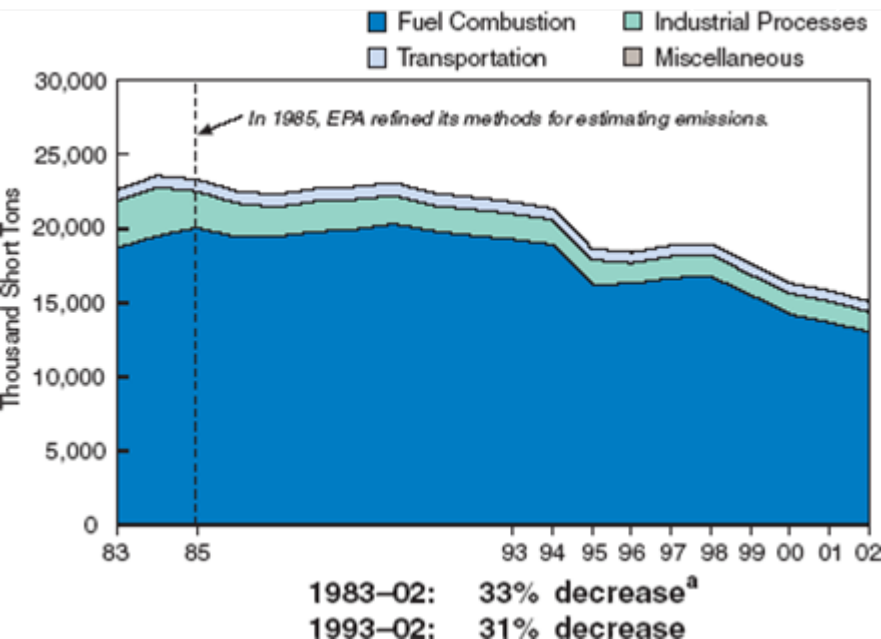
Normalized Mortality Rate

W = Watertown, Massachusetts
H = Harriman, Tennessee
L = St. Louis, Missouri
S = Steubenville, Ohio
P = Portage, Wisconsin
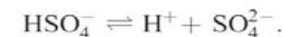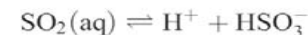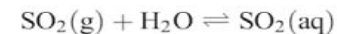T = Topeka, Kansas

Normalized Mortality Rate

More recent Population-based studies suggest that for each 10 ppb increase in 1-hour daily maximum level of ozone there is an increase in mortality risk of 0.39–0.87%, especially in individuals with pre-existing respiratory disease [Ito, et al., *Epidemiology* 16, 446–457, 2005]

# Aerosol formation in polluted environments
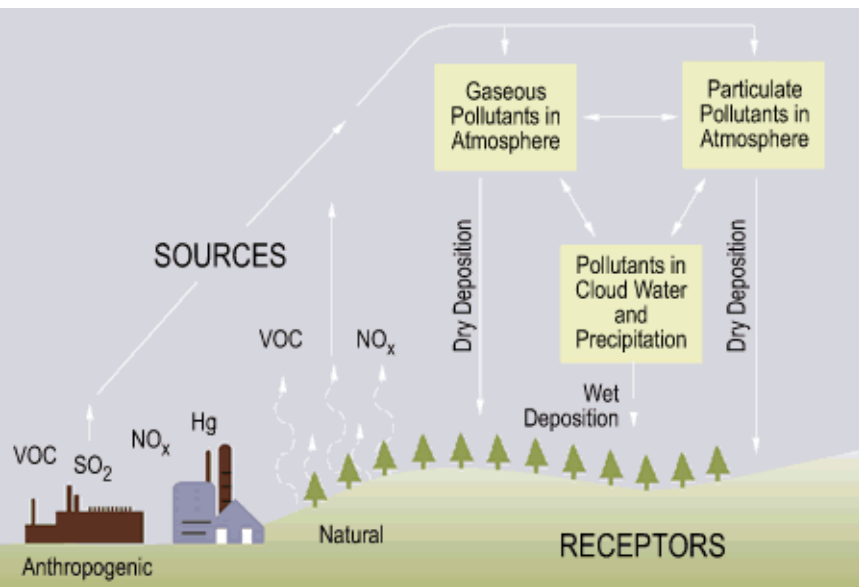
Oxidation of Sulfur dioxide (SO2) from by Hydrogen Peroxide (H2O2) produces small (< 2.5 micron) Sulfate (SO4) aerosol particles.

$$SO_2(g) + H_2O \rightleftharpoons SO_2(aq)$$

$$SO_2(aq) \rightleftharpoons H^+ + HSO_3^-$$

$$H_2O_2(g) + H_2O \rightleftharpoons H_2O_2(aq)$$

$$S(IV) + H_2O_2 \longrightarrow S(VI) + H_2O$$

$$HSO_4^- \rightleftharpoons H^+ + SO_4^{2-}.$$

In-cloud processing of Sulfate aerosols produces "acid rain"

Tropospheric Ozone Production

Ozone production is controlled by the abundance of precursors, such as Nitrogen oxides (NOx) and Volatile Organic Hydrocarbons (VOC)

Ozone Production (ppbv/hour)

NOx (ppbv)

VOC (ppbC)
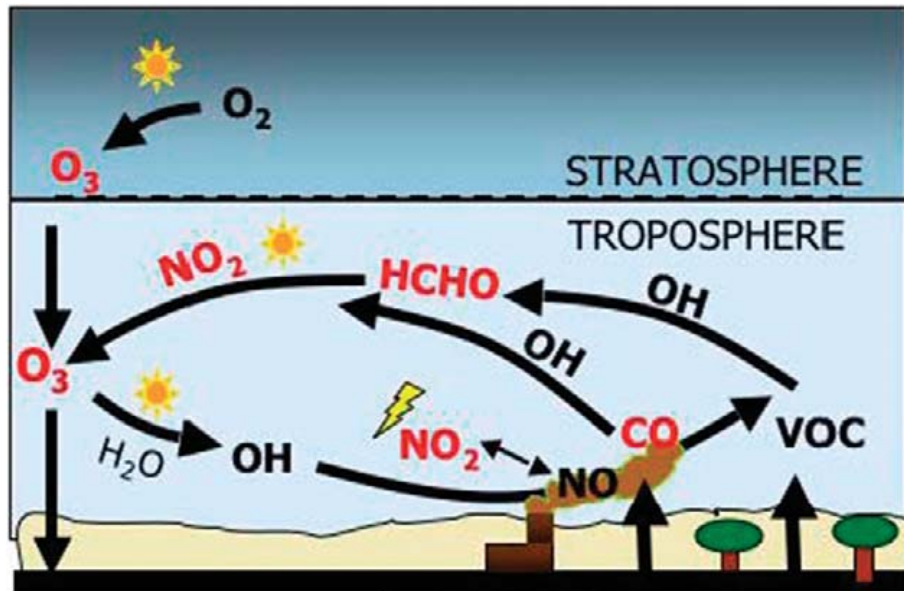
Schematic diagram of simplified tropospheric photochemistry. Species in red can be measured using existing satellite instrumentation.
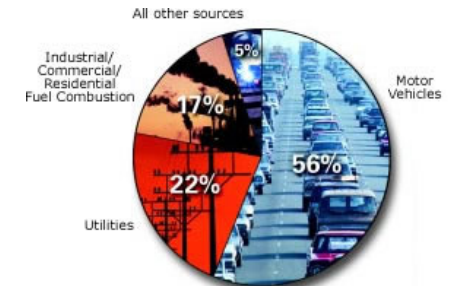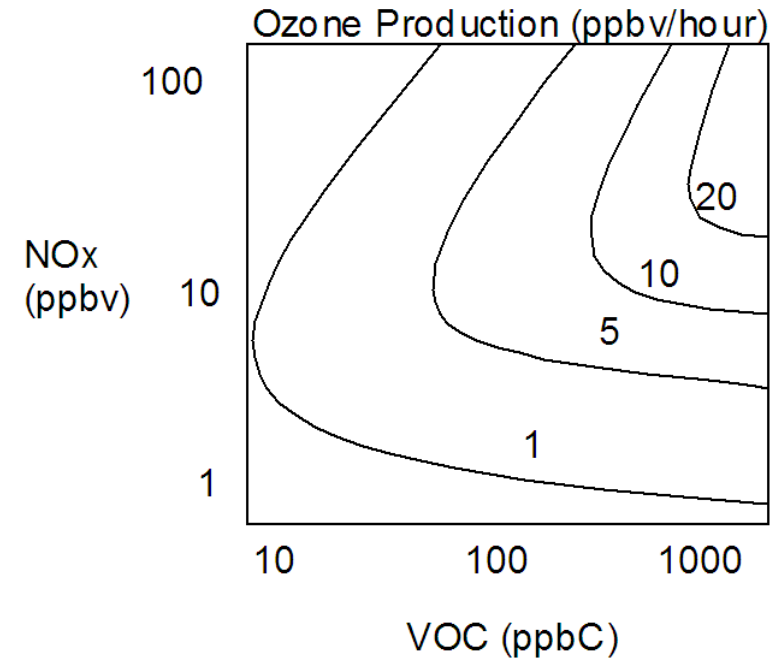
Sources of NOx
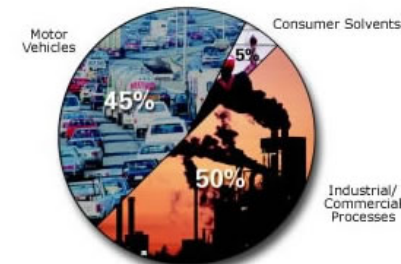
Sources of VOC

Variational data assimilation for tropospheric chemistry modeling

Hendrik Elbern, Hauke Schmidt, and Adolf Ebel

Institute for Geophysics and Meteorology, University of Cologne, Germany

Abstract. The method of variational adjoint data assimilation has been applied to assimilate chemistry observations into a comprehensive tropospheric gas phase model. The rationale of this method is to find the correct initial values for a subsequent atmospheric chemistry model run when observations scattered in time are available. The variational adjoint technique is esteemed to be a promising tool for future advanced meteorological forecasting. The stimulating experience gained with the application of four–dimensional variational data assimilation in this research area has motivated the attempt to apply the technique to air quality modeling and analysis of the chemical state of the atmosphere. The present study describes the development and application of the adjoint of the second–generation regional acid deposition model gas phase mechanism, which is used in the European air pollution dispersion model system. Performance results of the assimilation scheme using both model–generated data and real observations are presented for tropospheric conditions. In the former case it is demonstrated that time series of only few or even one measured key species convey sufficient information to improve considerably the analysis of unobserved species which are directly coupled with the observed species. In the latter case a Lagrangian approach is adopted where trajectory calculations between two comprehensively furnished measurement sites are carried out. The method allows us to analyze initial data for air pollution modeling even when only sparse observations are available. Besides remarkable improvements of the model performance by properly analyzed initial concentrations, it is shown that the adjoint algorithm offers the feasibility to estimate the sensitivity of ozone concentrations relative to its precursors.
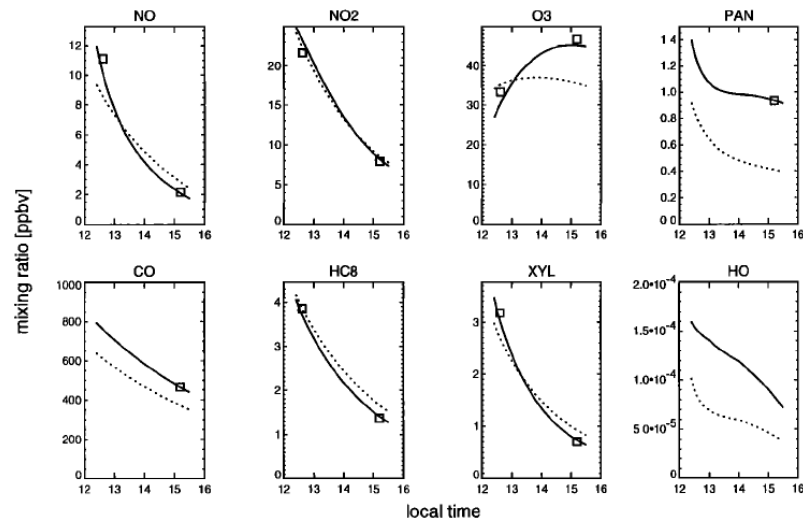
Figure 11. Assimilation results for the measurement stations Kappel (squares at 1237 LT observation time) and Schauinsland (squares at 1511 LT) shown by solid lines. First guess run is depicted by dotted lines. Simulation experiment with optimized parameters for vertical mixing, dry deposition, and drifting time between the stations is given.

The adjoint of the second generation Regional Acid Deposition Model (RADM2) [Stockwell et al., 1990] designed for use in mesoscale Eulerian tropospheric air quality models was developed.

The adjoint RADM2 mechanism was evaluated within the framework of a Lagrangian approach (two surface stations, 8.5km apart)

Concluded that variational adjoint data assimilation can be applied for comprehensive gas phase mechanism in the planetary boundary layer with few observations.

Table 3. Total of Species Measured at Stations Schauinsland, Kappel, Appertaining RADM2 Group, and Indication on Usage in the Assimilation Algorithm

| Species	RADM2 Group[a]	Kappel	Schauinsland	Assimilated
n-Butane	HC3		x	x
i-Pentane	HC5		x	x
n-Pentane	HC5		x	x
3-Methylpentane	HC5		x	x
2-Methylpentane	HC5	x	x	x
n-Hexane	HC5	x	x	x
i-Octane	HC5	x	x	x
2,4-Dimethylpentane	HC8	x	x	x
3-Methylhexane	HC8	x	x	x
n-Heptane	HC8	x	x	x
Methylcyclohexane	HC8	x	x	x
n-Octane	HC8	x	x	x
Hexene1	OLT		x	
Benzene	TOL		x	x
Ethylbenzene	TOL	x	x	x
Toluene	TOL	x	x	x
m/p-Xylene	XYL	x	x	x
o-Xylene	XYL	x	x	x
Isoprene	ISO	x	x	
O_3	O3	x	x	x
NO	NO	x	x	x
NO_2	NO2	x	x	x
NO_y	NO3, HNO3, ...	x	x	
PAN	PAN		x	x
CO	CO		x	x

[a] For the definition of the RADM2 groups see *Stockwell et al.* [1990].

Chemical data assimilation of Transport and Chemical Evolution over the Pacific (TRACE-P) aircraft measurements

Tianfeng Chai,[1] Gregory R. Carmichael,[1] Adrian Sandu,[2] Youhua Tang,[1] and Dacian N. Daescu[3]

[1] In this paper, the four-dimensional variational (4D-Var) technique is applied to assimilate aircraft measurements during the Transport and Chemical Evolution over the Pacific (TRACE-P) field experiment into a chemical transport model, Sulfur Transport Eulerian Model, version 2K1 (STEM-2K1). Whether data assimilation would produce better analyzed fields is examined. It is found that assimilating ozone observations from one of two independent flights improves model prediction of the other flight ozone measurements, which are withheld as validation data. The adjusted initial fields after only assimilating the total reactive nitrogen (NO_y) observations lead to better predictions of NO, NO_2, and PAN, based on their agreement with the withheld measurements. One experiment simultaneously assimilating the observations of O_3, NO, NO_2, HNO_3, PAN, and RNO_3 demonstrates that the model is able to match those measurements well by changing the initial fields. In addition, the model predictions of NO_y improve significantly after assimilating the aforementioned multiple observation species, which are independent of the withheld NO_y measurements. In the paper, we also show that the key species whose initial mixing ratios would significantly affect the agreement between model and measurements can be identified using adjoint sensitivity analysis. Such information can be used to reduce the number of control variables in the 4D-Var data assimilation. To speed up the optimization process in the 4D-Var, we enforce the concentration upper bounds through the limited memory–Broyden-Fletcher-Goldfarb-Shanno-B (L-BFGS-B) algorithm, and this proves to be effective.
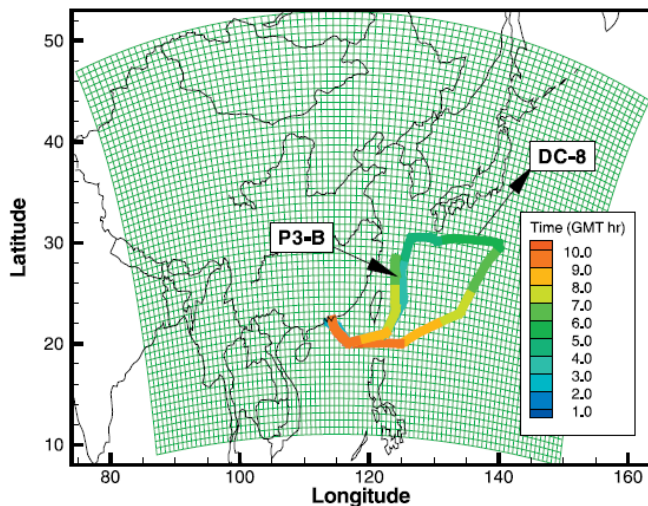
Full 4D-Var using SAPRC99 chemical mechanism [Carter, 2000], 93 chemical constituents, 213 reactions (including 30 photolysis reactions)

Kinetic Preprocessor (KPP) tool [Sandu et al., 2003; Daescu et al., 2003] used to generate both the forward and the adjoint chemistry code within the Sulfur Transport Eulerian Model version 2K1 (STEM-2K1) [Carmichael et al. 2003]

Assimilation of aircraft measurements obtained during the NASA Transport and Chemical Evolution over the Pacific mission (western Pacific, February–April 2001).

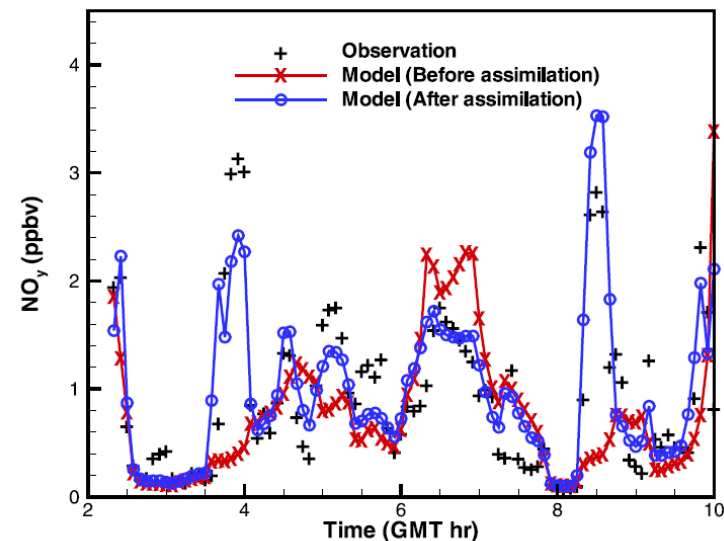Simultaneous assimilation of O3, NO, NO2, HNO3, PAN, and RNO3 significantly improves model predictions of NOy

Figure 17. Model predictions of NO_y before and after assimilating O_3, NO, NO_2, HNO_3, PAN, and RNO_3 measurements. The NO_y measurements were not used in the assimilation test. NO_y observation uncertainty is assigned as 18%.

Satellite remote sensing of Air quality

Table 2

Satellite remote sensing of air quality[a]

Instrument	Platform	Meas. period	Typical nadir res. (km)	Equator crossing time[b]	Global coverage (days)[c]	Spectral range (μm)	NO_2	HCHO	SO_2	CO	O_3	Aerosol optical thickness
GOME	ERS-2	1995–2003	320×40	10:30d	3	0.23–0.79	1	1	1		0.5–1.5	
MOPITT	Terra	2000–	22×22	10:30d	3.5	4.7				0.5–2		
MISR	Terra	2000–	18×18[e]	10:30d	7	4[d] λ 0.45–0.87						1
MODIS	Terra	2000–	10×10[e]	10:30d	2	36[d] λ						1
	Aqua	2002–		1:30a		0.41–14.2						
AIRS	Aqua	2002–	14×14	1:30a	1	3.7–16			1	0.5–1.5		
SCIAMACHY	ENVISAT	2002–	60×30	10:00d	6	0.23–2.3	1	1	1	1	0.5–1.5	
OMI	Aura	2004–	24×13	1:45a	1	0.27–0.50	1	1	1		0.5–1.5	1
TES	Aura	2004–	8×5	1:45a	n/a	3.3–15.4				0.5–1.5	1–2	
PARASOL	PARASOL	2004–	18×16	1:30a	1	9[d] λ, 0.44–1.0						1
CALIOP	CALIPSO	2006–	40×40	1:30a	n/a	0.53, 1.06						>30
GOME-2	MetOp	2006–	80×40	9:30d	1	0.24–0.79	1	1	1		0.5–1.5	
IASI	MetOp	2006–	12×12	9:30d	0.5	3.6–15.5				0.5–1.5	1–2	

[a] The number of independent degrees of freedom in the troposphere is given for each instrument. A value of 1 indicates a tropospheric column.

[b] Crossing time occurs at both AM and PM. Descending orbits are indicated by *d* and ascending orbits by *a*.

[c] Value given for clear-sky conditions. Clouds impede the retrieval.

[d] Number of discrete wavelengths.

[e] Radiances for MISR and MODIS are acquired at between 205 m and 1.1 km, depending on channel. Resolutions reported here are for the standard operational aerosol products.

[From Martin, R. V., Atmospheric Environment, 2008]

Assimilation of satellite Aerosol and Carbon monoxide measurements

August 2006
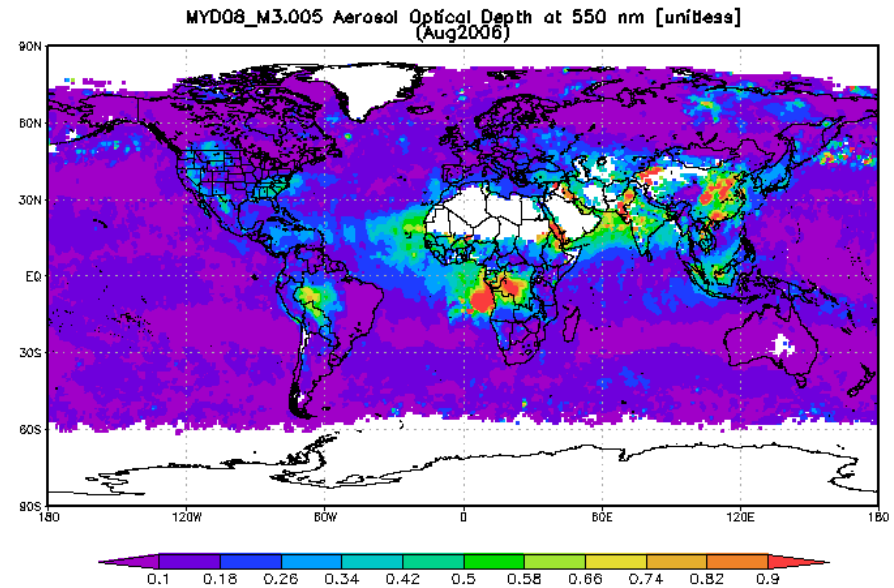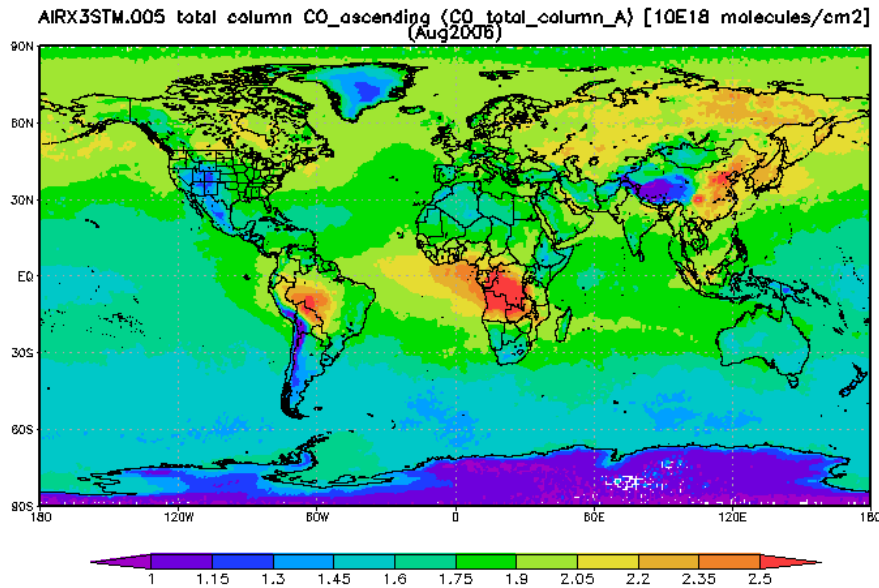
Global distribution of carbon monoxide (CO) From the Atmospheric Infrared Sounder (AIRS)

Global distribution of aerosol optical depth (AOD) from the Moderate Resolution Imaging Spectroradiometer (MODIS)

AIRS, and MODIS maps were produced with the Giovanni online data system [http://disc.sci.gsfc.nasa.gov/giovanni/]

Assimilation of Measurement of Air Pollution from Space (MAPS) CO in a global three-dimensional model

J.-F. Lamarque, B. V. Khattatov, J. C. Gille, and G. P. Brasseur

Atmospheric Chemistry Division, National Center for Atmospheric Research, Boulder, Colorado

Abstract. Observations of carbon monoxide (CO) by the Measurement of Air Pollution from Space (MAPS) instrument onboard the space shuttle were assimilated into a global three-dimensional chemistry-transport model using the Physical-space Statistical Analysis System approach. The assimilation considerably improved the calculated distribution of CO in the troposphere. On the global scale, the adjustment of the CO field resulting from the assimilation procedure was large at the beginning of the assimilation, suggesting discrepancies in the initial conditions of the model. As the model integration/assimilation progressed with time, transport caused the model to drift. This drift limited to a few days the "memory" of CO from its adjustment toward the observations. The assimilation of CO significantly influenced the distribution of other chemical species, even over the limited time periods (~ 10 days) analyzed.

MOZART (Model for Ozone And Related chemical Tracers) [Rasch et al., 1997]

Optimal Interpolation assimilation of Measurement of Air Pollution from Space (MAPS) (space shuttle, April and October of 1994) CO profile accounting for averaging kernel in observation operator.

The background variance was calculated assuming a fixed 30% relative error on the model CO field. Observational error standard deviation is set to a constant 20% relative error.

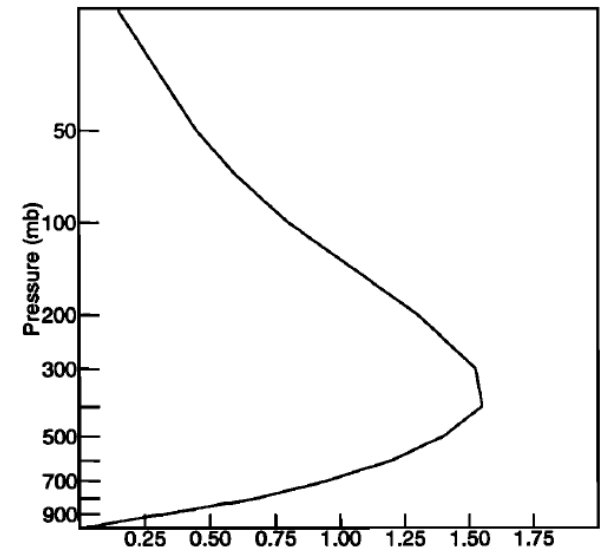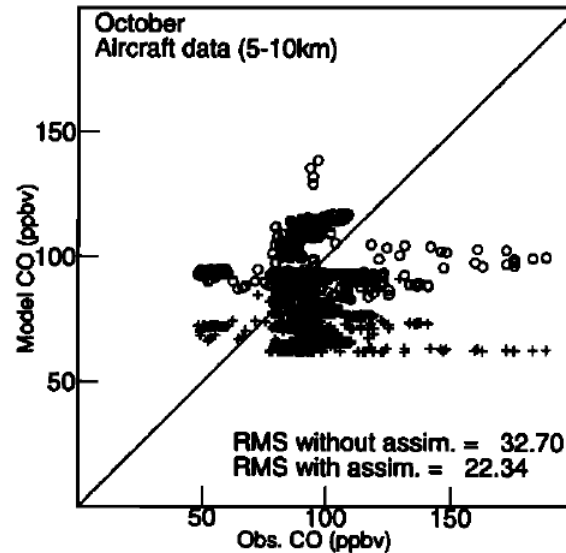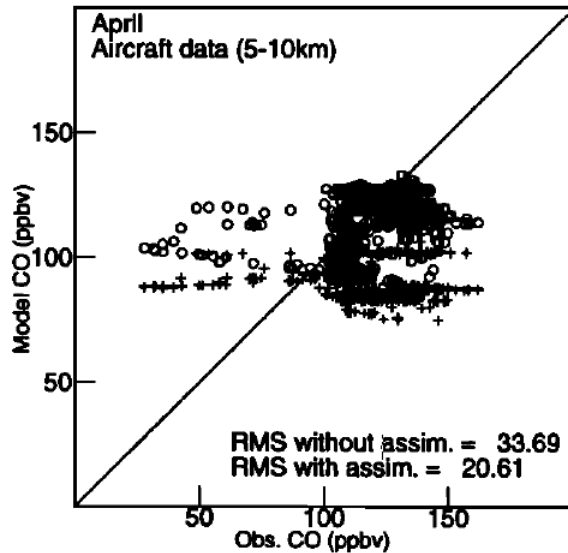Largest improvement (relative to observations) was found in mid troposphere (5-10km).

Figure 1. Averaging kernel for the MAPS CO channel. Adapted from *Reichle et al.* [1999].

Simulating aerosols using a chemical transport model with assimilation of satellite aerosol retrievals: Methodology for INDOEX

William D. Collins, Phillip J. Rasch, Brian E. Eaton, Boris V. Khattatov, and Jean-Francois Lamarque

National Center for Atmospheric Research, Boulder, Colorado

Charles S. Zender

Earth System Science, University of California at Irvine, Irvine, California

Abstract. A system for simulating aerosols has been developed using a chemical transport model together with an assimilation of satellite aerosol retrievals. The methodology and model components are described in this paper, and the modeled distribution of aerosols for the Indian Ocean Experiment (INDOEX) is presented by *Rasch et al.* [this issue]. The system generated aerosol forecasts to guide deployment of ships and aircraft during INDOEX. The system consists of the Model of Atmospheric Transport and Chemistry (MATCH) combined with an assimilation package developed for applications in atmospheric chemistry. MATCH predicts the evolution of sulfate, carbonaceous, and mineral dust aerosols, and it diagnoses the distribution of sea salt aerosols. The model includes a detailed treatment of the sources, chemical transformation, transport, and deposition of the aerosol species. The aerosol forecasts involve a two-stage process. During the assimilation phase the total column aerosol optical depth (AOD) is estimated from the model aerosol fields. The model state is then adjusted to improve the agreement between the simulated AOD and satellite retrievals of AOD. During the subsequent integration phase the aerosol fields are evolved using meteorological fields from an external model. Comparison of the modeled AOD against estimates of the AOD from INDOEX Sun photometer data show that the differences in daily means are -0.03 ± 0.06. Although the initial application is limited to the Indian Ocean, the methodology could be extended to derive global aerosol analyses combining in situ and remotely sensed aerosol observations.

Global Model of Atmospheric Transport and Chemistry (MATCH, version 3.3) [Rasch et al., 1997] aerosol model

Optimal Interpolation (OI) aerosol assimilation procedure [Lorenc, 1986] adapted from [Levelt et al., 1998; Lamarque et al.,1999]

Column-integrated AOD is derived from Advanced Very High Resolution Radiometers (AVHRR) radiances on NOAA 14 [Stowe et al., 1997]

Aerosol Optics

$$\tau_m = g^{-1} \int_0^{P_s} \sum_i \chi_i(p) q_i(p)\, dp. \qquad (2)$$

Here i is an index for aerosol species, χ_i is the optical extinction for each species, q_i is the corresponding aerosol mixing ratio, g is gravitational acceleration, and p_s is the surface pressure.

The optical extinctions can be specified as a product of a prescribed "dry" value and a hygroscopic growth factor that is a function of relative humidity (RH):

$$\chi_i = \chi_i(\text{RH} \ll 1)\, f_i(\text{RH}). \qquad (8)$$

The hygroscopic extinction correction can be significant, e.g., for sulfate aerosols, f_i in visible wavelengths increases from 1.7 to 7.0 as the relative humidity increases from 50 to 90% [*Kiehl et al.*, 2000].

Plate 1. Average aerosol optical depth at $\lambda = 630$ nm for March 1–14, 1999, from the standard integration.
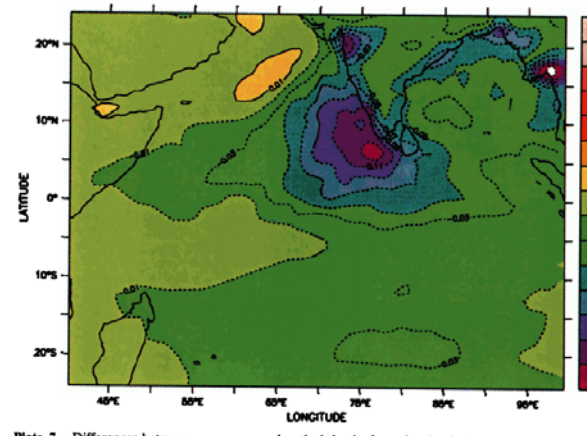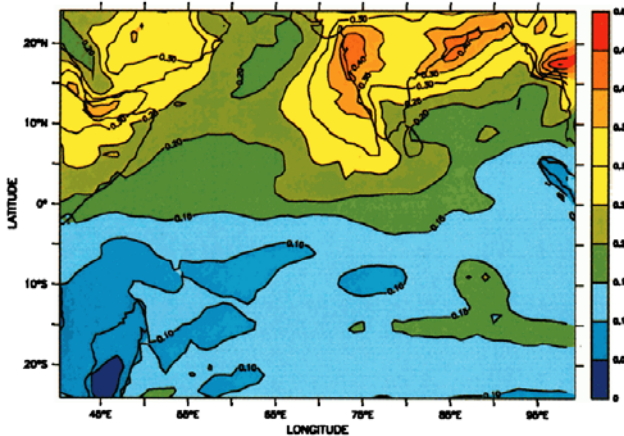
No AVHRR Assim

Plate 7. Differences between average aerosol optical depths from the simulation without assimilation the standard integration. Time period and wavelength are identical to Plate 1.

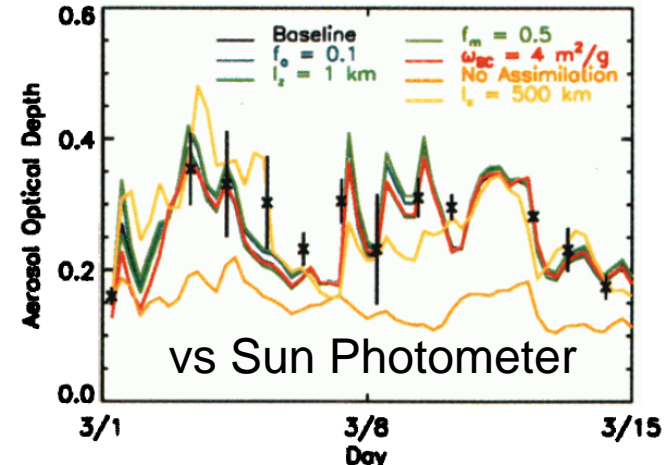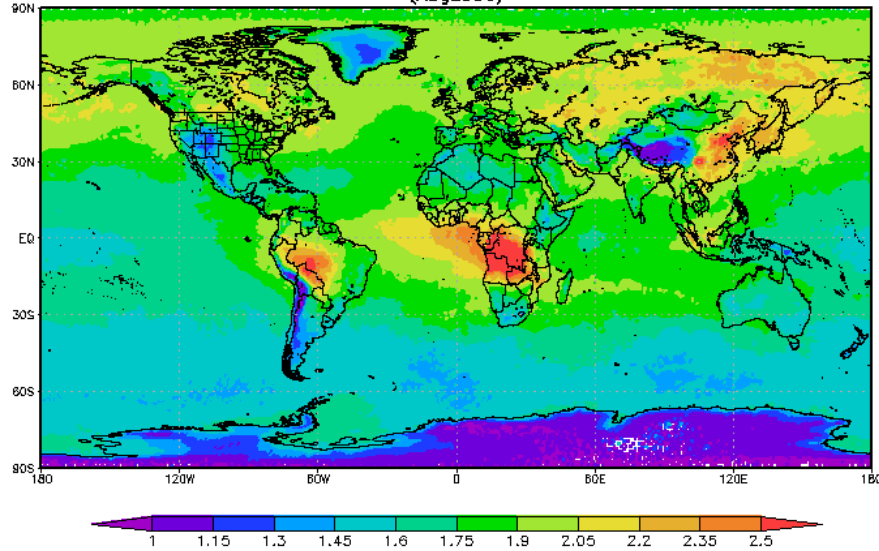With-without Assim

vs Sun Photometer

Plate 6. Comparison of daily-mean AOD from the assimilation system (solid lines) and from a Microtops Sun photometer (crosses) [*Satheesh and Ramanathan*, 2000]. The vertical bars represent the RMS differences between instantaneous measurements and the daily means. Sun photometer measurements of direct solar insolation are for $\lambda = 675$ nm, and the model AODs are estimated at $\lambda = 630$ nm: (a) baseline simulation and (b) sensitivity experiments (section 5) and baseline simulation for March 1–14, 1999.

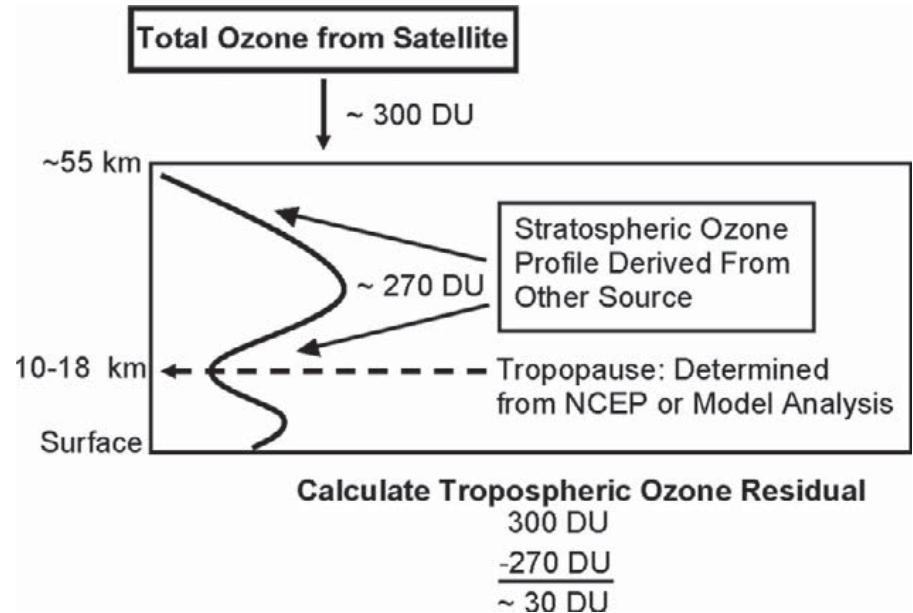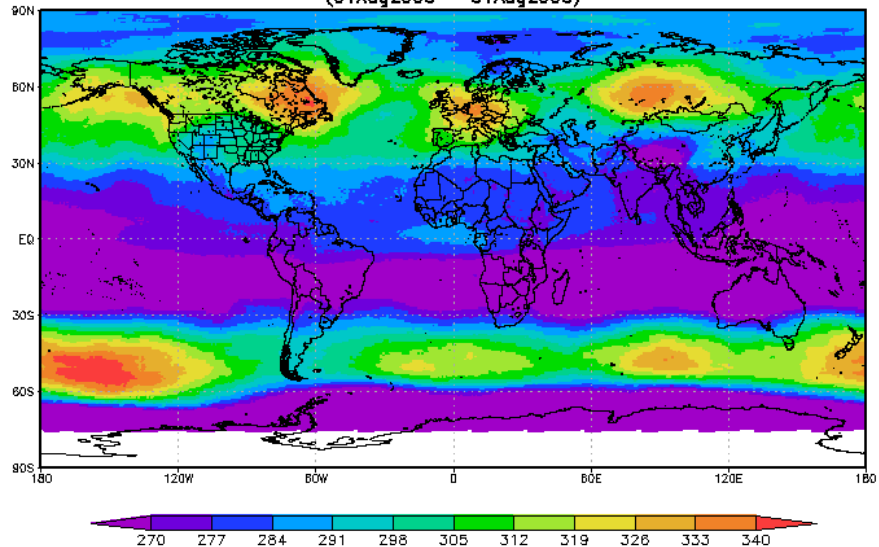# Assimilation of satellite O₃ measurements

AIRX3STM.005 total column CO_ascending (CO_total_column_A) [10E18 molecules/cm2] (Aug2006)

Total Ozone from Satellite

~ 300 DU

~55 km

~ 270 DU — Stratospheric Ozone Profile Derived From Other Source

10-18 km — Tropopause: Determined from NCEP or Model Analysis

Surface

Calculate Tropospheric Ozone Residual

300 DU
−270 DU
~ 30 DU

OMTO3e.003 Column Amount Ozone [DU] (01Aug2006 – 31Aug2006)

Challenge for O3 assimilation is separation of the stratosphere from troposphere to provide constraints on tropospheric analysis

AIRS and OMI maps were produced with the Giovanni online data system [http://disc.sci.gsfc.nasa.gov/giovanni/]

Constraining tropospheric ozone column through data assimilation

J.-F. Lamarque, B. V. Khattatov, and J. C. Gille

Atmospheric Chemistry Division, National Center for Atmospheric Research, Boulder, Colorado, USA

[1] Global distributions of the tropospheric ozone column (TOC) and its error are estimated by assimilating satellite observations of total ozone column and stratospheric ozone profiles in a global chemistry-transport model. A quantitative comparison of the calculated TOC with collocated ozonesondes observations shows good agreement over a wide range of latitudes for the period studied (July–September 1992), even at the daily timescale. In most cases, the difference with the ozonesonde-based TOC is within the calculated error estimate. Comparison with the TOC distribution by *Thompson and Hudson* [1999] does not lead to any quantitative conclusion due to a mix of similarities and differences, even in the geographical distribution of the TOC. A positive TOC bias with respect to ozonesondes is found in this study over Hilo and Irene, probably due to a misrepresentation of the transport of ozone in a region of strong TOC gradients. In September 1992 the LIDAR observations from the TRACE-A campaign are also assimilated. This is shown to provide a constraint on the TOC that significantly propagates across the Atlantic Ocean, indicating the importance of point measurements of ozone for constraining its large-scale distribution. *INDEX TERMS:* 0345 Atmospheric Composition and Structure: Pollution—urban and regional (0305); 0365 Atmospheric Composition and Structure: Troposphere—composition and chemistry; 3337 Meteorology and Atmospheric Dynamics: Numerical modeling and data assimilation; *KEYWORDS:* tropospheric ozone column, data assimilation

Assimilation of Microwave Limb Sounder (MLS) and Total Ozone Mapping Spectrometer (TOMS) total ozone column to estimate tropospheric ozone column (TOC).

MOZART (Model for OZone And Related Tracers) [Brasseur et al., 1998].

Suboptimal Kalman filter (OI) assimilation technique with explicit calculation of the evolution of the model error variance.

Results are compared with the TOC from available ozonesondes.

Table 2. Mean (Left Column) and Standard Deviation (Right Column) of the Difference (in DU) Between the Model Results and the Observations for a Set of Locations and Simulations[a]

	Latitude, °N	Longitude, °E	No Assimilation		Full Assimilation		TOMS Only		MLS v4		NCEP		T42	
Ascension	−8	346	12.7	8.2	1.5	6.9	4.6	7.2	6.2	7.3	8.8	6.7	−4.0	7.0
Brazzaville	−4	15	6.7	9.3	−3.1	8.0	0.4	8.2	1.6	7.2	−1.9	11.5	−7.8	8.5
Hilo	20	205	28.7	17.6	16.7	8.9	20.4	12.7	23.8	10.9	14.8	6.2	10.2	3.4
Irene	−25	28	27.2	9.3	12.3	3.3	15.1	4.4	18.1	4.0	14.7	8.4	3.7	3.8
Payerne	48	7	1.3	12.3|	−5.4	9.3	−5.8	10.0	−3.3	9.9	10.4	14.4	−14	9.3
Hohenp.	48	11	23.2	13.3	14.7	7.4	14.4	8.4	17.0	8.5	33.3	14.9	2.9	3.6
Tateno	36	140	23.8	11.0	14.0	8.3	18.0	8.9	18.7	8.9	18.3	11.5	13.9	9.8
Edmonton	54	246	8.5	9.2	5.4	8.0	3.8	8.0	6.0	8.0	17.3	12.9	0.2	6.1
Resolute	75	265	8.3	9.0	7.9	5.7	3.5	5.9	7.1	5.8	28.3	12.5	4.8	5.2
Syowa	−69	40	4.0	8.6	−4.8	9.7	−7.1	11.2	−2.1	8.4	4.13	8.2	−12	8.5

[a] See text for more details.
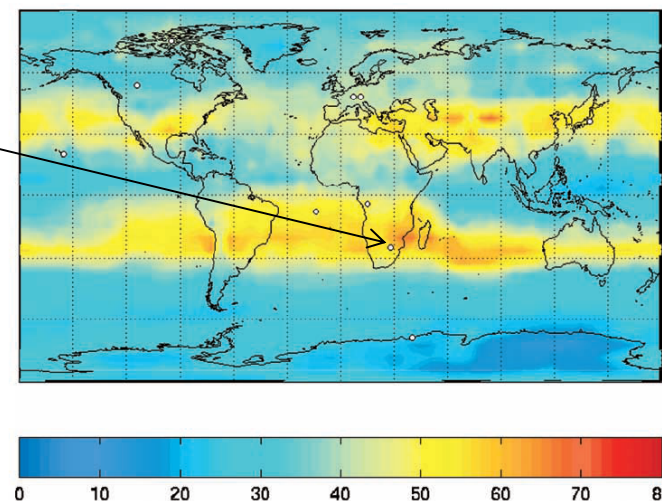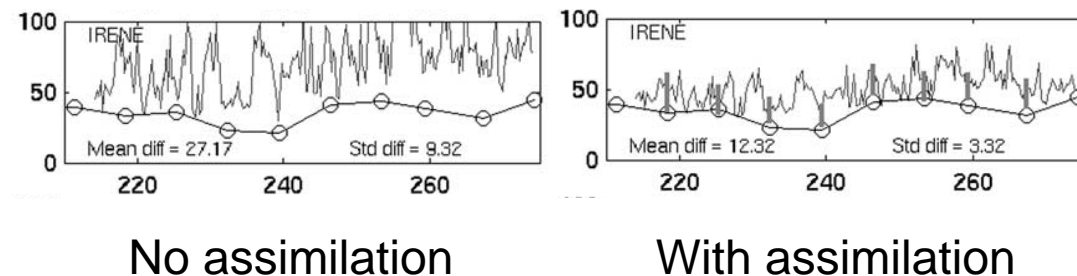

No assimilation

With assimilation

Figure 5. Global distribution of the TOC (in Dobson Units) from the full assimilation run for September 1992. The location of the 10 ozonesondes used in the analysis in section 3.1 are identified by the white circles.

Click Here for Full Article

Chemical data assimilation estimates of continental U.S. ozone and nitrogen budgets during the Intercontinental Chemical Transport Experiment–North America

Robert B. Pierce,[1] Todd Schaack,[2] Jassim A. Al-Saadi,[1] T. Duncan Fairlie,[1] Chieko Kittaka,[1] Gretchen Lingenfelser,[1] Murali Natarajan,[1] Jennifer Olson,[1] Amber Soja,[1] Tom Zapotocny,[2] Allen Lenzen,[2] James Stobie,[3] Donald Johnson,[2] Melody A. Avery,[1] Glen W. Sachse,[1] Anne Thompson,[4] Ron Cohen,[5] Jack E. Dibb,[6] Jim Crawford,[1] Didier Rault,[1] Randall Martin,[7] Jim Szykman,[8,9] and Jack Fishman[1]

[1] Global ozone analyses, based on assimilation of stratospheric profile and ozone column measurements, and NOy predictions from the Real-time Air Quality Modeling System (RAQMS) are used to estimate the ozone and NOy budget over the continental United States during the July–August 2004 Intercontinental Chemical Transport Experiment–North America (INTEX-A). Comparison with aircraft, satellite, surface, and ozonesonde measurements collected during INTEX-A show that RAQMS captures the main features of the global and continental U.S. distribution of tropospheric ozone, carbon monoxide, and NOy with reasonable fidelity. Assimilation of stratospheric profile and column ozone measurements is shown to have a positive impact on the RAQMS upper tropospheric/lower stratosphere ozone analyses, particularly during the period when SAGE III limb scattering measurements were available. Eulerian ozone and NOy budgets during INTEX-A show that the majority of the continental U.S. export occurs in the upper troposphere/lower stratosphere poleward of the tropopause break, a consequence of convergence of tropospheric and stratospheric air in this region. Continental U.S. photochemically produced ozone was found to be a minor component of the total ozone export, which was dominated by stratospheric ozone during INTEX-A. The unusually low photochemical ozone export is attributed to anomalously cold surface temperatures during the latter half of the INTEX-A mission, which resulted in net ozone loss during the first 2 weeks of August. Eulerian NOy budgets are shown to be very consistent with previously published estimates. The NOy export efficiency was estimated to be 24%, with NOx + PAN accounting for 54% of the total NOy export during INTEX-A.

Real-time Air Quality Modeling System (RAQMS) [Pierce et al., 2003] used to estimate the ozone and NOy budget over the continental United States.

Statistical digital filter (SDF) Optimal Interpolation (OI) analysis system [Stobie, 1985, 2000] univariate assimilation of stratospheric profile (HALOE, SAGE II, SAGE III) and total column (TOMS V8) ozone observations.

Assimilation of satellite-based profile and column ozone measurements have a positive impact on upper troposphere/lower stratosphere, particularly during the period when higher density SAGE III limb scattering measurements

Demonstration of impact of SAGE III stratospheric limb scattering measurements plus total column ozone on tropospheric ozone (precursor to OMPS on NPOESS)
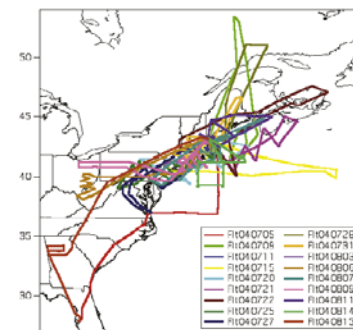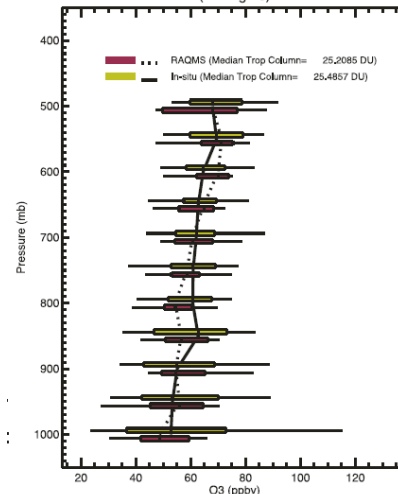
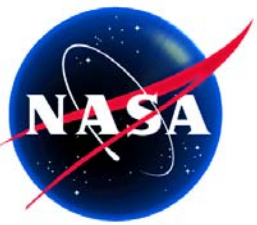## NASA DC8 Flights
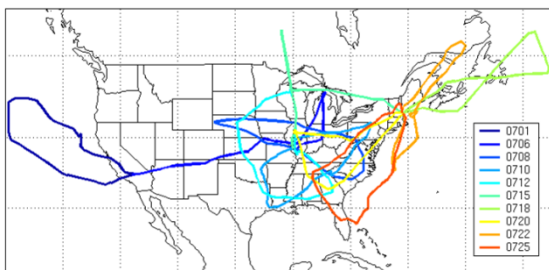
RAQMS_G/DC8 Insitu O3 (Avery)
(All Flights)
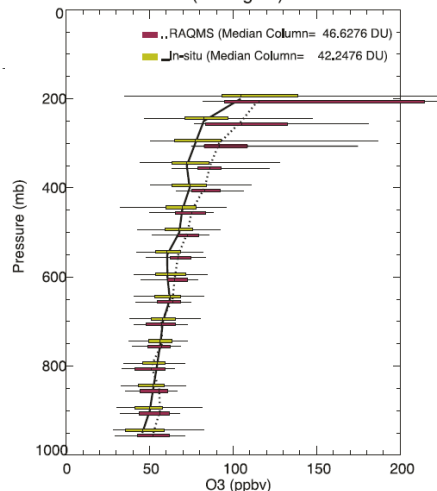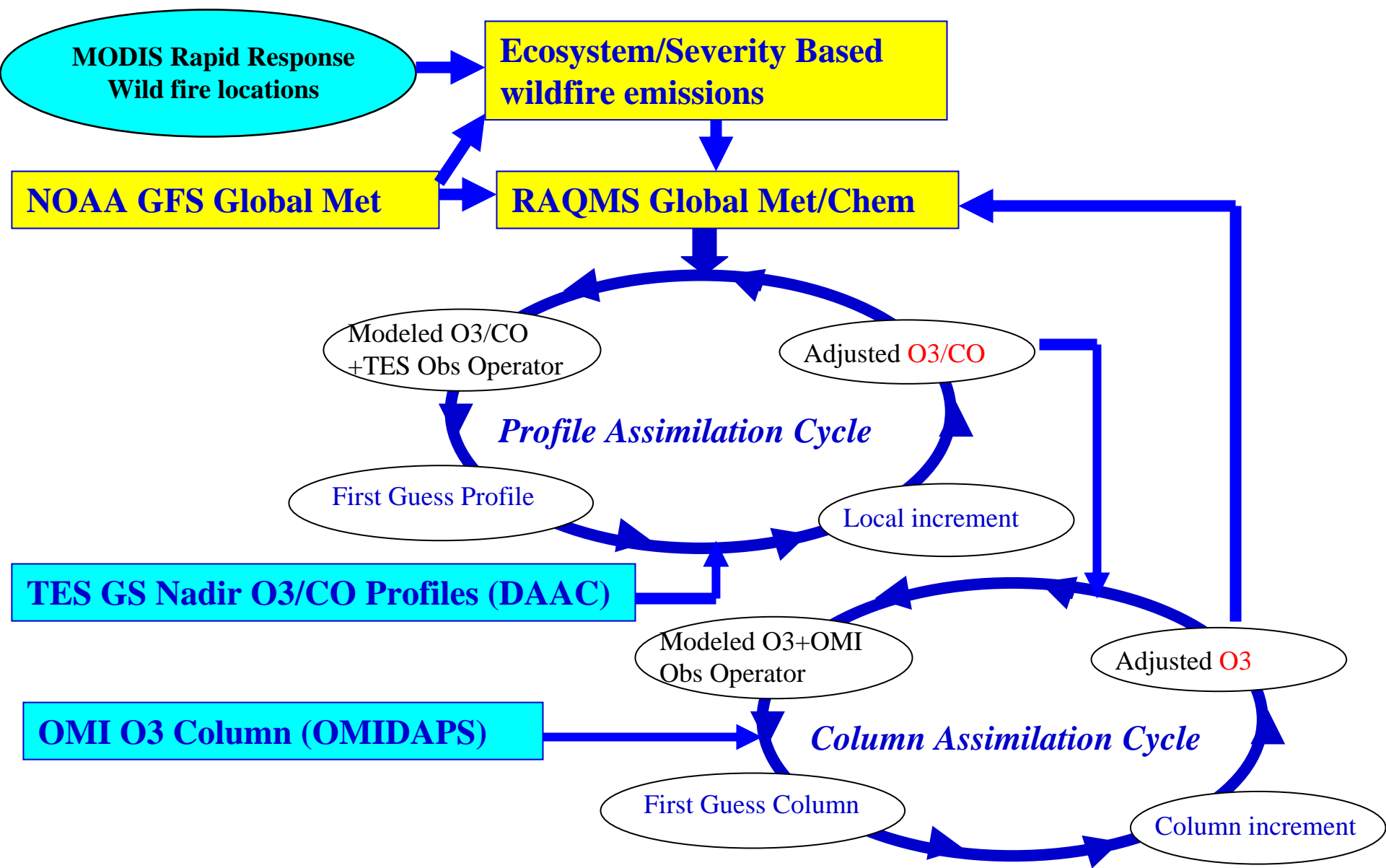
NOAA P3 Flights

RAQMS_G/P3 Insitu O3 (Ryerson)
(All Flights)

Model Description

1. **Online global chemical and aerosol assimilation/ forecasting system**

2. **UW-Madison sigma-theta hybrid coordinate model (UW-Hybrid) dynamical core**

3. **Unified stratosphere/troposphere chemical prediction scheme (LaRC-Combo) developed at NASA LaRC**

4. **Aerosol prediction scheme (GOCART) developed by Mian Chin (NASA GSFC).**

5. **Statistical Digital Filter (OI) assimilation system developed by James Stobie (NASA/GFSC)**
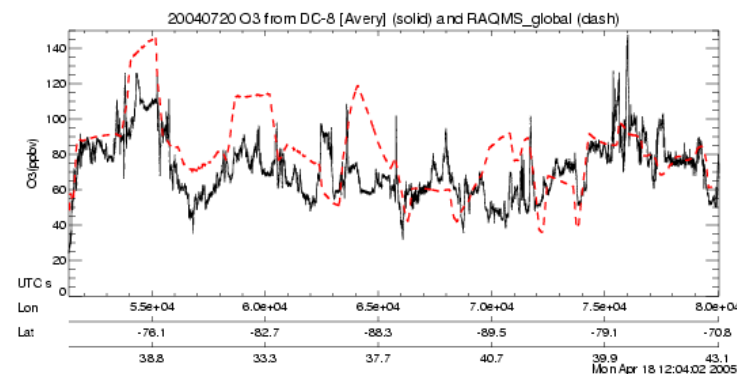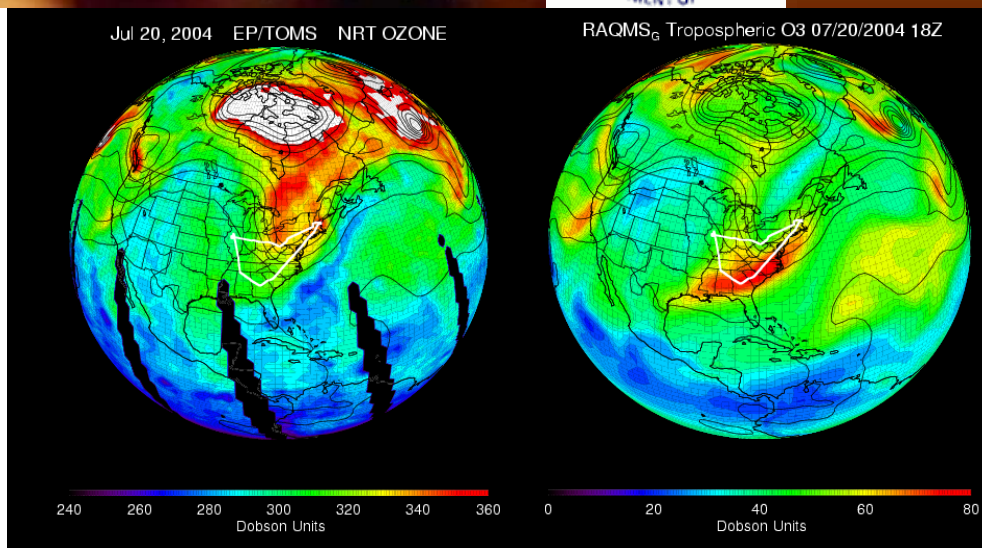
RAQMS has been used to support airborne field missions [Pierce et al, 2003, 2007, 2008], develop capabilities for assimilating satellite trace gas and aerosol retrievals [Pierce et al., 2007, 2008, Fishman et al., 2008, Sunita et al., 2008] and assess the impact of global chemical analyses on regional air quality predictions [Song et al., 2008, Tang et al., 2008]

RAQMS 2006 OMI/TES O3/CO Assimilation Procedure

MODIS Rapid Response Wild fire locations

Ecosystem/Severity Based wildfire emissions

NOAA GFS Global Met

RAQMS Global Met/Chem

Modeled O3/CO +TES Obs Operator

Adjusted O3/CO

Profile Assimilation Cycle

First Guess Profile

Local increment

TES GS Nadir O3/CO Profiles (DAAC)

Modeled O3+OMI Obs Operator

Adjusted O3

OMI O3 Column (OMIDAPS)

Column Assimilation Cycle

First Guess Column

Column increment

Pierce, R. B., et al. (2009), Impacts of background ozone production on Houston and Dallas, Texas, air quality during the Second Texas Air Quality Study field mission, J. Geophys. Res., 114, D00F09, doi:10.1029/2008JD011337.

Accounting for averaging kernel and apriori
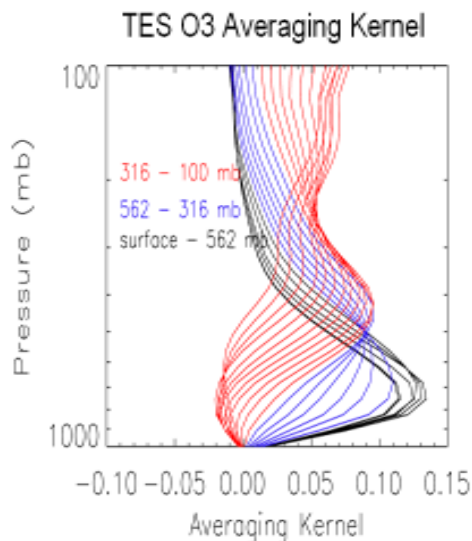
$$X_r = X_a + A_{xx}(X_t - X_a)$$

where:
X_r = retrieval
X_a = apriori
X_t = truth

and:
$A_{xx} = dX_r/dX_t$

A_{xx} **is the averaging kernel which determines the sensitivity of the retrieval to the true state of the atmosphere. The vertical resolution is defined as the full-width-half-maximum of the rows of the averaging kernel.**
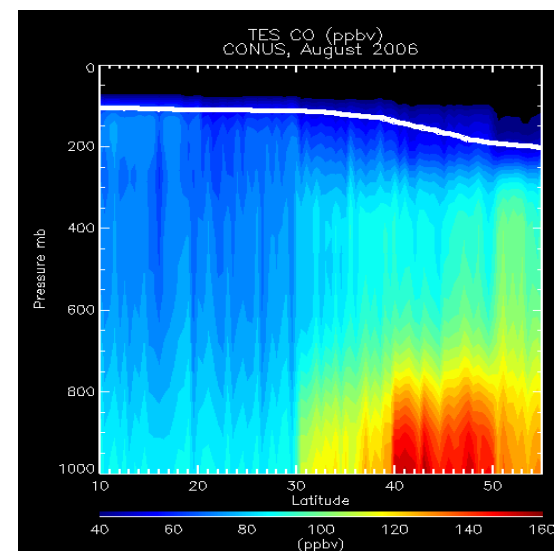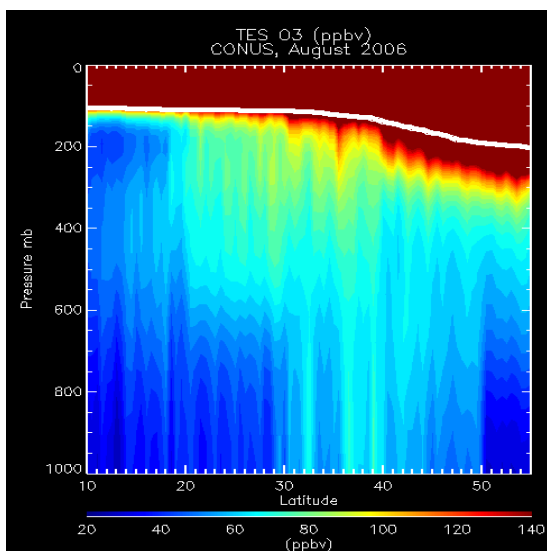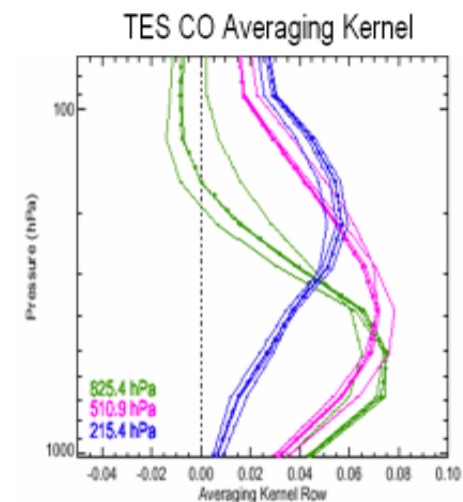
August 2006 Tropospheric Emission Spectrometer (TES) O3 and CO retrievals

Comparison of RAQMS OMI+TES reanalysis with IONS ozonesondes
(373 sondes, August, 2006)

PI: ANNE M. THOMPSON Penn State

RAQMS OMI+TES Tropospheric Ozone Column (August 01-31, 2006)

RAQMS TES/OMI Data denial Studies

Bias (%)	No Assimilation	TES Assimilation	TES+OMI Assimilation
Column	- 8.47	- 3.46	+ 0.30
Stratospheric	-12.87	- 12.17	+ 0.06
Middle Stratosphere	-17.63	- 17.60	- 5.18
Lower Stratosphere	- 4.31	- 2.40	+ 9.51
Tropospheric	- 5.05	+ 3.32	+ 0.49
Upper Troposphere	- 3.65	+ 2.21	- 11.31
Lower Troposphere	- 6.44	+ 4.42	+ 12.29

Pierce, R. B., et al. (2009), Impacts of background ozone production on Houston and Dallas, Texas, air quality during the Second Texas Air Quality Study field mission, J. Geophys. Res., 114, D00F09, doi:10.1029/2008JD011337.

RAQMS 2006 Data Denial Study

Time period: August 2006
Initial Conditions: July 15th, 2006
(Baseline RAQMS OMI+TES ozone analysis)
Validation: 2006 IONS ozonesonde network (373 sondes)

Procedure:
Compare RAQMS analyses with ozonesonde
1) No Assimilation
2) OMI (Cloud Cleared) only
3) TES (O3&CO)
4) MLS+TES CO

August 2006 NO ASSIM Zonal mean CO/O3
(July 15, 2006 OMI+TES IC)

Zonal Mean RAQMS_noassim August 2006 co

Zonal Mean RAQMS_noassim August 2006 o3
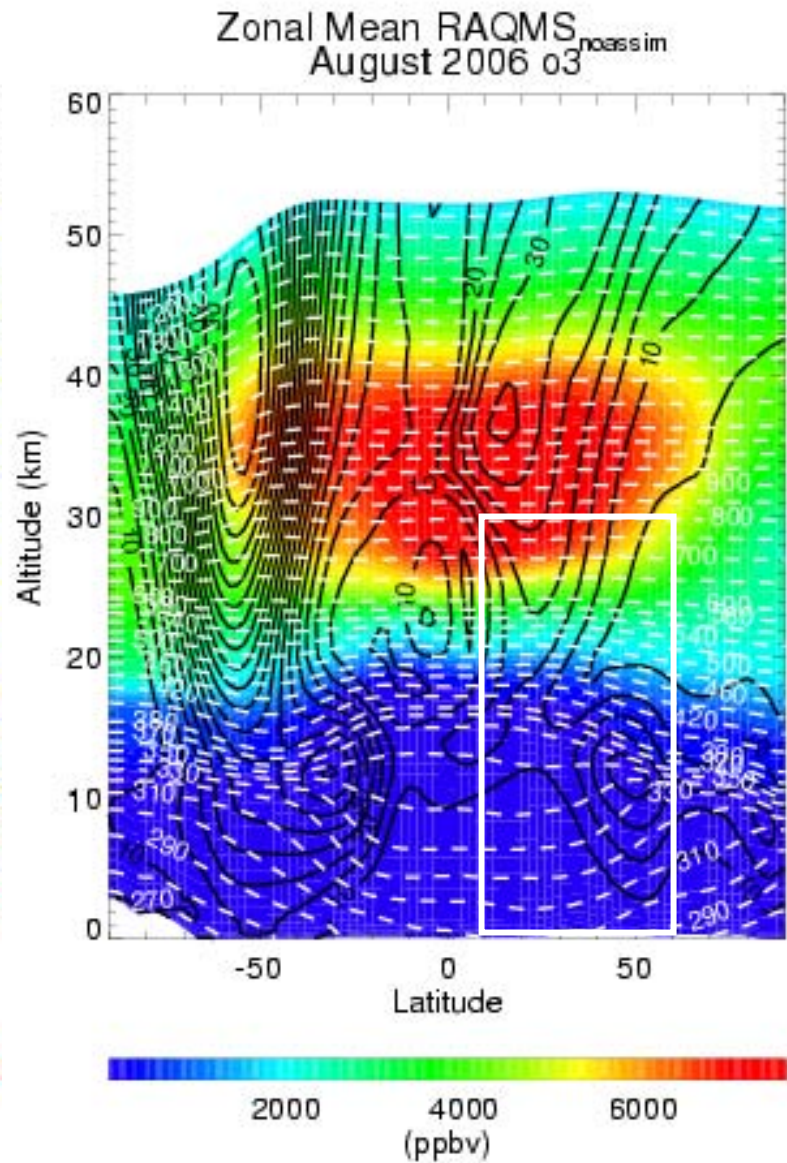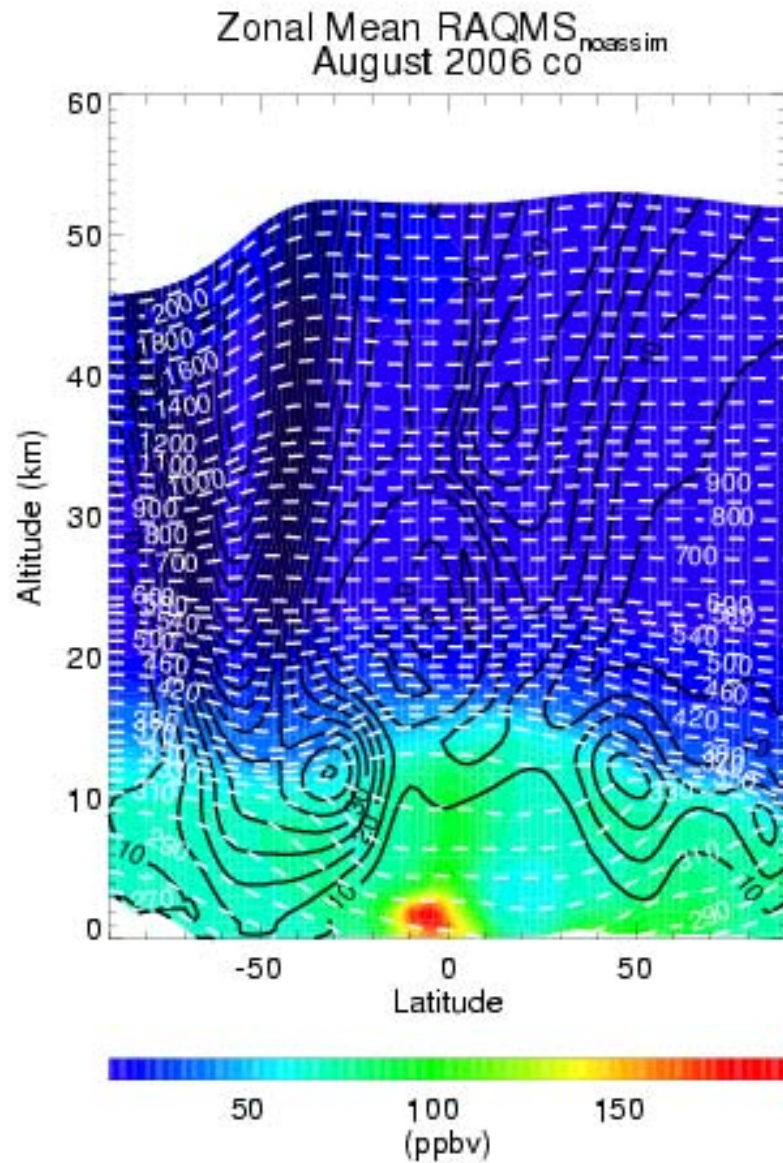
August 2006 <u>OMI Assim-NO ASSIM</u> Zonal mean Delta CO/O3
(July 15, 2006 OMI+TES IC)

Zonal Mean delta_co
RAQMS$_{OMIassim}$-RAQMS$_{noassim}$ August 2006

Small (~2%) change in CO

Zonal Mean delta_o3
RAQMS$_{OMIassim}$-RAQMS$_{noassim}$ August 2006
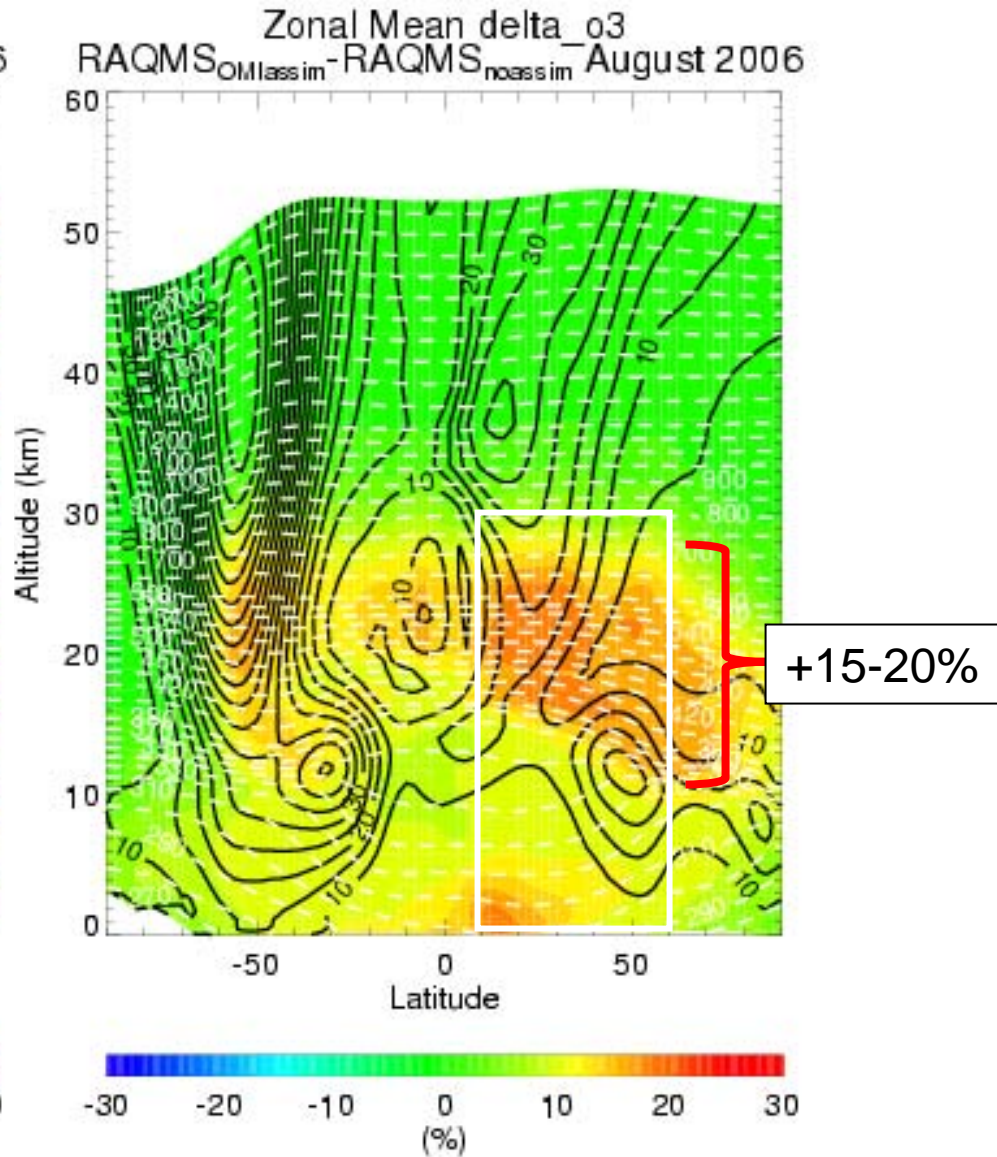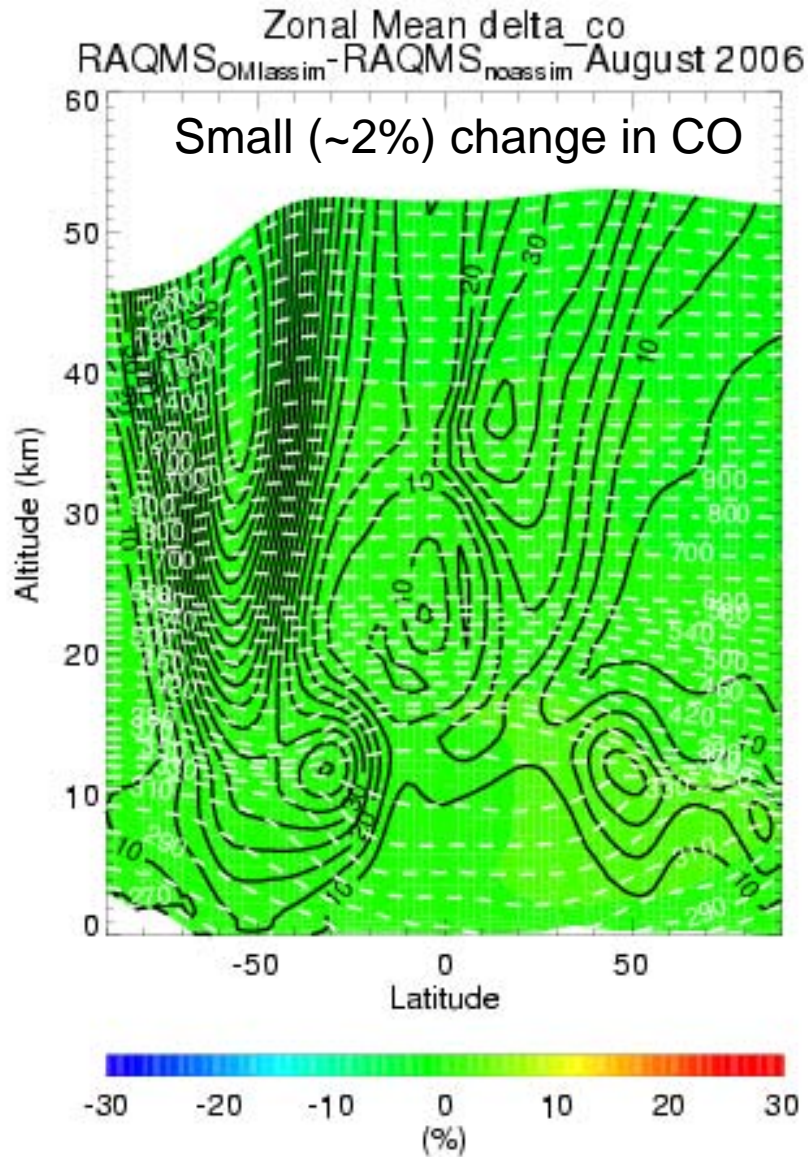
+15-20%

August 2006 TES Assim-NO ASSIM Zonal mean Delta CO/O3 (July 15, 2006 OMI+TES IC)

Zonal Mean delta_co
RAQMS$_{TESsassim}$-RAQMS$_{noassim}$ August 2006

(+/-) 15-20% change in (NH/SH)

Zonal Mean delta_o3
RAQMS$_{TESsassim}$-RAQMS$_{noassim}$ August 2006

+15-20%
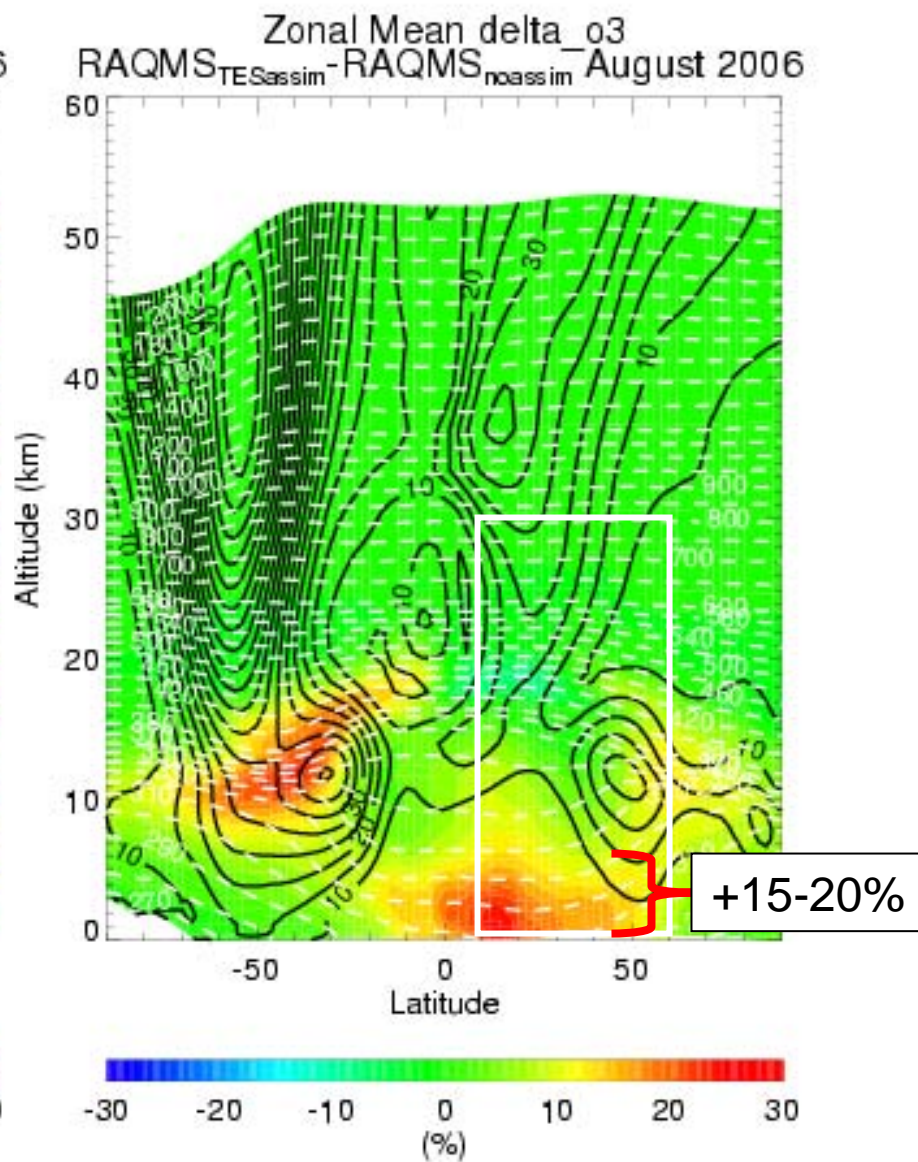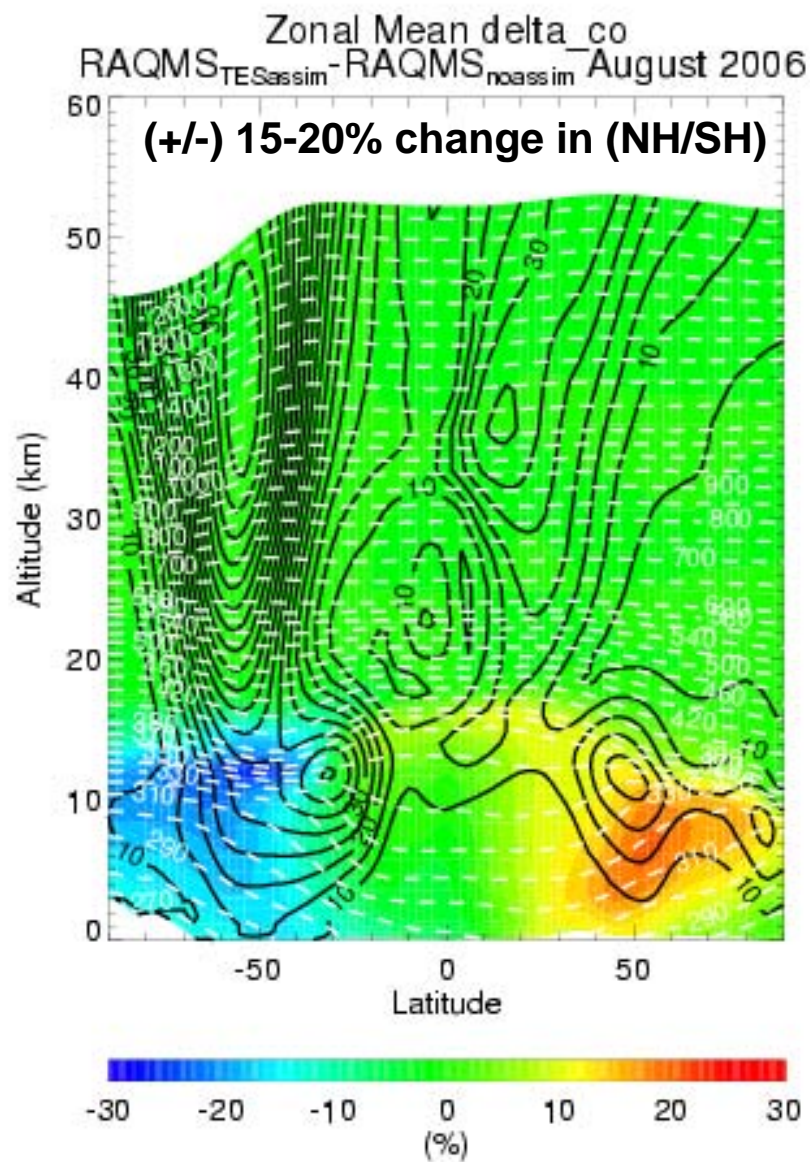
Multi-sensor impact study:

MLS (above 100mb)
TES CO
MODIS AM/PM AOD ← **Addition of Aerosol Assimilation**

Improved Baseline:

Corrected error in dz calculation (impacts emissions)
Improved tropical biomass burning estimates
Aerosol influence on photoysis calculations (GOCART aerosols)

August 2006 TESCO/MLS/MODIS-NO ASSIM Zonal mean Delta CO/O3 (July 15, 2006 OMI+TES IC)

Left panel: Zonal Mean delta_co — $\text{RAQMS}_{TES(CO)/MLS/MODIS\,assim} - \text{RAQMS}_{noassim}$ August

(-) 20% change in (SH)
(+) 15-20% change in (NH)

Right panel: Zonal Mean delta_o3 — $\text{RAQMS}_{TES(CO)/MLS/MODIS\,assim} - \text{RAQMS}_{noassim}$ August 2006

+10-30%
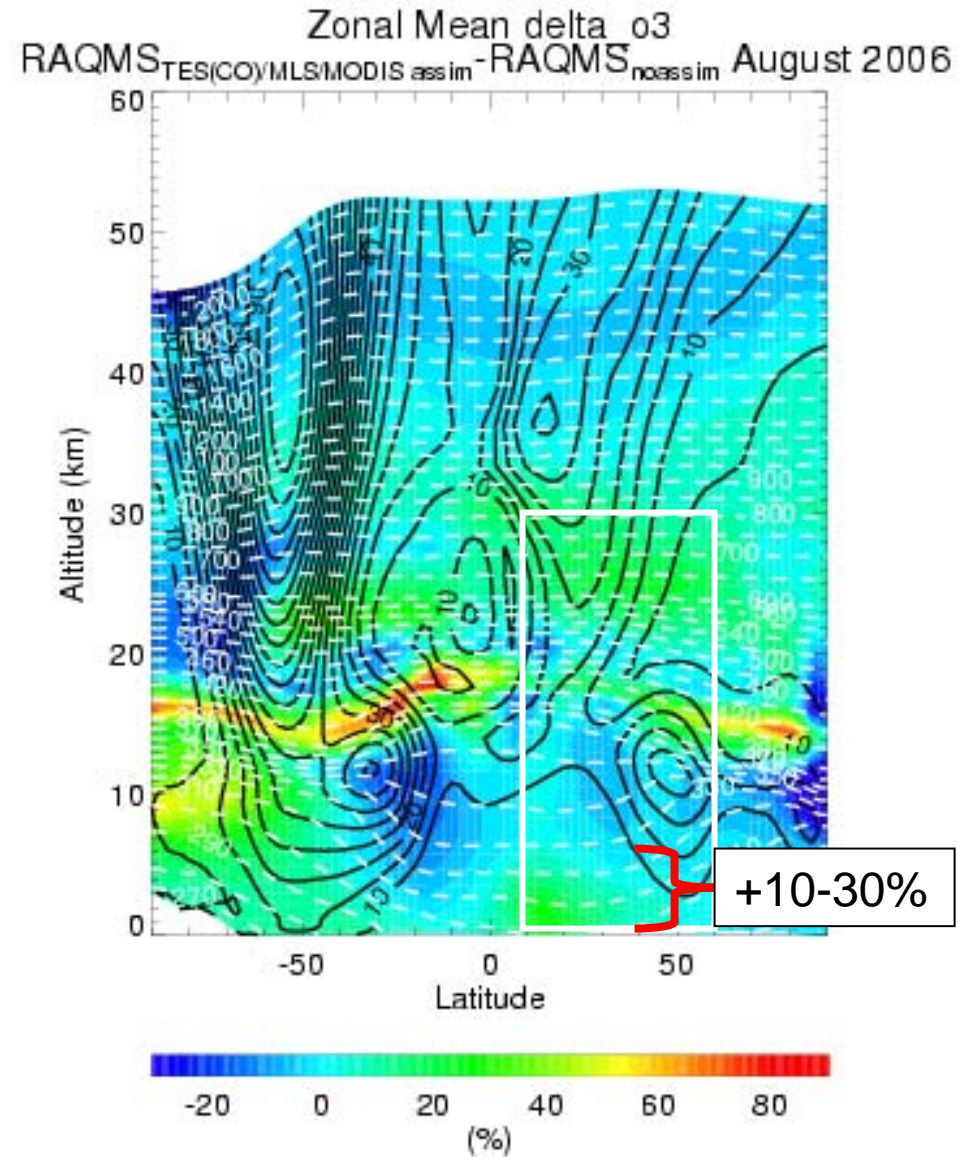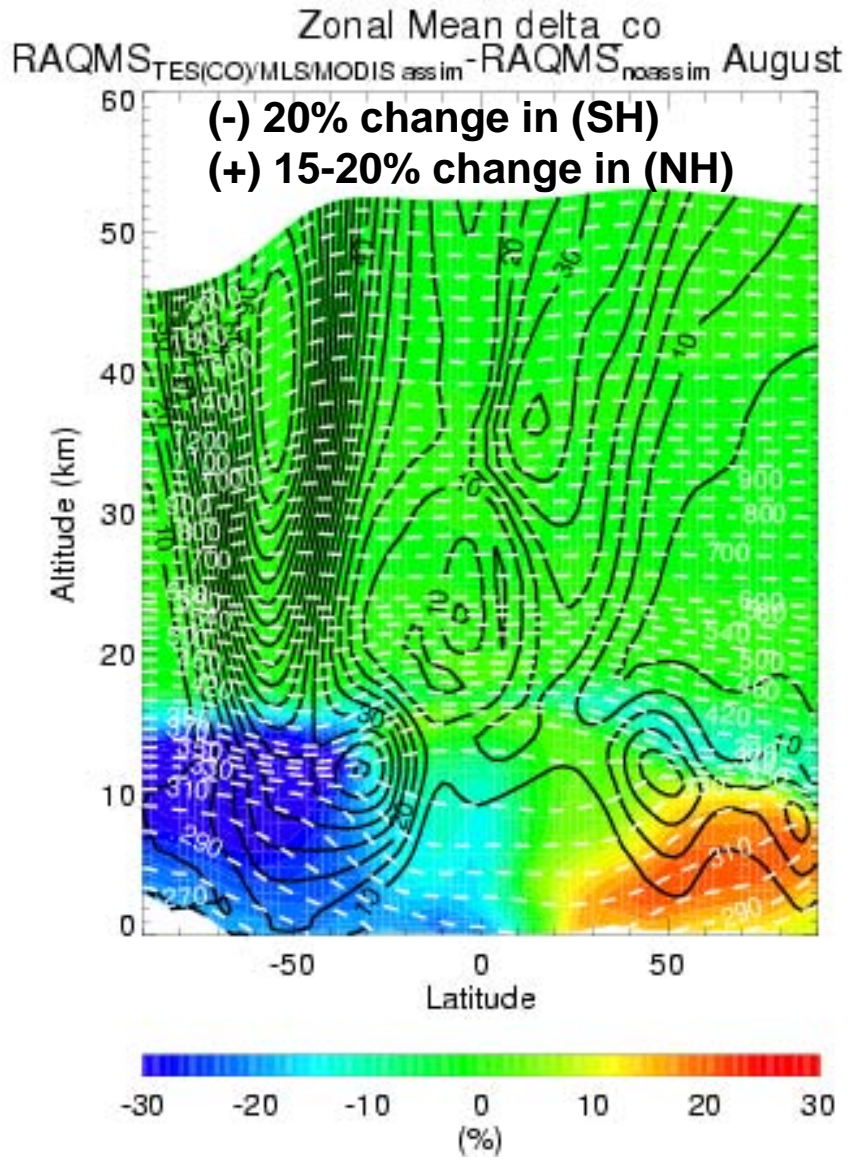
August 2006 TES (CO)/MLS/MODIS ASSIM vs IONS
(July 15, 2006 OMI+TES IC)
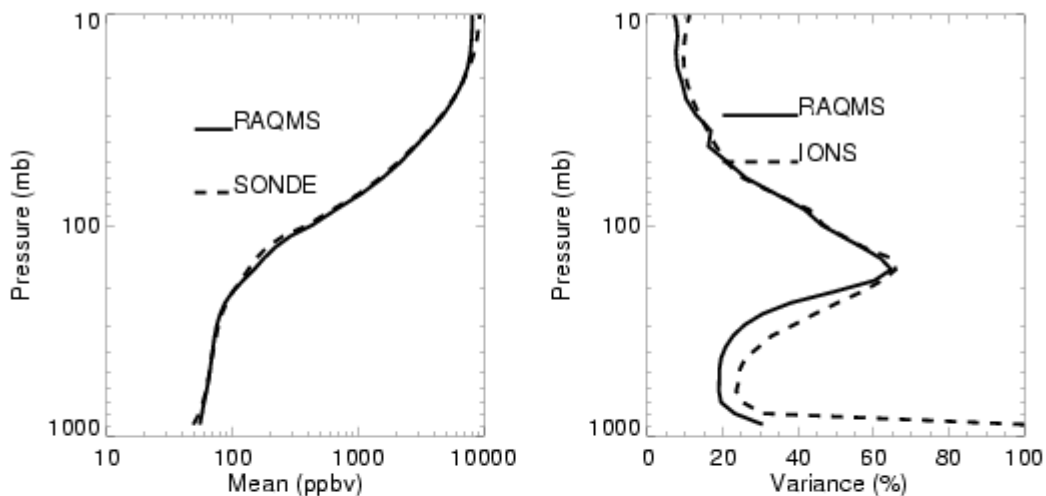
RAQMS/Sonde TES CO/MLS O3/MODIS AOS assim O3 (IONS06, August 01-31, 2006 (373 sondes)

Improved Variance
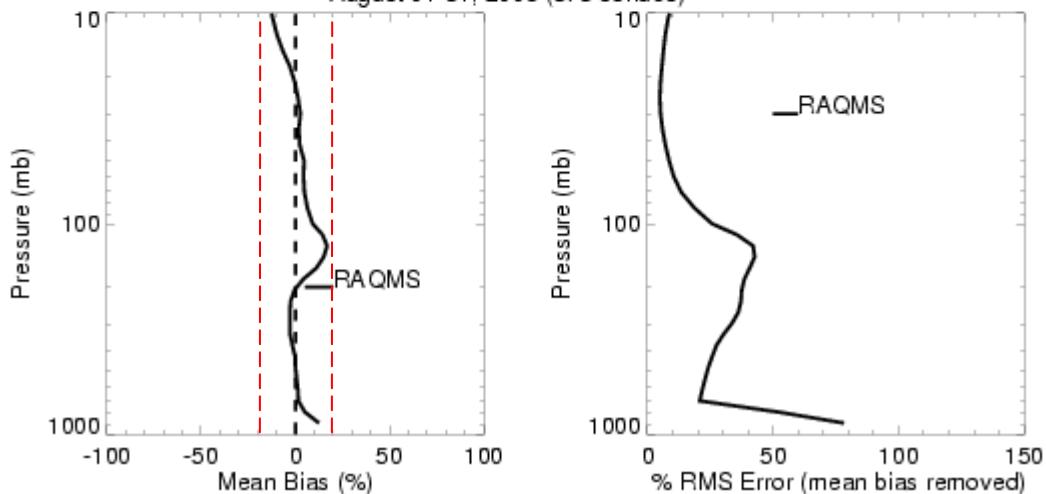
Tropospheric biases: <10%
Stratospheric biases: <10%
Tropopause biases: +20%

MODIS Rapid Response Wild fire locations

Ecosystem/Severity Based wildfire emissions

NOAA GFS Global Met

RAQMS Global Met/Aerosol

Column Assimilation Cycle

Modeled aerosol mass

Adjusted aerosol mass

Forward model

Inverse model

First Guess AOD

AOD increment

MODIS AM/PM AOD

Forward model:
Compute layer/species extinction based on tabulated extinction efficiency and hydroscopic growth factors

Inverse model:
Distribute total AOD increment across aerosol dry mass based on layer/species extinction accounting for extinction due to hydroscopic growth

•*Applied to SO4, Dust, BC, OC (not Sea Salt)*

Forward model:

$$AOD = \sum_k \sum_i q_{ik} \beta_{ik} dz, \quad q_{ik}\beta_{ik} = \textbf{ext}_{ik}$$

where q_{ik} is the mass mixing ratio and β_{ik} is the mass specific extinction of aerosol species i at the vertical level k. dz is the thickness of the layer. The mass specific extinction is a function of the local relative humidity.

Inverse model:

1) Obtain new extinction for each species

$$\textbf{ext\_new}_{ik}=\textbf{ext\_1stguess}_{ik}+\textbf{aodinc}_i*\textbf{ext\_1stguess}_{ik}/\textbf{aod1stguess}_i$$

2) Obtain new total (water+aerosol) mass for each species based on mass extinction coefficient

$$\textbf{totalmass\_new}=\textbf{ext\_new}_{ik}/\textbf{mass\_ext}_{ik}$$

3) extract new dry mass of aerosol based on mole fraction of aerosol in mixture

$$\textbf{aeromass\_new} = \frac{\textbf{totalmass\_new}*\textbf{mole\_frac\_aero}*\textbf{mw}_{\textbf{aero}}}{(\textbf{mw}_{\textbf{h2o}}*\textbf{mole\_frac\_h2o}+\textbf{mw}_{\textbf{aero}}*\textbf{mole\_frac\_aero})}$$

where **mole_frac_h2o=vmr_h2o/(vmr_aero+vmr_h2o)**
and   **mole_frac_aero=vmr_aero/(vmr_aero_vmr_h2o)**

Aeronet Sun photometer validation August 2006

August 2006 550nm AOD Bias (Aeronet-RAQMS)
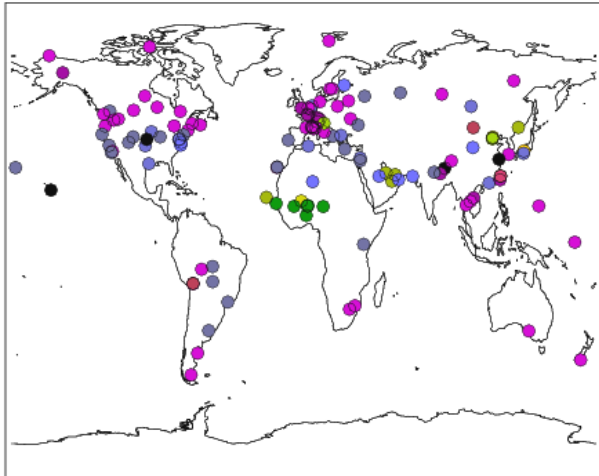
RAQMS AOD (ASSIM)
August 01–31, 2006
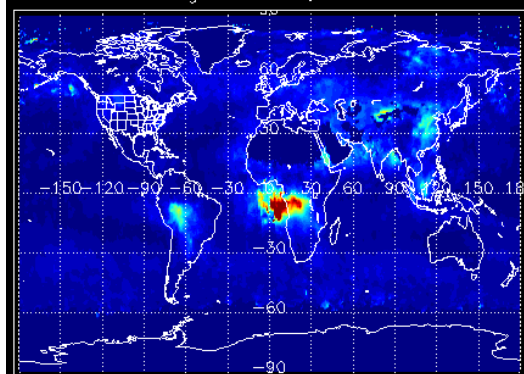
August 2006 550nm AOD RAQMS/Aeronet Correlation

Bias
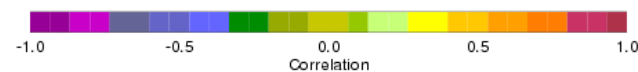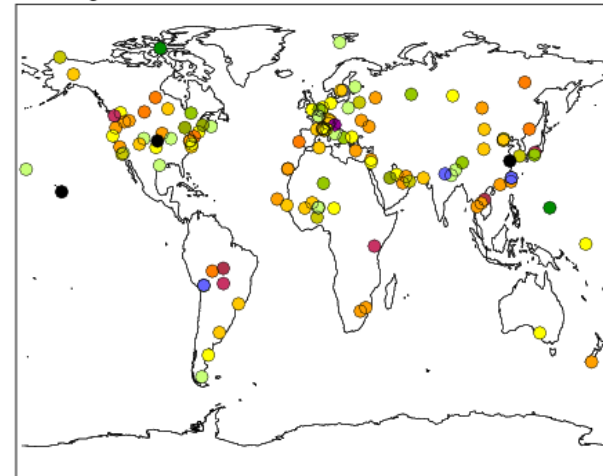
August 2006 RAQMS vs Aeronet 550nm AOD
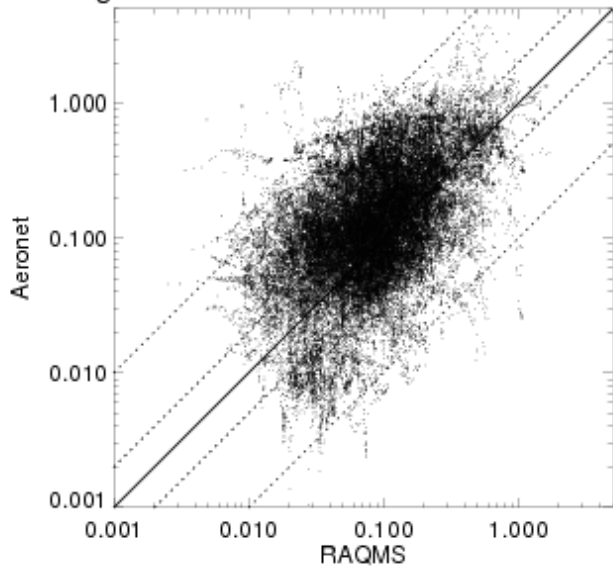
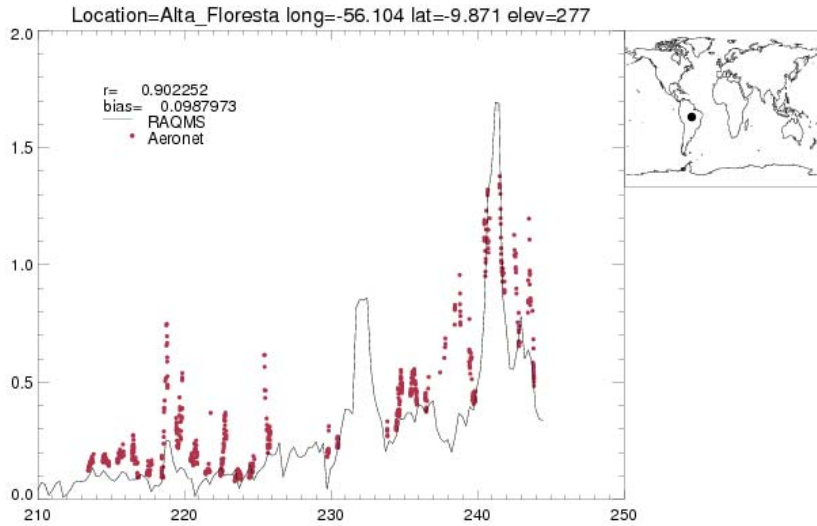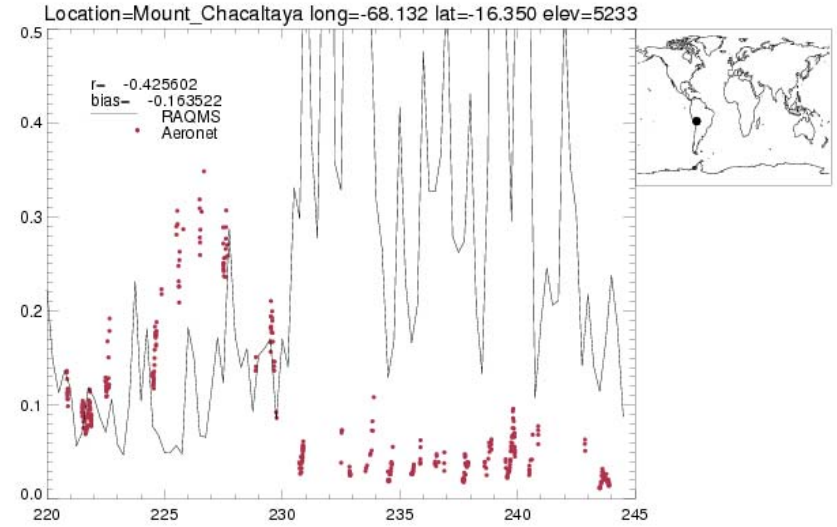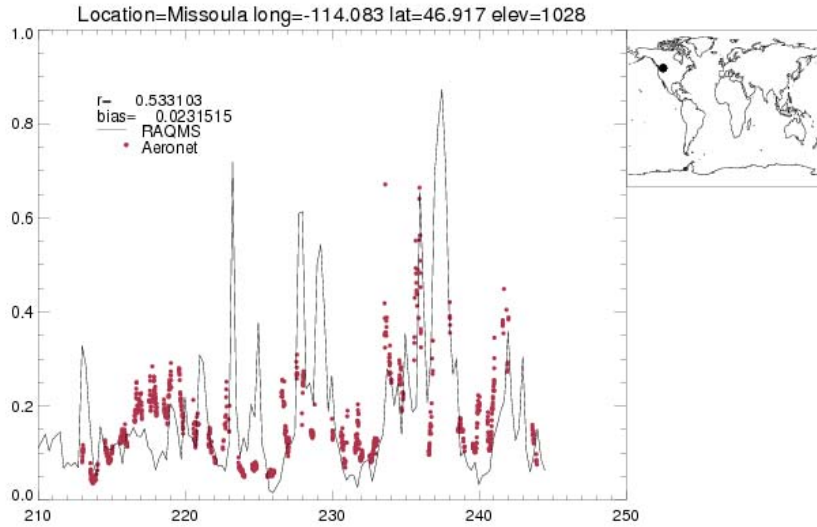MODIS AOD August 01–31, 2006

Correlation
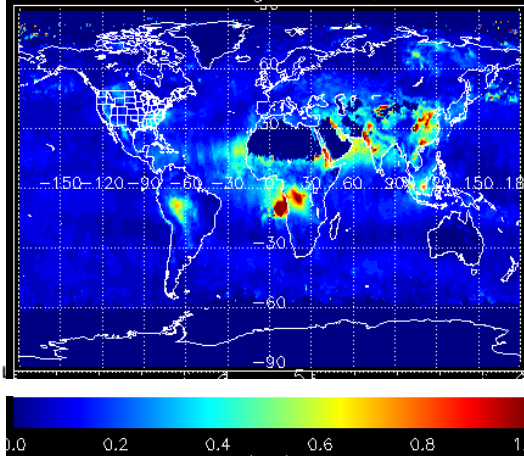
August 2006 550nm AOD Histogram
Aeronet (Red) RAQMS (Black)
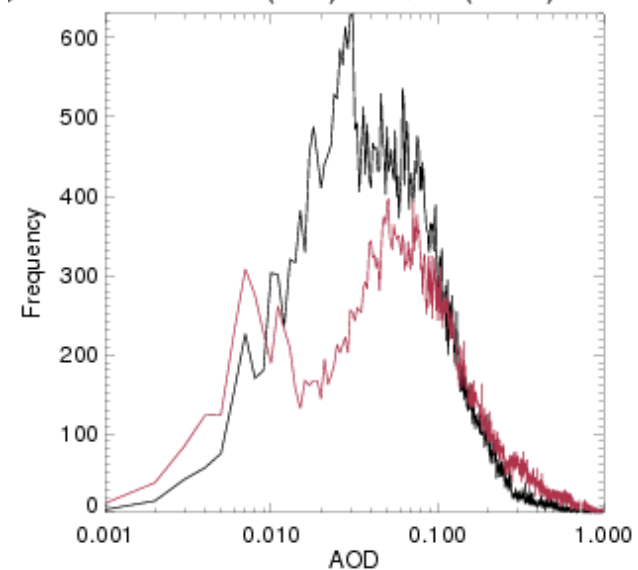
**Aerosol Robotic Network (AERONET)
is global network of Sun photometers
[Holben et al., 1998]**

Selected Aeronet vs RAQMS AOD timeseries
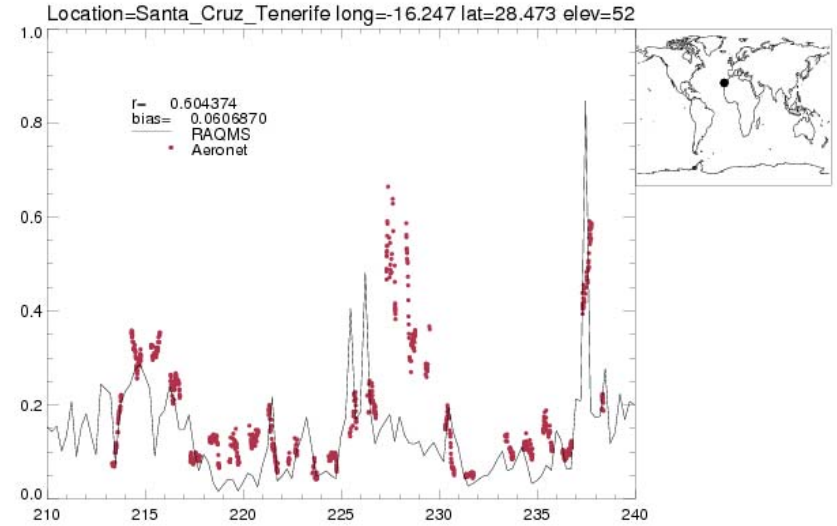
GEMS

GEMS: Global and regional Earth-system Monitoring using Satellite and in-situ data

GEMS themes:

Greenhouse Gases (GHG)
Global Reactive Gases (GRG)
Aerosols (AER)
Regional Air Quality (RAQ)
Production (PRO) & Validation (VAL)

Development of constituent and aerosol assimilation/forecasting within ECMWF Integrated Forecast System (IFS) Framework

TOWARD A MONITORING AND FORECASTING SYSTEM FOR ATMOSPHERIC COMPOSITION
The GEMS Project

BY A. HOLLINGSWORTH, R. J. ENGELEN, C. TEXTOR, A. BENEDETTI,
O. BOUCHER, F. CHEVALLIER, A. DETHOF, H. ELBERN, H. ESKES,
J. FLEMMING, C. GRANIER, J. W. KAISER, J.-J. MORCRETTE,
P. RAYNER, V.-H. PEUCH, L. ROUIL, M. G. SCHULTZ,
A. J. SIMMONS, AND THE GEMS CONSORTIUM

The European GEMS project is building a comprehensive monitoring and forecasting system for atmospheric composition on both global and regional scales.

With the advance of satellite remote sensing of the Earth's atmosphere, a clearer picture is starting to emerge of how natural and anthropogenic emissions are influencing the composition of the atmosphere on a global scale. While climate and pollution problems, such as the Antarctic ozone hole (Farman et al. 1985), increase in atmospheric CO_2 (Keeling et al. 1976) and pollution around cities, have often been first detected by ground-based measurements, satellite observations have the capability of showing the large-scale patterns. Good examples are the geostationary images of desert dust plumes stretching all the way from the Sahara to South America (see information online at http://oiswww.eumetsat.org/WEBOPS/iotm/iotm/20040306_dust/20040306_dust.html), observations of the Antarctic ozone hole by various satellite sensors (e.g., www.nasa.gov/vision/earth/environment/ozone_resource_page.html), and the recent global views of tropospheric NO_2 pollution as measured by the Global Ozone Monitoring Experiment (GOME), the Scanning Imaging Absorption Spectrometer for Atmospheric Cartography (SCIAMACHY), and the Ozone Monitoring Instrument (OMI; information at www.knmi.nl/omi/publ-n/metingen/no2/metingen_no2_nrt.html). These examples clearly show ▶

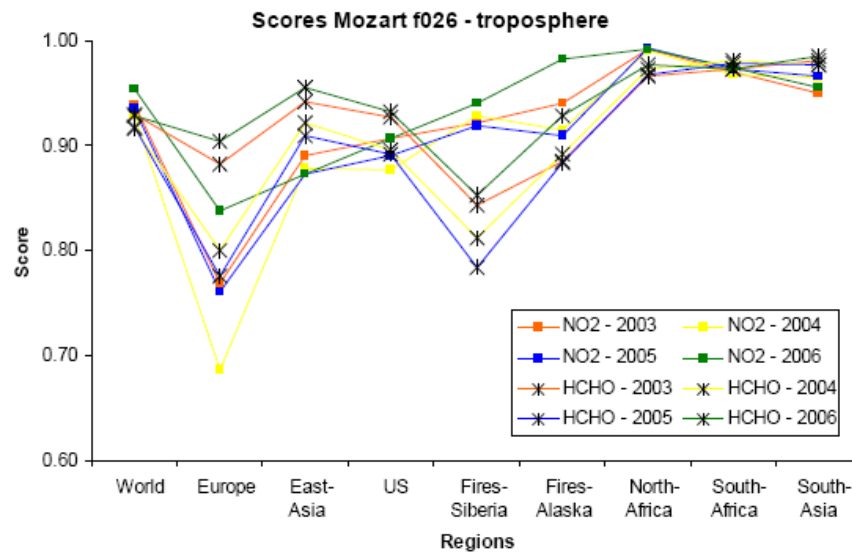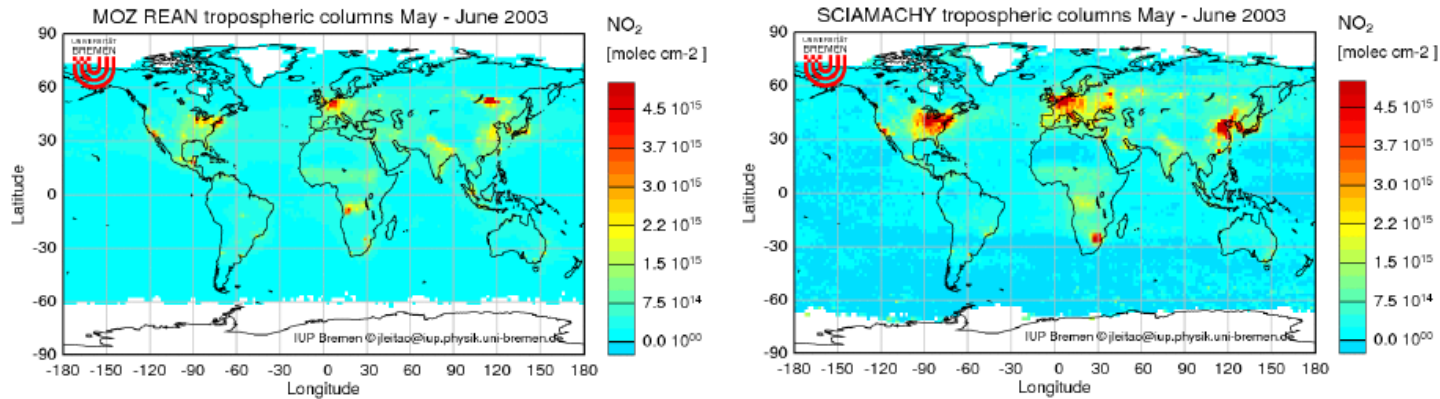Detail of MODIS visible image over northwestern Europe. See Fig. 9 for more information.

AMERICAN METEOROLOGICAL SOCIETY

AUGUST 2008 BAMS | 1147

GRG Main Objectives

•Build a system for routine forecasts and reanalyses of global reactive gases relevant for

   •**air pollution (long-range transport / RAQ boundaries)**

   •**climate change (oxidizing capacity, ozone)**

   •**stratospheric ozone**

   •**ecosystem monitoring (deposition fluxes)**

•Integrate tropospheric and stratospheric chemistry into the IFS model at ECMWF

•Assimilate satellite retrievals of O_3, CO, NO_2, CH_2O and SO_2 into the IFS model

Modelling Approach

•Use existing CTMs + coupling software, ensemble approach with 3 CTMs

   •MOCAGE

   •MOZART

   •TM5

From "GEMS Global Reactive Gases strategy and achievements" Martin Schultz - Jülich

Tropospheric NO$_2$ column

From "GEMS Global Reactive Gases strategy and achievements" Martin Schultz - Jülich

From "GEMS Global Reactive Gases strategy and achievements" Martin Schultz - Jülich
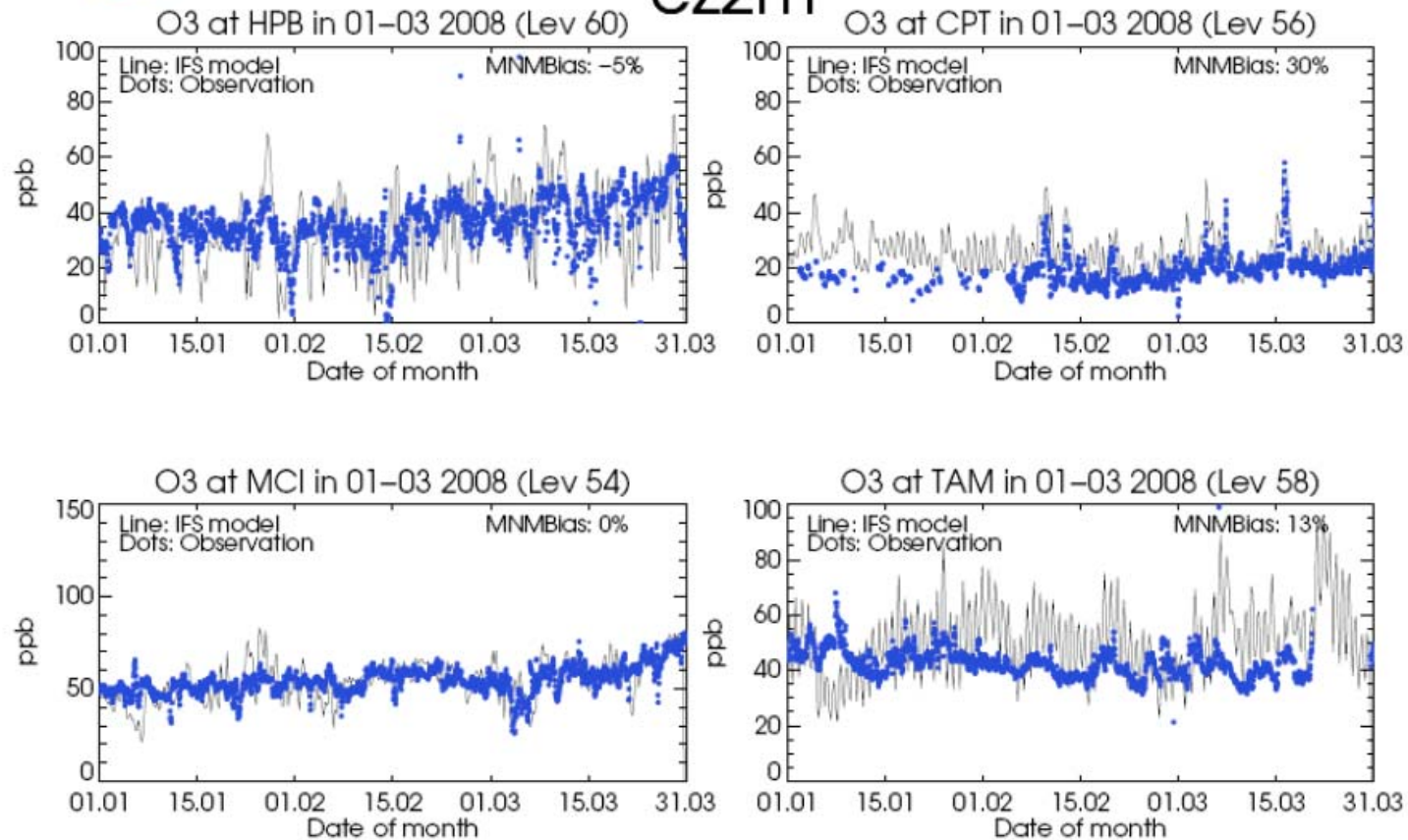
GEMS-aerosol

• Aerosol model with the ECMWF IFS framework
(12 variables*, emissions, transformation, sinks)

• 4D-VAR assimilation of MODIS data
(1 variable: total AOD)

• Focus is global monitoring, forecasting is a by-product

• T159, L60 (reanalysis), L91 (NRT forecast)

 * 1 DMS+SO2, 1 SU, 2 OC, 2 BC, 3 DU, 3 SS

From "Overview of the GEMS-aerosol project" Olivier Boucher – Met Office

Model evaluation with Aeronet sun photometers

	Reanalysis	Forecast	Aeronet
Mean AOD	0.269	0.242	0.218
Correlation	0.82	0.67	
RMS	0.114	0.133	
Std Mod/Obs	0.81	0.76	
Month Bias	41%	43%	

Averages at Aeronet stations during days of measurement
Based on # 1225 monthly means in 2003
from worldwide Aeronet network
no mountain sites, stations below 1000m

Michael Schulz
Jan Griesfeller
Nicolas Huneeus
Stefan Kinne

From "Overview of the GEMS-aerosol project" Olivier Boucher – Met Office

Model evaluation with Aeronet sun photometers

Biomass burning aerosols
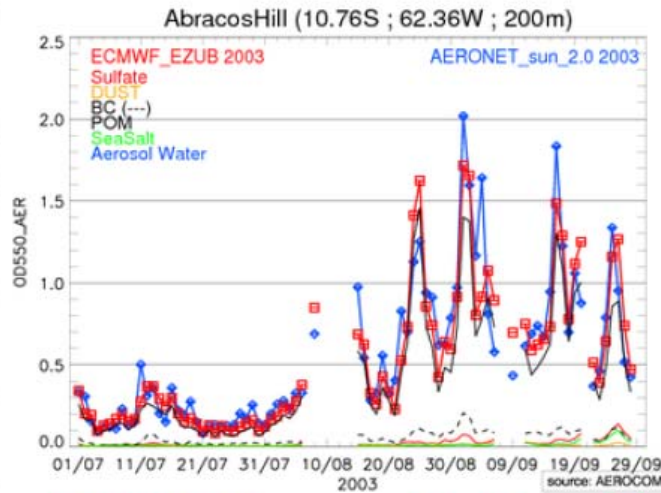
ECMWF reanalysis with MODIS AOD assimilation
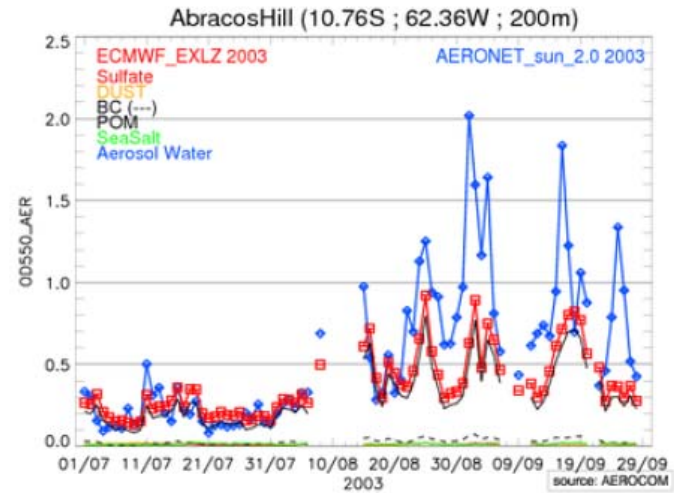
ECMWF forecast 00h

against Aeronet sun photometer AOD obs

Michael Schulz
Jan Griesfeller
Nicolas Huneeus
Stefan Kinne

From "Overview of the GEMS-aerosol project" Olivier Boucher – Met Office

Operational AOD assimilation
Naval Research Laboratory (NRL)

Aerosol physics uses a version of the NRL operational Atmospheric Variational Data Assimilation System (NAVDAS) called NAVDAS-Aerosol Optical Depth (NAVDAS-AOD)

- 2D variational approach
- constant aerosol mass adjustment for all species
- no adjustment for hydroscopic growth

Used to improve the NRL Aerosol Analysis and Prediction System (NAAPS)'s aerosol forecasting capability

Meteorological analysis and forecast fields from the Navy Operational Global Analysis and Prediction System (NOGAPS)

NAVDAS-AOD assimilates over-water MODIS AOD from the NOAA NESDIS Near Real Time Processing Effort (NRTPE) (latency of 3 h or less in most cases)

Strict QA procedure is necessary to remove outliers associated with cloud artifacts [Zhang and Reid, 2006]

Zhang, J., J. S. Reid, D. L. Westphal, N. L. Baker, and E. J. Hyer (2008), A system for operational aerosol optical depth data assimilation over global oceans, J. Geophys. Res., 113, D10208, doi:10.1029/2007JD009065

African Case Study 30 May 2006

Figure 2. (a) MODIS true color image for 30 May 2006; (b) daily averaged MODIS (Terra + Aqua) τ for the same day as Figure 2a. Notice that with the stringent data cleaning processes, Figure 2b may be different from the plot that is created using the operational level 2 MODIS aerosol product; (c) NAAPS τ analysis for 1200 z, 30 May 2006, without the use of NAVDAS-AOD; (d) NAAPS τ analysis for 1200 z, 30 May 2006, with 5 months of data assimilation.

Aeronet Sun photometer validation

Aeronet comparisons limited to the coastal and island AERONET sites
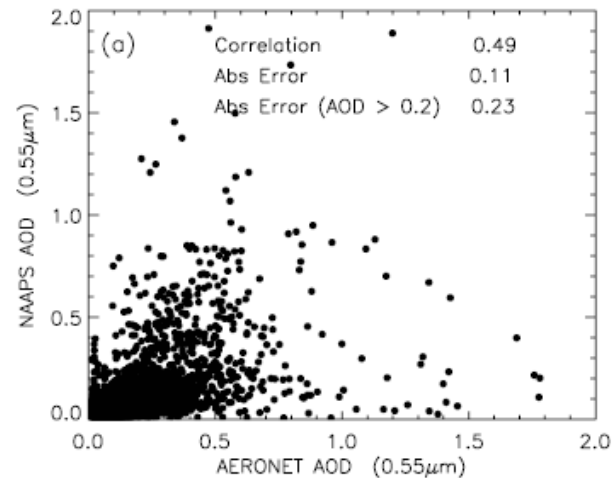
January-May 2006 No Assimilation
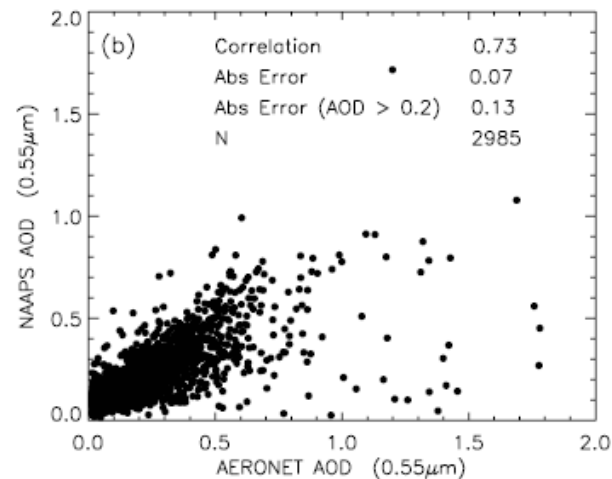
January-May 2006 MODIS Assimilation

Figure 3. (a) AERONET versus NAAPS τ for 5-month (January–May 2006) NAAPS nonassimilation run; (b) AERONET versus NAAPS τ for 5-month (January–May 2006) NAAPS run with the aerosol data assimilation process.

GOES and MODIS fire detections
From Fire Locating and Modeling of Burning Emissions (FLAMBE')

2009061500-2009061523 GOES(red) MODIS(purple)

June 15, 2009

http://www.nrlmry.navy.mil/aerosol/
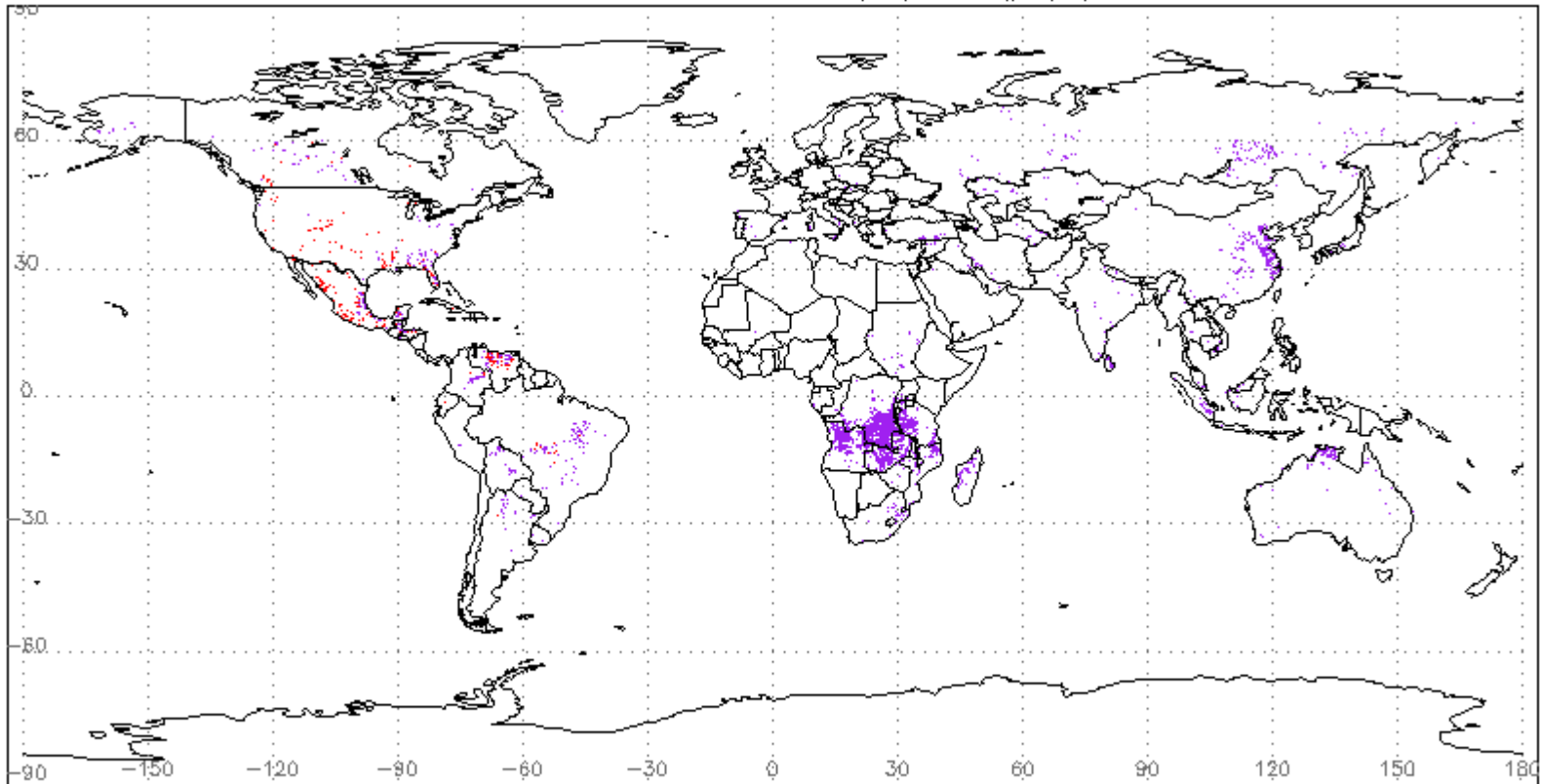
NAAPS Smoke Analysis

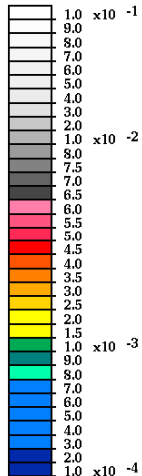2009061500-2009061523 GDES(red) MODIS(purple) NAAPS Smoke(see colorbar)

0.1　0.2　0.4　0.8

Smoke

June 15, 2009

http://www.nrlmry.navy.mil/aerosol/
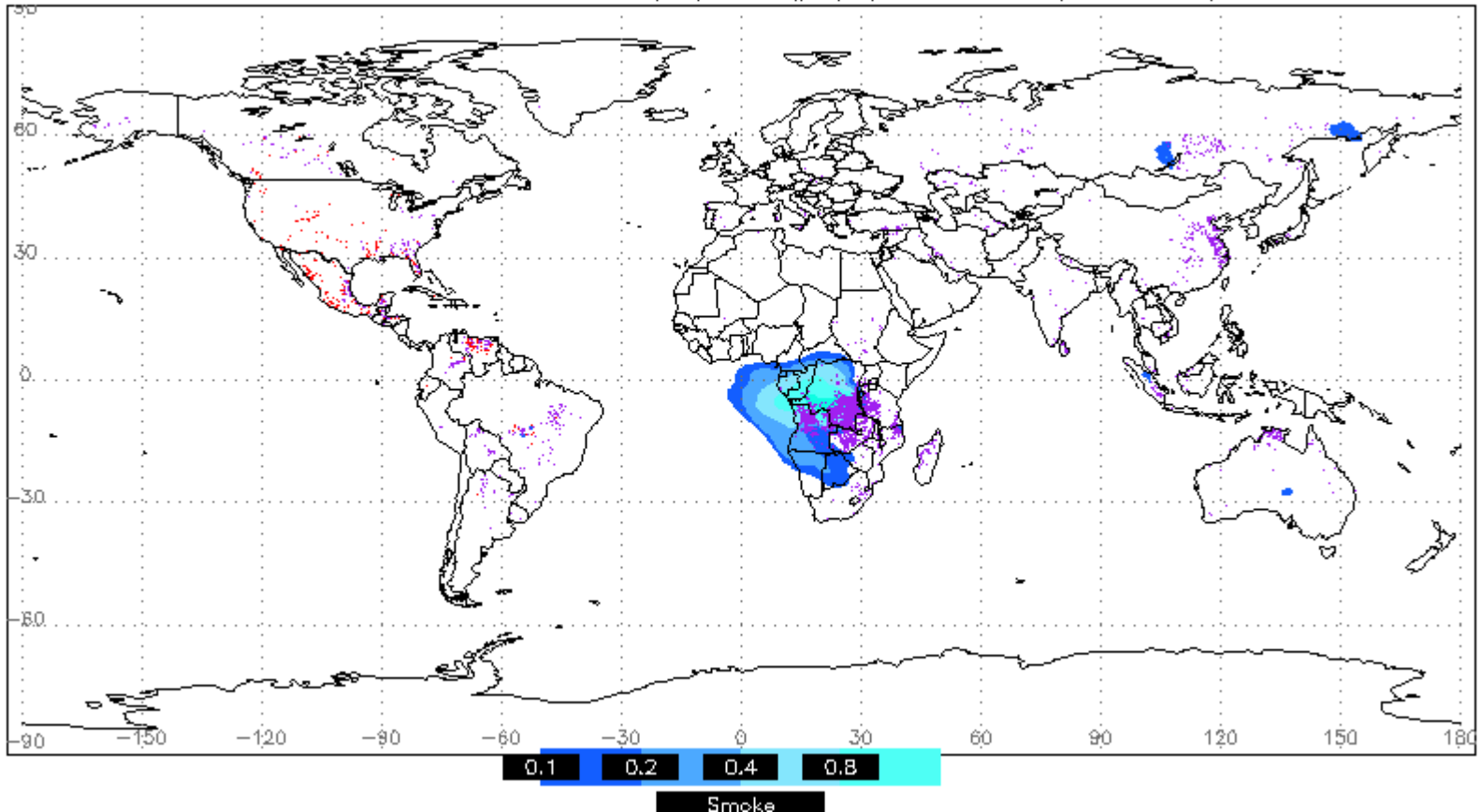
NAAPS Smoke+Dust Analysis

2009061500–2009061523 GOES(red) MODIS(purple) NAAPS Smoke(see colorbar)

Dust: 0.1 0.2 0.4 0.8

Smoke: 0.1 0.2 0.4 0.8

June 15, 2009

http://www.nrlmry.navy.mil/aerosol/
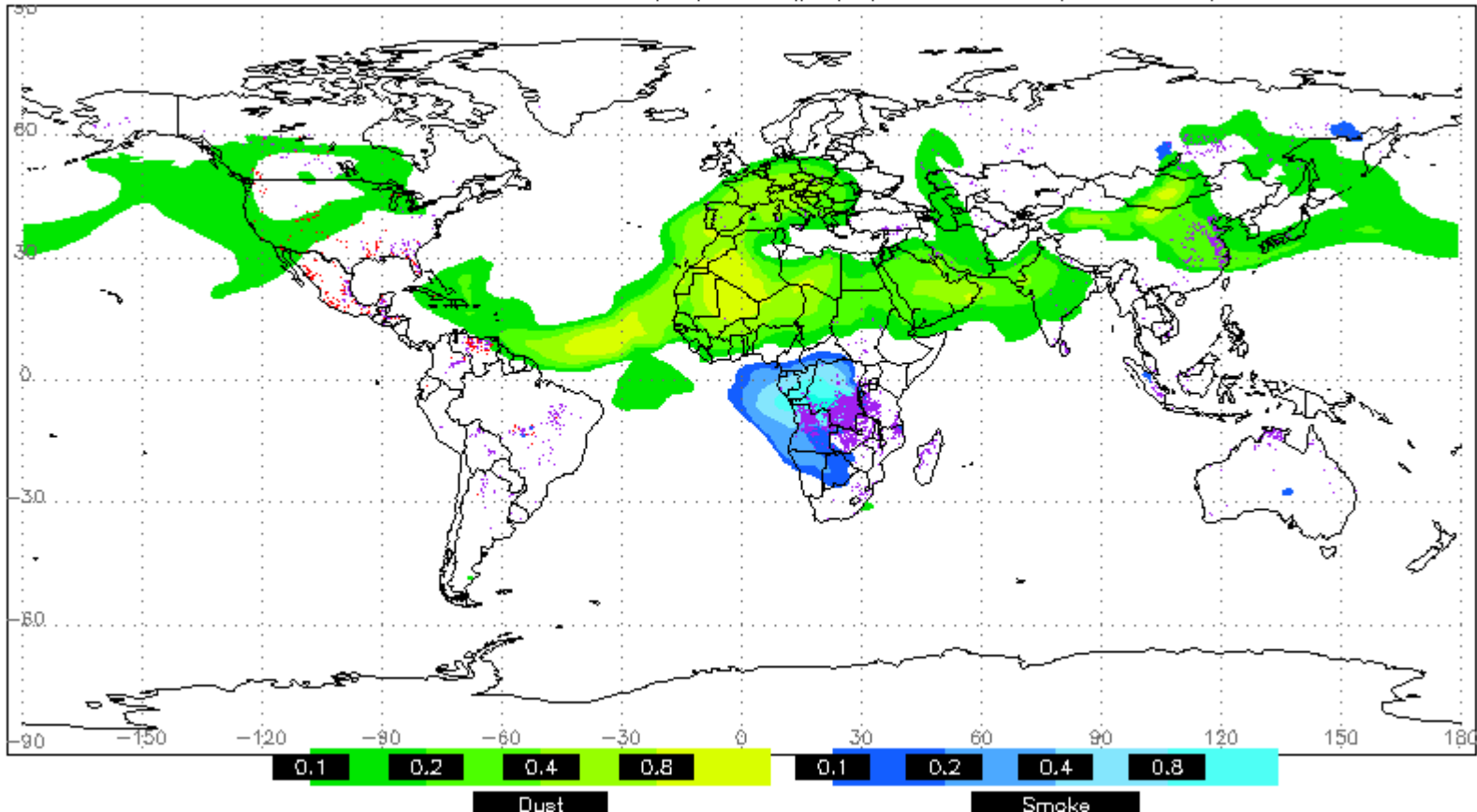
NAAPS Smoke+Dust+Sulfate Analysis
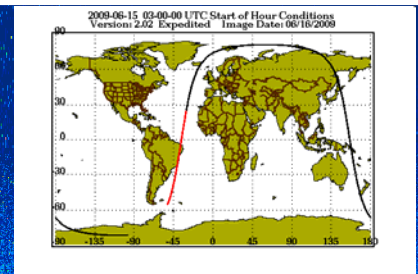

2009061500-2009061523 GOES(red) MODIS(purple) NAAPS Sulfate (see colorbar)

June 15, 2009

http://www.nrlmry.navy.mil/aerosol/
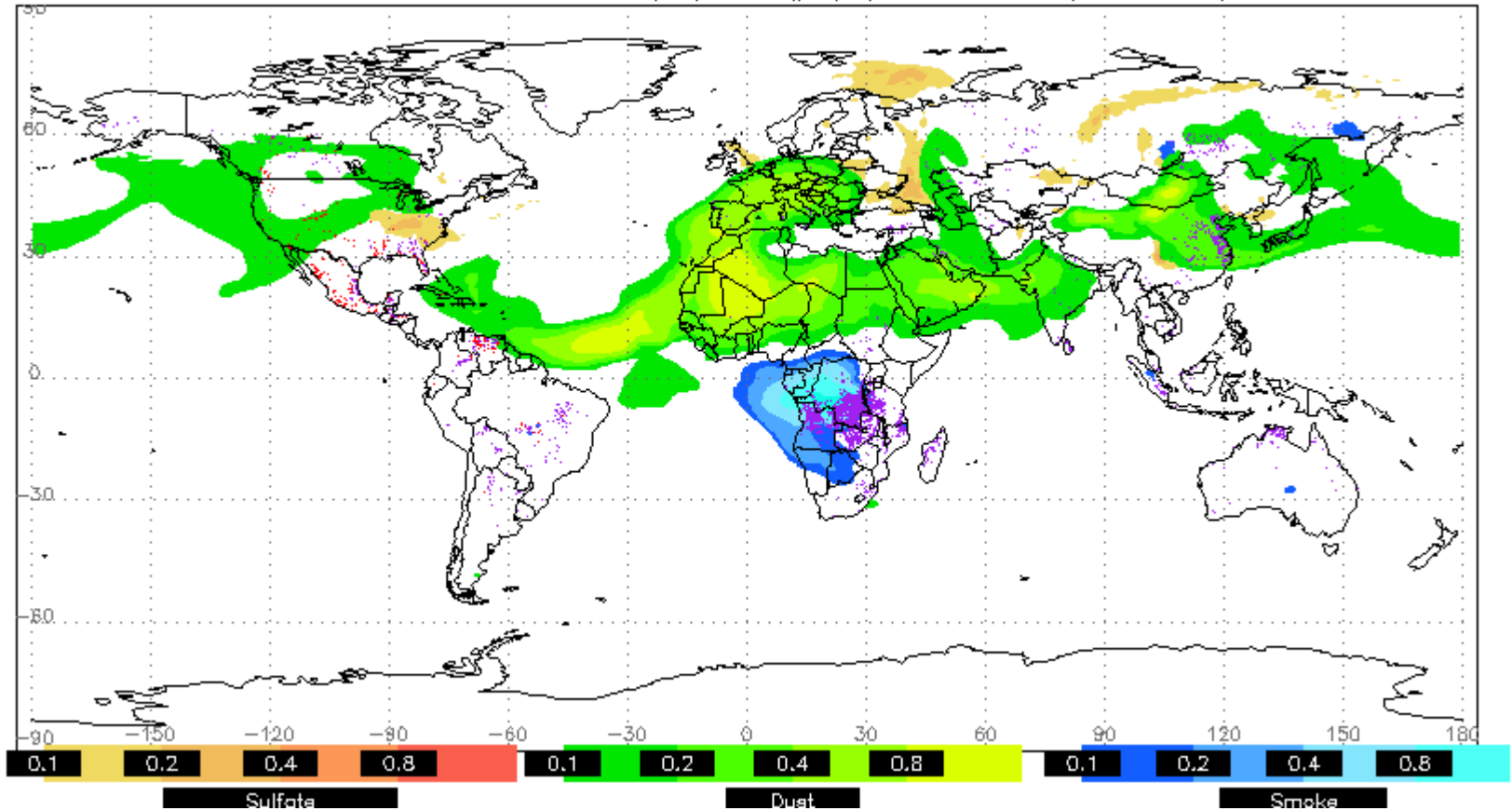
MODIS AOD

MYD08_D3.051 Aerosol Optical Depth at 550 nm [unitless]
(15Jun2009)

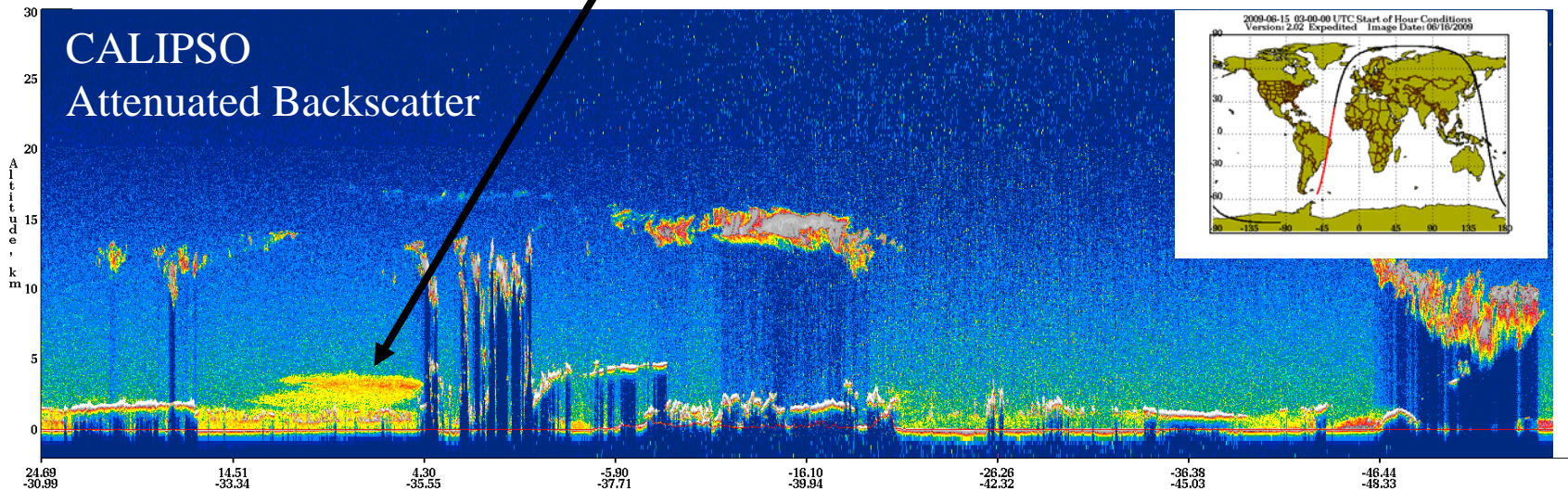**June 15, 2009**

http://www.nrlmry.navy.mil/aerosol/
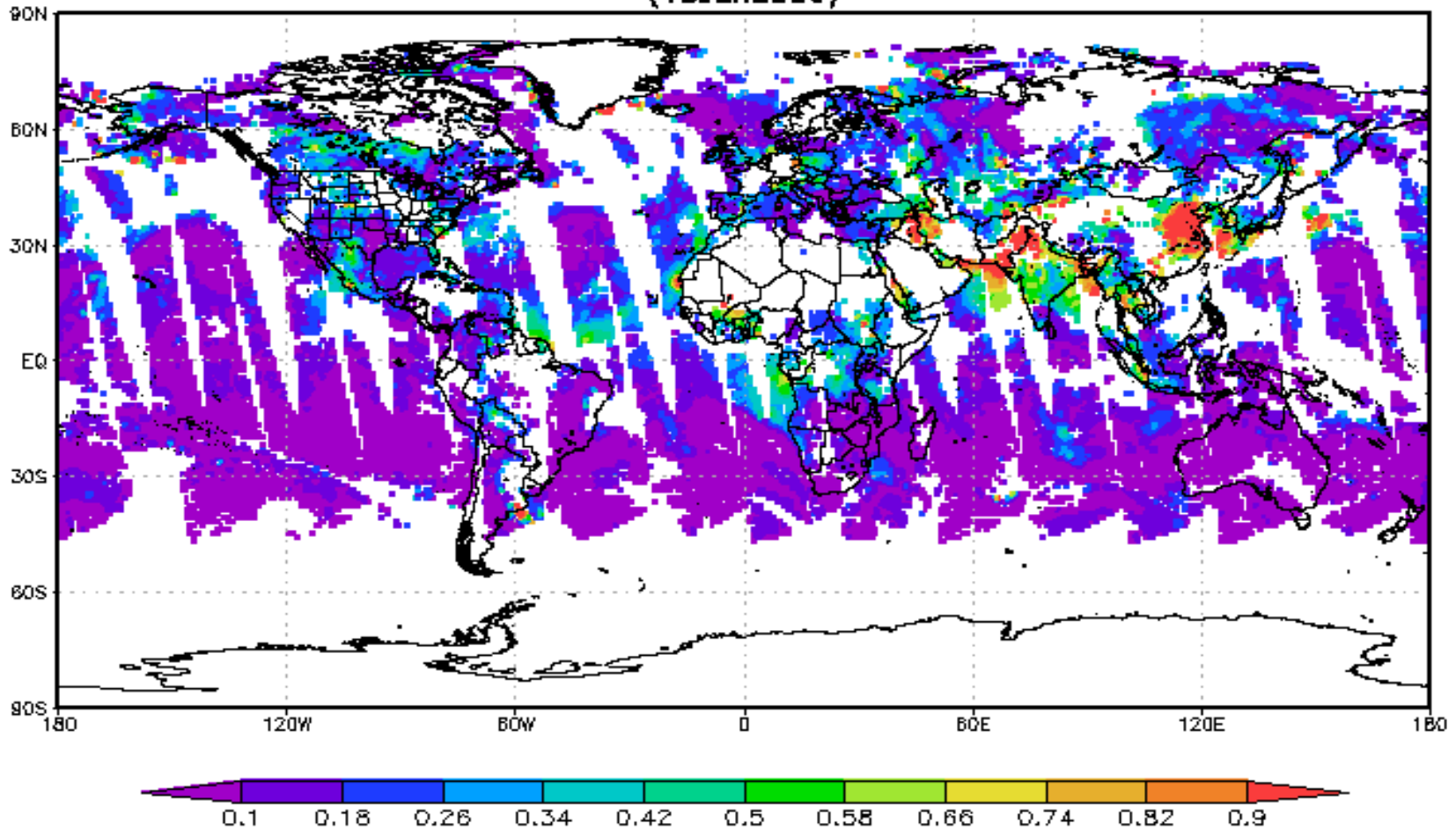
NAAPS Dust Analysis vs CALIPSO

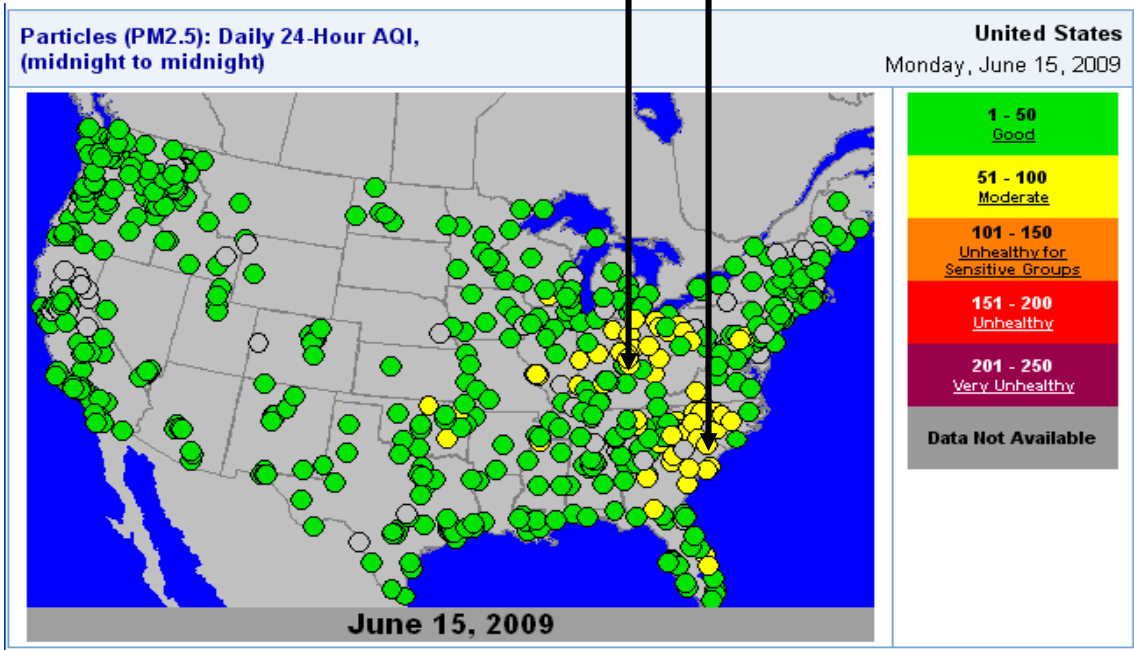2009061500–2009061523 GOES(red) MODIS(purple) NAAPS Sulfate (see colorbar)
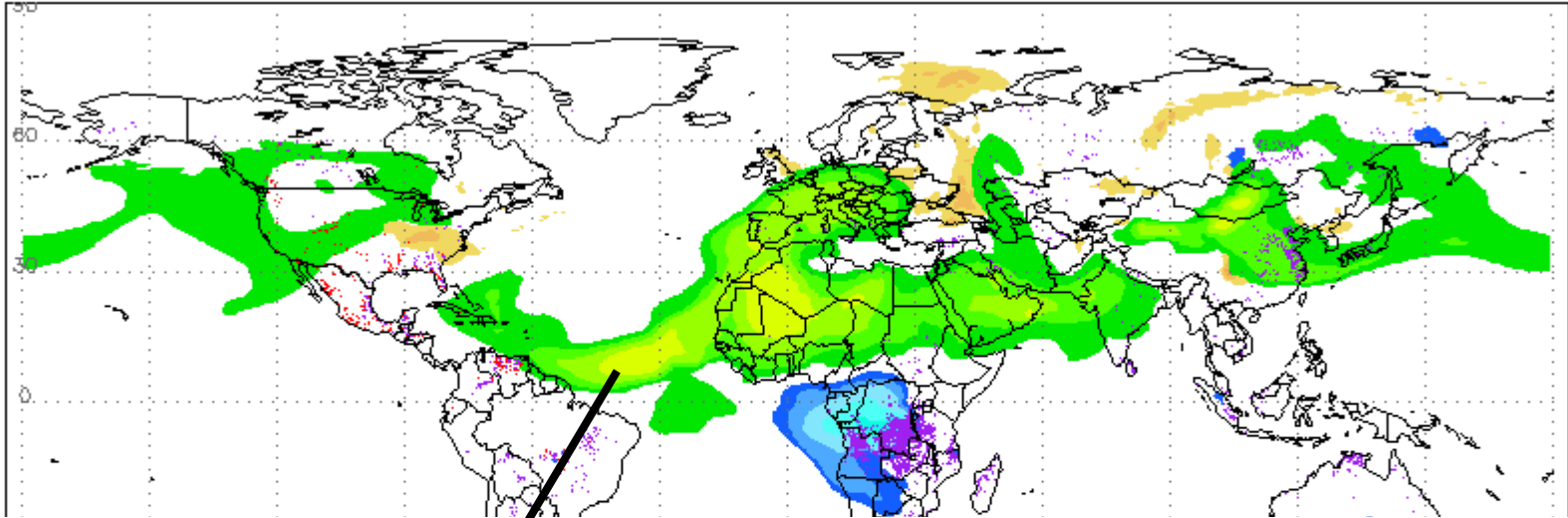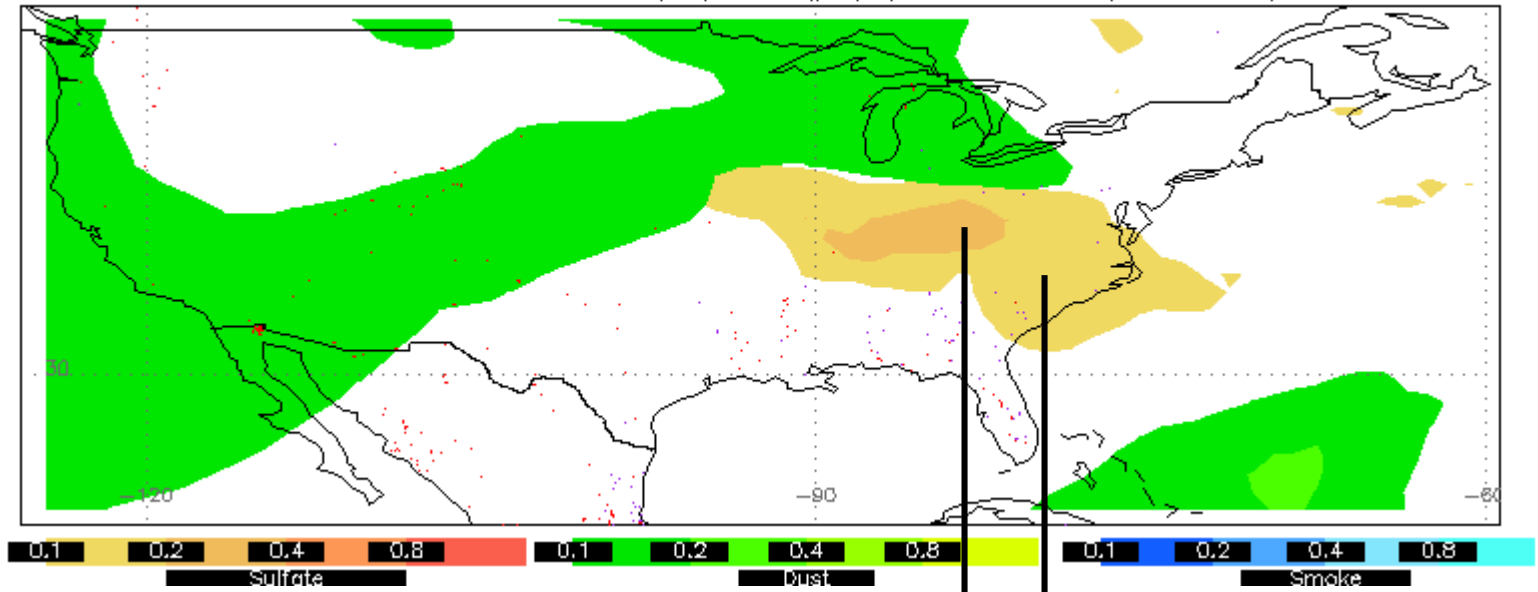
532 nm Total Attenuated Backscatter, /km /sr   Begin UTC: 2009-06-15 04:07:44.7562   End UTC: 2009-06-15 04:30:00.1561
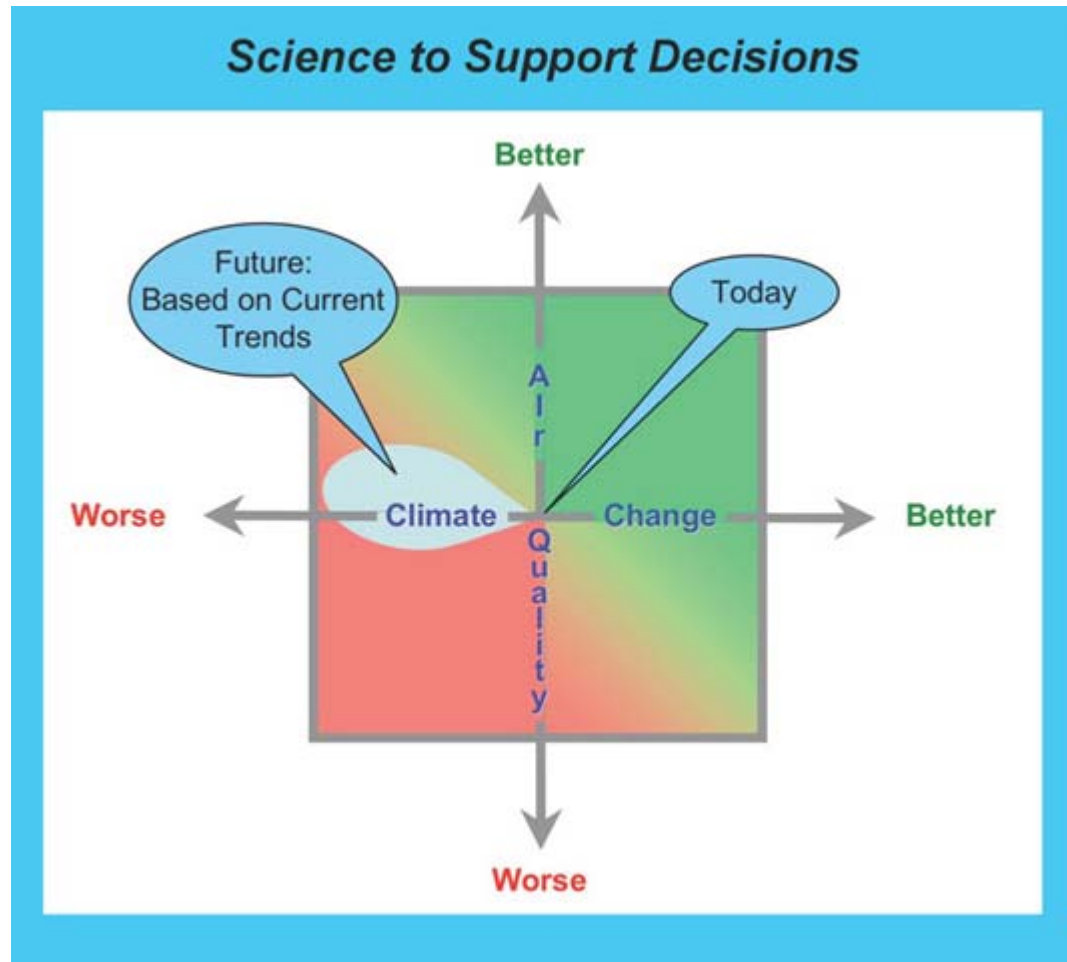
Version: 2.02 Expedited   Image Date: 06/16/2009

CALIPSO
Attenuated Backscatter

NAAPS Sulfate Analysis vs EPA AIRNow PM2.5 Air Quality Index (AQI)

2009061500–2009061523 GOES(red) MODIS(purple) NAAPS Sulfate (see colorbar)

Sulfate   Dust   Smoke

Particles (PM2.5): Daily 24-Hour AQI,
(midnight to midnight)

United States
Monday, June 15, 2009

1 - 50 Good
51 - 100 Moderate
101 - 150 Unhealthy for Sensitive Groups
151 - 200 Unhealthy
201 - 250 Very Unhealthy
Data Not Available

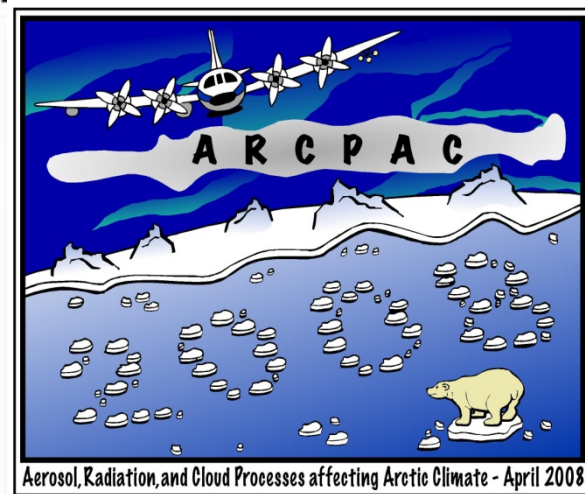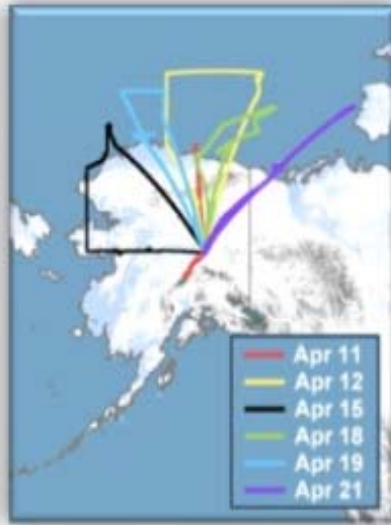June 15, 2009

http://airnow.gov/

# Links between air quality and global climate change

The gray ellipse represents the direction of current trends in the U.S.

During April 2008, as part of the International Polar Year (IPY), NOAA's Climate Forcing and Air Quality Programs engaged in an airborne field measurement campaign in the Alaskan Arctic . The Aerosol, Radiation, and Cloud Processes affecting Arctic Climate (ARCPAC) field mission (Fairbanks AK) focused on direct measurements of properties and processes associated with non-greenhouse-gas atmospheric climate forcing
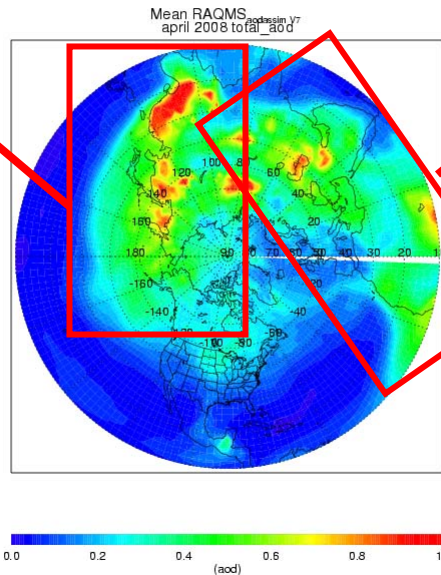
Website: http://www.esrl.noaa.gov/csd/arcpac/
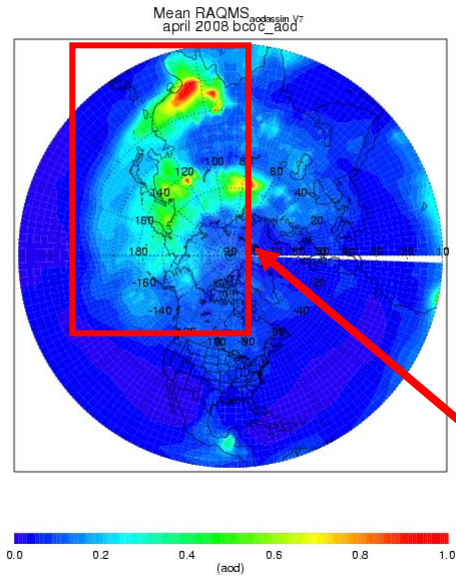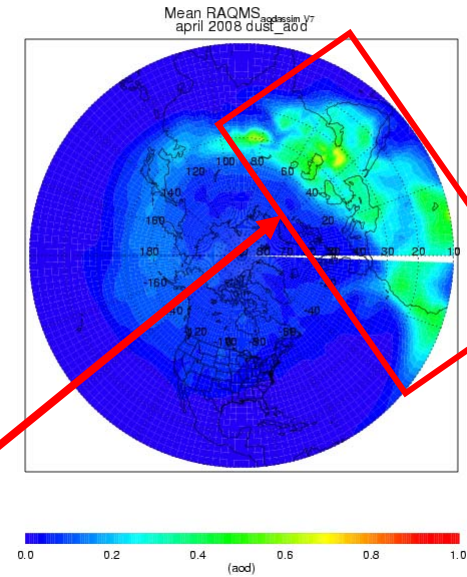
RAQMS April 2008 AOD Partitioning

Carbon

Dust

Total

April 2008 RAQMS vs Aeronet 550nm AOD (v7ems/dzfix)

rms = 0.180213
bias= -0.0509267
r = 0.702086
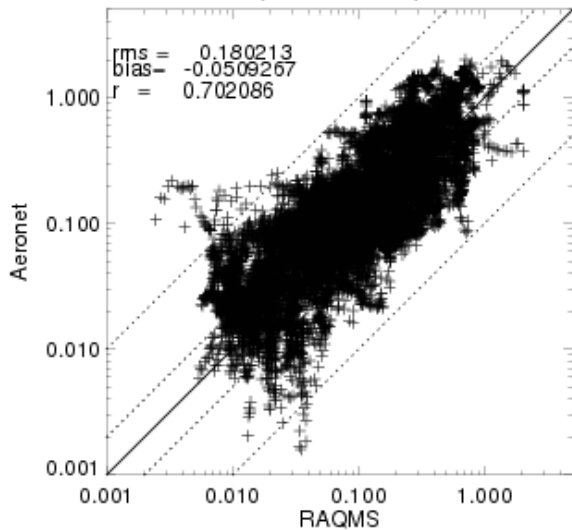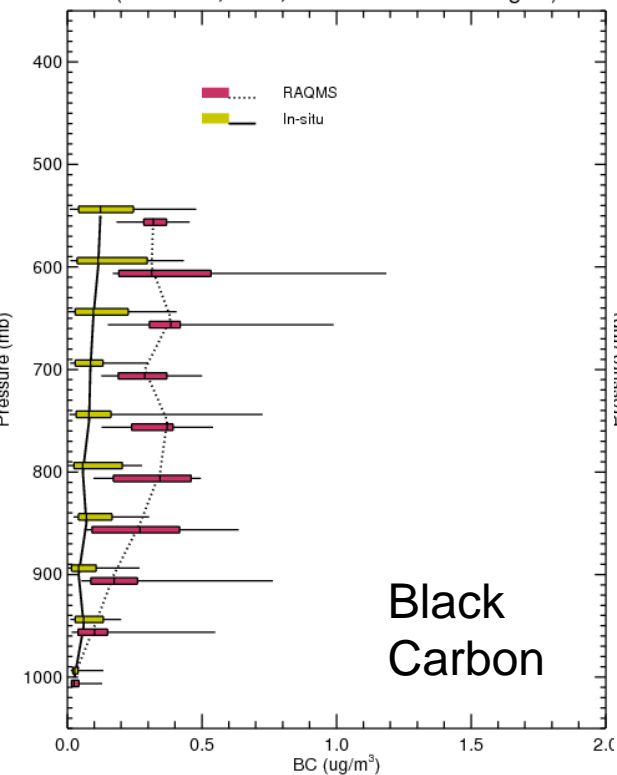
April 2008 550nm AOD Histogram
Aeronet (Red) RAQMS (Black) (v7ems/dzfix)
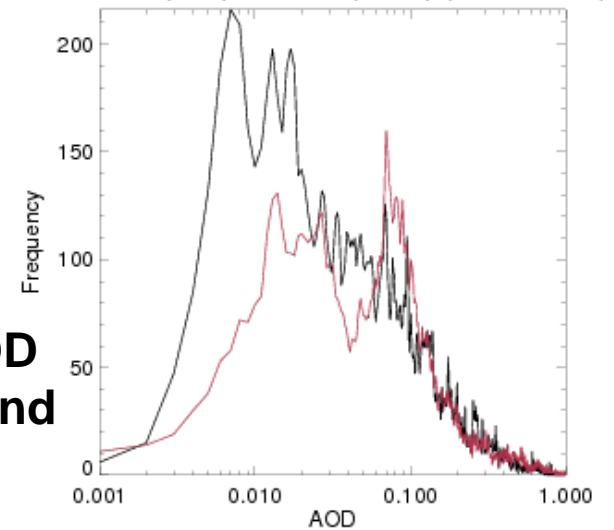
Majority of April 2008 AOD is due to Carbonaceous and Dust aerosols

RAQMS/NOAA P3 Insitu BC (Spackman) (v7ems/dzfix) (4/12-4/21, 2008, All Arctic ARCPAC Flights)

RAQMS/NOAA P3 Insitu SO4 (Middlebrook) (v7ems/dzfix) (4/11-4/21, 2008, All Arctic ARCPAC Flights)
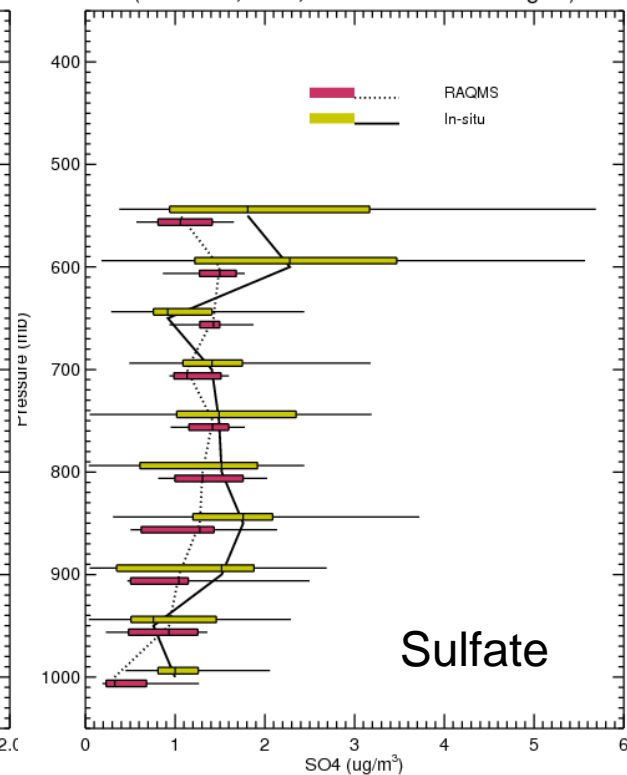
RAQMS/NOAA P3 Insitu OC (Middlebrook) (v7ems/dzfix) (4/11-4/21, 2008, All Arctic ARCPAC Flights)

Black Carbon

Sulfate
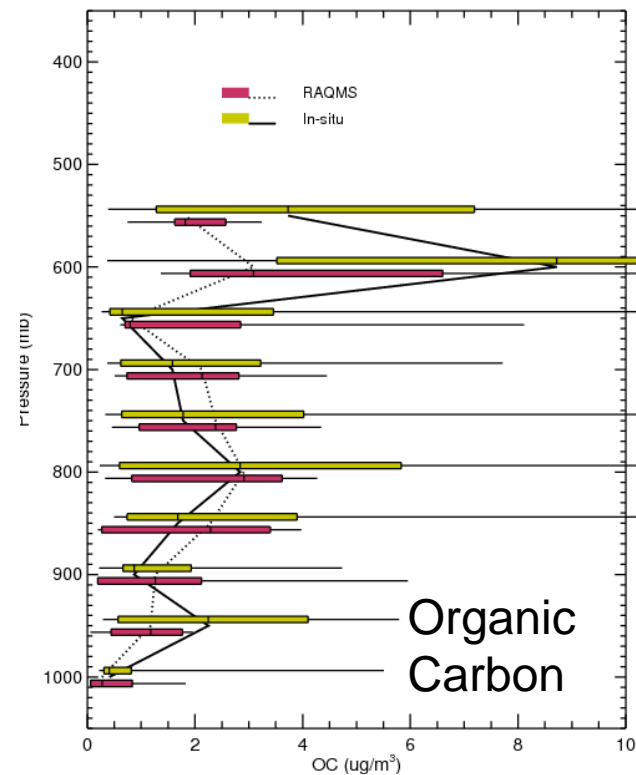
Organic Carbon

WP-3D Flight Track Map

Flight tracks in Alaska.
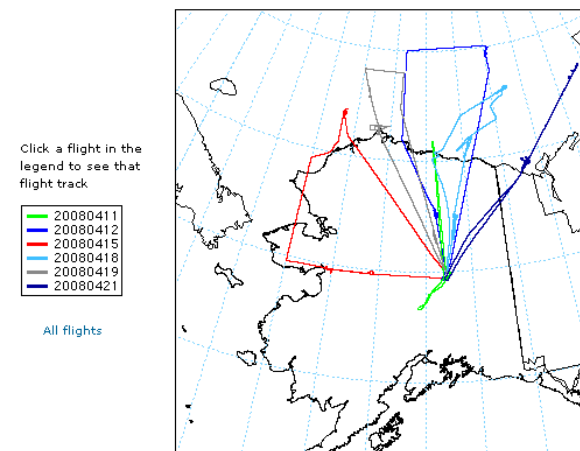
MODIS aerosol optical depth (AOD) assimilation results in good agreement with P3 insitu SO4 and Organic Carbon (OC) measurements but overestimates Black Carbon (BC) mass.

NOAA P3 insitu data provided by Ryan Spackman and Ann Middlebrook (NOAA/ESRL)

Arctic aerosol indirect effects during ARCPAC

Use RAQMS analyzed aerosol extinction to sort MODIS Liquid Effective Radius as a function of Cloud Liquid Water Content to investigate Arctic first indirect effect

April 2008 (60-90N) MODIS Cloud Liquid Effective Radius

decrease in r_e

Cloud effective radius (micron)
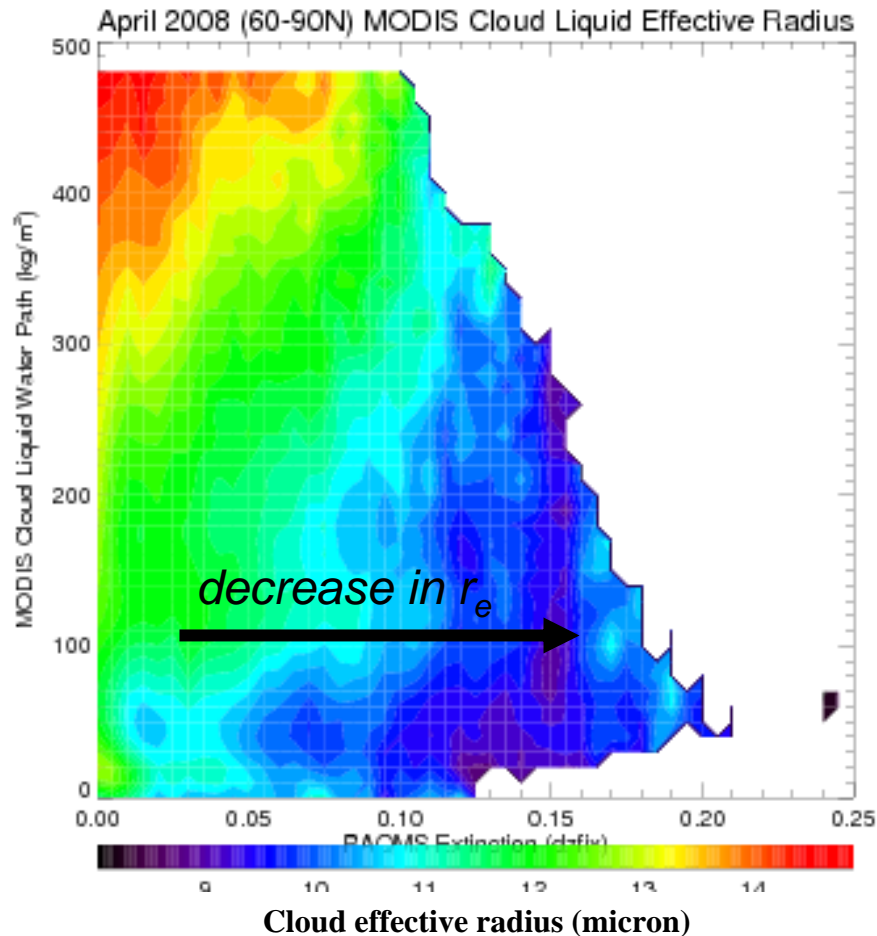
Evidence for First (Twomey) indirect Effect: Aerosol loading increases cloud droplet number concentration resulting in a decrease in average cloud droplet size (effective radius) for a fixed liquid water content (LWC).

Impacts of aerosols on Arctic radiative forcing

Shortwave effects: Decreased droplet size due to aerosol loading leads to *increased cloud albedo* and additional reflection of shortwave radiation to space and leads to *surface cooling*.

High snow/ice albedo minimizes this effect in the Arctic

Longwave effects: Decreased droplet size due to aerosol loading *increases the longwave emissivity* of optically thin clouds, which leads to increased emitted longwave radiation [Curry and Ebert, 1992, Curry 1993] and *surface longwave heating*.

Observational studies have shown that the longwave aerosol indirect effect can lead to significant (3.4 Wm^{-2}) positive radiative forcing in the Arctic [Lubin and Vogelmann, 2006].

Links between air quality and global climate change

RF Terms		RF values (W m⁻²)	Spatial scale	LOSU
Long-lived greenhouse gases	CO_2 / N_2O / CH_4 Halocarbons	1.66 [1.49 to 1.83]	Global	High
		0.48 [0.43 to 0.53] 0.16 [0.14 to 0.18] 0.34 [0.31 to 0.37]	Global	High
Ozone	Stratospheric Tropospheric	-0.05 [-0.15 to 0.05] 0.35 [0.25 to 0.65]	Continental to global	Med
Stratospheric water vapour from CH_4		0.07 [0.02 to 0.12]	Global	Low
Surface albedo	Land use Black carbon on snow	-0.2 [-0.4 to 0.0] 0.1 [0.0 to 0.2]	Local to continental	Med - Low
Total Aerosol — Direct effect		-0.5 [-0.9 to -0.1]	Continental to global	Med - Low
Total Aerosol — Cloud albedo effect		-0.7 [-1.8 to -0.3]	Continental to global	Low
Linear contrails		0.01 [0.003 to 0.03]	Continental	Low
Solar irradiance		0.12 [0.06 to 0.30]	Global	Low
Total net anthropogenic		1.6 [0.6 to 2.4]		

Radiative Forcing (W m⁻²)

©IPCC 2007: WG1-AR4

Thank you!